

NASA TN D-1793

56p.



N 63 17301

Code -1

TECHNICAL NOTE

D-1793

CENTER-LINE PRESSURE DISTRIBUTIONS ON TWO-DIMENSIONAL
BODIES WITH LEADING-EDGE ANGLES GREATER THAN THAT
FOR SHOCK DETACHMENT AT MACH NUMBER 6 AND
ANGLES OF ATTACK UP TO 25°

By Theodore J. Goldberg, George C. Ashby, Jr.,
and James G. Hondros

Langley Research Center
Langley Station, Hampton, Va.

NATIONAL AERONAUTICS AND SPACE ADMINISTRATION
WASHINGTON

June 1963

Colby

CHANGE PAGE COPY

NATIONAL AERONAUTICS AND SPACE ADMINISTRATION

TECHNICAL NOTE D-1793

CENTER-LINE PRESSURE DISTRIBUTIONS ON TWO-DIMENSIONAL
BODIES WITH LEADING-EDGE ANGLES GREATER THAN THAT
FOR SHOCK DETACHMENT AT MACH NUMBER 6 AND
ANGLES OF ATTACK UP TO 25°

By Theodore J. Goldberg, George C. Ashby, Jr.,
and James G. Hondros

SUMMARY

17301

Center-line pressure distributions were obtained for two-dimensional sharp-nose parabolic arc, circular arc, and wedge bodies having a leading-edge angle greater than that for shock detachment (aerodynamically blunt bodies) at Mach number of 6 for angles of attack up to 25° . The maximum pressure coefficient was found to increase continuously from the shock-attachment value to the stagnation value behind a normal shock between leading-edge deflection angles of 42° and 51° . Only the data for contoured bodies having leading-edge angles of 66° or greater are correlated very well by the generalized Newtonian theory. However, at all angles of attack for all aerodynamically blunt bodies having curved surfaces, the agreement between the generalized Newtonian theory and the measured values of pressure coefficient was reasonably good for surface-deflection angles above 30° . This theory can be used to predict pressures on most two-dimensional bodies by the methods shown herein. With few exceptions, at a given deflection angle the pressure distributions rearward of the maximum pressure on the lower and upper surfaces of aerodynamically blunt wedges are essentially coincident with those of wedges having higher and lower half-angles, respectively. In addition, the pressure distributions of these wedges are in good agreement aft of the maximum-pressure point with those of a flat plate at corresponding deflection angles to the lower surface above 53° and to the upper surface above 31° .

INTRODUCTION

There is a large amount of available experimental and theoretical information in the hypersonic speed range for bodies having either rounded leading edges and therefore detached shock waves or sharp leading edges with attached shock waves. However there is very little, if any, available data in this speed range for the class of bodies with sharp leading edges having detached shock waves. The purpose of the present investigation is to provide some information in that area.

This report presents the center-line pressure distributions on a series of two-dimensional bodies having leading-edge angles from 42° to 90° which were measured in the Langley 20-inch Mach 6 tunnel at angles of attack up to 25° . In addition the means by which the pressure distributions can be predicted are also presented.

SYMBOLS

C_p	pressure coefficient, $\frac{p_1 - p_\infty}{\frac{1}{2}(\gamma p_\infty M_\infty)}$
M_∞	free-stream Mach number
p_1	local pressure, lb/sq in.
p_t	total or stagnation pressure, lb/sq in.
p_∞	free-stream pressure, lb/sq in.
s	distance along body surface from nose, in.
s_w	total length of wedge surface, in.
t	half the maximum body thickness, in.
x, y	body coordinates
α	angle of attack, deg
γ	ratio of specific heats
δ	local inclination of the body surface referenced to wind axis, deg
θ	local inclination of body surface referenced to body axis, deg

Subscripts:

geom	geometric
l	lower surface
le	leading edge
max	maximum
stag	stagnation behind a normal shock
u	upper surface

APPARATUS AND METHODS

Wind Tunnel and Models

This investigation was conducted in the Langley 20-inch Mach 6 tunnel. The tunnel, which has been described in reference 1, is a blowdown-to-atmosphere type which operates at a maximum stagnation temperature of 600° F and a maximum stagnation pressure of 600 lb/sq in. The air is dried by an activated alumina dryer designed to provide a dewpoint temperature of -40° F at 600 lb/sq in.

The three groups of 5 two-dimensional models used in this investigation consisted of wedges and parabolic and circular arcs. Each group had leading-edge angles of 42°, 54°, 66°, 78°, and 90°. These models will herein be referred to by their leading-edge angles and contours. These contours were selected because they represent a large portion of the entire class of two-dimensional sharp-nose bodies having a leading-edge angle greater than that for shock detachment at a Mach number of 6. For a given deflection angle the wedge and the parabolic arc represent the minimum and maximum surface curvature of the present investigation, respectively, while the circular arc represents an intermediate curvature. Although the theoretical shock-detachment angle at Mach 6.0 is 42.4°, it was felt that a perfectly sharp leading edge could not be fabricated and that the shock for a 42°-leading-edge-angle model would be detached. This leading-edge angle would represent the lower limit of the aerodynamically blunt range. All models had a span of 4.00 inches and a thickness of 4.00 inches. The models were adapted with a 2.56-inch-long cylindrical section on the rear by using a "quick-disconnect" type connection to facilitate model changes. Photographs of the models and of the model attached to the support connection are shown in figures 1 and 2, respectively. Model dimensions are given in table I along with x,y locations of orifices, local inclinations at orifices, and surface distance-to-thickness ratios. Extensions, which were added to both sides of the 78° parabolic arc body to check the two dimensionality of the flow along the center line, were each 3 inches wide and contoured to match the basic body. A row of orifices on one of the extensions was located at the same position relative to the edge (2 inches inboard) as those on the basic body. This body was selected because it was the longest and any disturbance emanating from the tips of the models would affect the most rearward orifices. The 78° parabola with extensions is shown in figure 2. Model orifice sizes for the basic models and extensions were 0.021 inside diameter near the leading edges and 0.063 inside diameter at all other orifice locations.

The models were supported in the tunnel by the goose-neck support system shown in figure 3, which moved the model 25° in angle of attack in the horizontal plane. A mechanically operated counter geared to the vertical shaft of the support system was used to measure the angle of attack. Deflections due to air loads were negligible because of the stiffness of the sting support.

Tests

All models were tested in 5° increments over an angle-of-attack range of 0° to 25°. In addition, the 42°-leading-edge models were tested in 1° increments at angles of attack from 0° to 15°.

All tests reported herein were conducted at a stagnation pressure and temperature of 400 lb/sq in. absolute and 400° F which yields a Reynolds number of 7.6×10^6 per foot.

Pressure data were recorded by photographing a mercury manometer for pressures greater than 1 lb/sq in. absolute. For pressures of 1 lb/sq in. absolute or less a butyl phthalate manometer was used to obtain greater accuracy because of the low specific gravity of the fluid. Tunnel stagnation pressures were measured with a 0 to 600 lb/sq in. Bourdon gage. All pressures were photographically recorded simultaneously.

Data Reduction and Accuracy

Previous tunnel calibrations have shown that at any instant the Mach number throughout the test section varies by only ± 0.02 . However, the Mach number level varies from 5.94 to 6.04 depending upon time - the time during each run, the time between runs, and the total time elapsed. This fact makes it extremely difficult, if not impossible, to obtain an exact calibration curve of Mach number against time. The data, therefore, were initially reduced at an average Mach number of 6. This procedure resulted in sufficient data scatter to make difficult an analysis of data trends. One obvious trend emerged, however, which led to a better definition of test Mach numbers. This trend is shown in figure 4 where the maximum pressure coefficients obtained on the various bodies are presented as a function of the flow-deflection angles at which they were obtained. At flow-deflection angle for shock detachment ($\delta = 42^\circ$) the data agree with oblique shock theory. At higher flow-deflection angles the data approach and even exceed the stagnation-pressure-coefficient value at flow-deflection angles considerably less than 90° . The degree by which the data exceed $C_{p,\text{stag}}$, of course, is indicative of the data scatter. Since the data exceed $C_{p,\text{stag}}$ by as much as 4 percent which is much greater than measuring accuracy, the scatter is attributed to a true Mach number variation different from the assumed constant value of 6.0. By using the data trend shown in figure 4, a more representative Mach number variation for reducing the data was obtained by the following procedure. For each model the ratio of maximum-local to tunnel-stagnation pressure was assumed to be equal to the total pressure ratio across a normal shock. This ratio was then used to compute the corresponding Mach number for each model and α combination. At the angles of attack where the resulting Mach numbers fell within the known tunnel range these values of Mach number were used to reduce the data. The Mach numbers so obtained were applicable to all bodies except the 42° wedge at angles of attack below 7° and the 42° parabolic and circular arc bodies below $\alpha = 10^\circ$. For the 42° bodies at 0° angle of attack, the Mach numbers were computed by assuming the measured maximum pressure to be given by oblique shock theory. Since these Mach numbers again fell within the known range of tunnel Mach number, they were used to reduce the data for these models. For the angles of attack of the 42° bodies between 0° and 7° or 10° , as the case may be, a linear variation of Mach number with angle of attack between these limits was assumed. This assumption appears to be justifiable because the variation of tunnel Mach number with time is quasi-linear and in the same direction.

The center line of the body was considered to be the dividing line between the upper and lower surfaces at all angles of attack. The location of the maximum pressure point was determined from faired curves of P_1/P_t against θ on the upper and lower surfaces. Where no peak occurred beyond the first orifice, the values of P_1/P_t and θ at the first orifice were used to compute $C_{p,\max}$ and δ_{\max} . Where a peak occurred downstream of the first orifice, the faired values were used to compute $C_{p,\max}$ and δ_{\max} .

It should be noted that the data for the 78° parabolic arc body is the least reliable at angles of attack below 15° because the first orifice on the lower surface was inadvertently plugged. At 0° angle of attack the first orifice on the upper surface was used but it was located at an angle of about 8° less than that of the leading edge. At 5° and 10° angle of attack, the second orifice on the lower surface, which was located at an angle of about 12° less than the leading edge, was used. Therefore, the free-stream Mach number computed from the pressures at these orifices for these angles of attack is too high and results in a value of C_p which is too high. It is only this error in Mach number which raises a question as to the reliability of the data for the 78° body.

The maximum error of the measured pressures is believed to be less than 1 percent of the maximum measured value on the body. Model alignment and angles of attack are believed to be accurate to about $\pm 1/2^\circ$. The accuracy of the x, y coordinates of the model orifices is ± 0.001 inch. The measured coordinates were used to compute the slopes for all orifices.

RESULTS AND DISCUSSION

Experimental Results

Basic data.- The pressure distributions of the 78° parabolic arc model with and without extension pieces at $\alpha = -10^\circ$, 0° , and 10° are presented in figure 5 to show the two dimensionality of the flow. Flow blockage prevented any measurements at higher angles of attack; therefore, the agreement between the distributions on the body with and without the extensions establishes only that the flow along the center line of this, the longest, body is two dimensional up to $\alpha = 10^\circ$. However, all other bodies have the same span but are shorter; therefore, the flow along their center line, with the possible exception of the wedges having higher leading-edge angles, should also be two dimensional up to $\alpha = 10^\circ$.

Pressure distributions of the 15 models tested are presented in figures 6, 7, and 8 for angles of attack up to 25° . In addition, schlieren photographs of all the bodies near 0° angle of attack are presented in figure 9 to show the variation of the shock shape with changes in leading-edge angle and body contour.

Maximum pressure coefficient.- One of the most important results of these tests is that stagnation pressure occurs on all of the bodies in this investigation having a leading-edge deflection angle greater than about 51° and that the maximum pressure coefficient for all bodies has its locus along a single representative curve. (See fig. 10.) The portion of the curve between

shock-detachment angle and 51° may be questionable because of the small uncertainty in the value of free-stream Mach number and the inability to locate the first orifice directly at the apex of the nose. However, if the maximum known tunnel Mach numbers were used to compute the pressure coefficients for this portion of the curve, it would shift the deflection angle at which stagnation occurs only about 2° to approximately 49° . In reference 2 stagnation pressure on a flat plate was measured at a deflection angle of 45° . The unrealistic maximum pressure coefficients that are predicted for bodies in this investigation by two modifications to the Newtonian theory are also shown in figure 10 for comparison.

On the upper surface, figure 11 shows that all measured values of $C_{p,\max}$ do not lie along a single curve but vary with leading-edge angle and angle of attack. However, for each leading-edge angle the values of $C_{p,\max}$ for all shapes tested generally fall along the same curve with the exception of the 78° and 90° bodies. As the leading-edge angle increases, the variation of $C_{p,\max}$ with deflection angle approaches that predicted by modified Newtonian theory until at $\delta_{le} = 90^\circ$ the curved-surface bodies agree with this theory.

Location of maximum pressure coefficients.- The location of the maximum pressures would be expected to occur at the point where the slope relative to the flow is the greatest - herein referred to as the geometric location. A comparison of the geometric and measured slopes at which the maximum pressures occurred on both the lower and upper surfaces of the parabolic and circular arc bodies is shown in figure 12. It must be remembered that physical limitations prevented the installation of the first orifice exactly at the leading edge. Therefore, in comparing the measured with the geometric location of $C_{p,\max}$, they will be considered to coincide whenever the measured values differ from the geometric by the same difference as that indicated at 0° angle of attack. On the lower surface (fig. 12(a)) only for the 90° circular arc body do the measured and geometric locations coincide over the angle-of-attack range investigated. For all other bodies the measured location of $C_{p,\max}$ moves off the nose before its angle relative to the flow becomes 90° . This result is attributed to the pressure bleed-off around the sharp leading edge. For bodies having leading-edge angles up to and including 66° , the measured location of $C_{p,\max}$ moves off the nose when its angle relative to the flow becomes approximately 67° . This is also true for the wedges, as can be seen in figures 8(b) to (f). However, the maximum difference between the geometric and measured location for any body through the angle-of-attack range of the tests is only about 8° . On the upper surface the location of the maximum pressure might be expected to remain at the nose over the angle-of-attack range of the test. Figure 12(b) shows this to be true only for the 78° and 90° bodies. For bodies having leading-edge angles below 78° the location of $C_{p,\max}$ is seen to move off the nose at angles of attack less than 20° . This result can be attributed to leading-edge separation around the nose followed by flow reattachment as indicated in figures 6, 7, and 8.

Comparison of center-line pressure distributions on wedges and a flat plate at corresponding deflection angles.- Another important result which can be obtained from these tests is the effect of leading-edge angle on the pressure distributions over the wedge surfaces at a given inclination to the flow. The

lower- and upper-surface pressure distributions, in terms of $C_p/C_{p,\max}$ against s/s_w for wedges at approximately constant surface-deflection angles are presented in figure 13. The surface-deflection angles are only approximately constant because the wedge angles were varied in 12° increments whereas the angle of attack was varied in 5° increments. It can be seen that the maximum pressure point moves rearward on the lower surface with decreasing wedge angle only for deflection angles greater than about 66° and on the upper surface with increasing wedge angle only for deflection angles less than about 66° . The effect of leading-edge angle on wedge surface-pressure distributions is seen to be slight because, with few exceptions, at a given deflection angle, the pressure distributions rearward of the maximum pressure point on the lower and upper surfaces are essentially coincident with those of corresponding surfaces of wedges having higher and lower half-angles, respectively. Thus the wedge-surface pressure distributions are primarily a function only of flow-deflection angles. The effect of leading edge is confined to those regions ahead of the location of the maximum pressure coefficient. Since the value of $C_{p,\max}$ on the lower surface is a constant (as shown in fig. 13), the pressure coefficients aft of the maximum pressure point on the lower surface at a given location of all wedges at the same deflection angles are also coincident. However, on the upper surface the value of $C_{p,\max}$ varies not only with deflection angle but also with wedge angle at the same deflection angle; therefore, the pressure coefficients at a given location on the upper surface of wedges at the same deflection angles are not coincident. It should be noted that at $\delta = 66^\circ$ and above, the distributions on the lower and upper surfaces for the same δ agree. This can be seen from figures 13(a) and 13(b) since the data for each body at $\alpha = 0$ are presented in both.

Also included in figure 13 are flat-plate pressure distributions from reference 2 at approximately the same deflection angles as the wedge surfaces. In general, the pressure distributions of the wedges are in good agreement aft of the maximum pressure point with those of the flat plate at deflection angles of the lower surface above 53° and of the upper surface above 31° . This agreement might not be envisioned since in a subsonic-flow field behind a normal shock, the upper surface would be expected to affect the pressures on the lower surface of the wedge. It is interesting to note that for deflection angles from 27° to 37° the values of $C_{p,\max}$ for the upper surface of wedges at angles of attack other than 0° are about the same as those for a flat plate at corresponding deflection angles.

Prediction of Pressures on Aerodynamically Blunt Bodies

Having obtained the pressure data on these bodies it is of interest to determine if there is a simple method of predicting pressures on two-dimensional aerodynamically blunt bodies. Probably the most widely used method of predicting pressures and forces (because of its simplicity and ease of calculating) is some form of the Newtonian theory

$$C_p = K \sin^2 \delta$$

Various modifications of this theory have been found to give reasonably good predictions of the pressure distribution on different bodies, if the proper value of K is chosen. For example, it is shown in reference 3 that with $K = (\gamma + 1)$, the theory is applicable only to bodies having small leading-edge angles; and in reference 4, with $K = C_p, \text{stag}$, theory is limited to bodies having 90° leading-edge slopes. As can be seen in figure 10, neither of these modifications is applicable to the bodies of this investigation.

A more recent consideration of the Newtonian theory is presented in reference 5 which suggests that in the general case K has the form $\frac{C_{p,\max}}{\sin^2 \delta_{\max}}$, thus acknowledging that K is not necessarily constant. This resulted in the generalized Newtonian theory

$$\frac{C_p}{C_{p,\max}} = \frac{\sin^2 \delta}{\sin^2 \delta_{\max}}$$

which was shown to predict the surface-pressure distribution reasonably well for pointed-nose bodies having a leading-edge angle less than that for shock detachment, as well as for bodies having a 90° leading-edge slope. (Unpublished work also shows that this generalized form of Newtonian theory can be derived by resorting to the tangent-wedge or tangent-cone approximations.) Therefore, it was decided to investigate this method for use in predicting the pressures on the two-dimensional aerodynamically blunt bodies studied herein.

Wedges.- Since the prediction of the pressure distribution for any body by means of the generalized Newtonian theory is basically dependent upon the body having a changing slope, it obviously cannot be applied in the same manner to wedges as to bodies having curved surfaces. However, it is shown in reference 5, that by using pressures computed from attached shock theory, the generalized Newtonian theory is applicable from one wedge to another, for wedge angles less than shock detachment at 0° angle of attack. For the aerodynamically blunt wedges of the present investigation it is apparent from figure 8 that the large and varied pressure gradients require any correlation with generalized Newtonian theory from one wedge to another, or from one surface to another for the same wedge at angle of attack, to be made at more than one point along the surface of the bodies. Even if this could be done with reasonably good results, the pressure distribution of one wedge would first have to be known. In view of the fact that experimental values must be resorted to, and since the data of the present investigation cover the range of aerodynamically blunt wedges, the pressure distribution of any wedge in this regime can be obtained by interpolating these data. In addition, the good agreement in pressure distribution from wedge to wedge at the same deflection angles, as well as the agreement from wedges to a flat plate at corresponding deflection angles (fig. 13), enables the pressure distribution to be obtained for either of the two types of bodies if one is known.

Parabolic and circular arc bodies.- Since the lower and upper surfaces of the bodies of the present investigation are separated by a sharp leading edge, which is shown in figures 6 and 7 to result in flow separation and reattachment

at some angles of attack and, therefore, a difference in the value of K between the two surfaces, the theory might not be expected to apply from surface to surface. Therefore, the data for each surface are reduced in the generalized Newtonian form by using their respective measured $C_{p,\max}$ values. The results for the parabolic and circular arc models together with the generalized Newtonian theory prediction using the measured $C_{p,\max}$ and its associated δ_{\max} are presented in figures 14 and 15.

As can be seen from figures 14 and 15, the data for both the parabolic arc and circular arc bodies can be divided into two distinct correlation groups; bodies having a leading-edge angle closest to that for shock attachment (42° and 54°) and bodies having leading-edge angles much greater than shock attachment (66° to 90°). The data for the former group are not correlated with any consistency by the generalized Newtonian theory, whereas the data of the latter group were in general correlated very well for both surfaces by the theory.

The agreement between the measured and theoretical values in percent of the measured C_p cannot be made directly from figures 14 and 15 because the $C_{p,\max}$ values are not constant for all bodies on either surface. Therefore, a majority of the measured and predicted values of C_p together with their differences in percent of measured C_p are presented in table II. As might be expected the agreement is best near the nose where the body slope is high and becomes progressively poorer as the surface inclination decreases; however, the disagreement does not in general become poorer than about 20 percent of measured C_p down to a surface inclination of 30° (the limit to which modified Newtonian theory is known to predict the pressures very well on cylinders). The very high percentage errors at inclinations below 30° may not be very significant because the pressures are very low over this region. There are points between the nose and the maximum pressure point on both surfaces of some bodies at angle of attack which cannot be predicted by the generalized Newtonian theory because the value of $\frac{\sin^2 \delta}{\sin^2 \delta_{\max}}$ becomes greater than 1. But considering all points above deflection angles of 30° , the theory predicts about 85 percent of them within 10 percent of the measured C_p . It should be noted that whereas the data for the lower surface appear to be in better agreement with the theory than those of the upper surface in figures 14 and 15, table II shows that, on the basis of the percentage of measured C_p , both surfaces show about the same agreement for inclinations above 30° . The agreement for the circular arc bodies was, in general, better than that for the parabolic arc bodies and indicated that for the same leading-edge angle the gradient of slope along the body may be the important factor in determining how well the generalized Newtonian theory predicts the pressure distribution for two-dimensional aerodynamically blunt bodies, that is, the more rapidly the slope changes, the poorer the correlation.

Application of Generalized Newtonian Theory to Any Two-Dimensional
Aerodynamically Blunt Body Having Curved Surfaces

It has been shown that the pressure distributions of the aerodynamically blunt bodies having curved surfaces of the present investigation agree reasonably well with the generalized Newtonian theory. However, in order to use this theory to predict the pressures on any body without resorting to experimentation, it is necessary to know a pressure at a given slope on the surface. Since the measured locations of the maximum pressures are shown in figure 12 to occur reasonably close to the geometric locations and because the maximum pressure on the lower surface is equal to stagnation value for the majority of deflection angles between shock detachment and 90° (fig. 10), it would be convenient to utilize the maximum pressure on the lower surface to predict the pressures over the whole body. An analysis shows that this can be accomplished as follows:

On the lower surface $C_{p,\max} = C_{p,\text{stag}}$ for $\delta_{le} \geq 51^\circ$, while for $\delta < 51^\circ$, $C_{p,\max}$ for deflection angles between 42° and 51° can be obtained from

$$\frac{C_{p,\max}}{C_{p,\text{stag}}} = \frac{\sin^2 \delta_{le}}{\sin^2 51^\circ}$$

The values of $C_{p,\max}$ obtained in this manner for these deflection angles are shown in figure 10 and are in good agreement with the measured values. For deflection angles equal to or less than shock detachment, $C_{p,\max}$ is obtained from oblique shock theory.

The pressure distribution for the lower surface at each angle of attack can then be computed from

$$\frac{C_p}{C_{p,\max}} = \frac{\sin^2 \delta}{\sin^2 \delta_{\max, \text{geom}}}$$

and the pressure distributions for the upper surface can be obtained at any angle of attack from

$$\frac{C_p}{C_{p,\max}(\alpha=0^\circ)} = \frac{\sin^2 \delta}{\sin^2 \delta_{le}(\alpha=0^\circ)}$$

The pressure coefficients predicted by this method for the parabolic and circular arc bodies are presented in table II. In general, these values are about the same as those obtained from the generalized Newtonian theory by using the values of $C_{p,\max}$ at their actual locations on each surface and are within about 20 percent of the measured C_p at deflection angles above 30° . Some of the points between the nose and the actual location of the maximum pressure point, which could not be predicted by the generalized Newtonian theory by using $C_{p,\max}$ at

its actual location for each surface, are not predicted by this method within this accuracy. However, on the whole, about 85 percent of all points at deflection angles above 30° are predicted within 10 percent of the measured C_p value.

The good agreement between the generalized Newtonian theory and the data of the present investigation as well as the results for bodies having a leading-edge angle less than that for shock detachment in reference 5 indicate that this theory may be applicable to all two-dimensional bodies except aerodynamically blunt wedges.

CONCLUSIONS

An investigation of the center-line pressure distributions on two-dimensional sharp-nose bodies having a leading-edge angle greater than that for shock detachment at a Mach number of 6 and angles of attack up to 25° has resulted in the following conclusions:

1. Stagnation pressure behind a normal shock was measured on all bodies having a leading-edge deflection angle greater than about 51° and the maximum pressure coefficient for all bodies has its locus along a single representative curve which continuously increases with increasing deflection angle between shock detachment and about 51° .
2. With few exceptions the center-line pressure distributions rearward of the maximum pressure point on the lower and upper surfaces of aerodynamically blunt wedges are primarily a function only of surface-deflection angle and essentially independent of leading-edge angle. In addition, the pressure distributions of these wedges are in good agreement aft of the maximum pressure point with those of a flat plate at corresponding deflection angles to the lower surface above 53° and to the upper surface above 31° .
3. Only the data for contoured bodies having leading-edge angles of 66° or greater are correlated very well by the generalized Newtonian theory. However, at all angles of attack for all aerodynamically blunt bodies having curved surfaces, the agreement between the generalized Newtonian theory and the measured values of C_p was reasonably good for surface-deflection angles above 30° (for 85 percent of the points in this region the theoretical values of C_p were within 10 percent of the measured C_p).
4. The generalized Newtonian theory can be used to predict the center-line pressures on aerodynamically blunt contoured bodies because the maximum pressures and their locations can be predetermined.

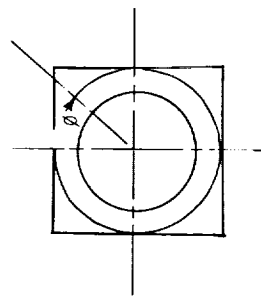
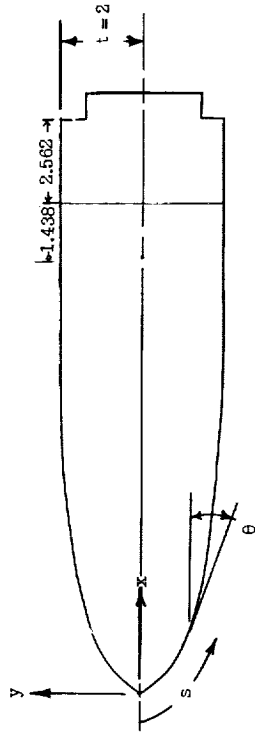
Langley Research Center,
National Aeronautics and Space Administration,
Langley Station, Hampton, Va., February 27, 1963.

REFERENCES

1. Ashby, George C., Jr., and Fitzgerald, Paul E., Jr.: Longitudinal Stability and Control Characteristics of Missile Configurations Having Several Highly Swept Cruciform Fins and a Number of Trailing-Edge and Fin-Tip Controls at Mach Numbers From 2.21 to 6.01. NASA TM X-335, 1961.
2. Hondros, James G.: Pressure Distributions on Two-Dimensional Sharp-Leading-Edge Flat Plates With Sweep Angles of 0° , 30° , and 45° at a Mach Number of 6 and Angles of Attack From 0° to 90° . NASA TN D-1371, 1962.
3. Laitone, Edmund V.: Exact and Approximate Solutions of Two-Dimensional Oblique Shock Flow. Jour. Aero. Sci., vol. 14, no. 1, Jan. 1947, pp 25-41.
4. Lees, Lester: Hypersonic Flow. Fifth International Aeronautical Conference (Los Angeles, Calif., June 20-23, 1955), Inst. Aero. Sci., Inc., 1955, pp 241-276.
5. Love, E. S.: Generalized-Newtonian Theory. Jour. Aero/Space Sci. (Reader's Forum), vol. 26, no. 5, May 1959, pp. 314-315.

TABLE I - MODEL DIMENSIONS AND ORIFICE LOCATIONS

(a) Parabolic arc models



42° parabolic arc					
Orifice location	Slope θ, deg	s/t	θ/t	ϕ, deg	
x, in.	y, in.	x, in.	y, in.	x, in.	
0.067	-0.060	41.25	0.045	180	
.226	-1.196	59.44	.149		
.407	-1.342	37.46	.265		
.565	-1.457	35.80	.363		
.726	-1.568	34.15	.448		
1.227	-1.886	29.35	.756		
1.512	-1.035	26.80	.918		
1.861	1.199	23.88	1.130		
2.455	1.359	20.82	1.324		
2.698	1.512	17.66	1.558		
3.829	1.782	10.75	2.142		
4.306	1.875	8.26	2.385		
4.774	1.933	6.02	2.619		
5.241	1.975	3.97	2.854		
5.720	1.999	2.03	3.093		
6.999	2.000	0	3.133		
.172	-1.18	40.0	.114		
.282	-2.26	38.42	.185		
.412	-3.38	37.41	.268		
.571	-1.56	35.75	.320		
.730	-1.59	34.11	.464		
.968	-1.725	31.76	.606		
1.226	-1.877	29.44	.755		
1.518	-1.034	26.90	.921		
1.862	-1.197	23.87	1.111		
2.257	-1.359	20.81	1.325		
2.702	-1.512	17.64	1.560		
3.836	-1.794	10.71	2.113		
4.305	-1.873	8.26	2.383		
4.776	-1.932	6.01	2.620		
5.242	-1.972	3.97	2.854		
5.718	-1.994	2.05	3.092		
6.174	-2.000	.35	3.321		
6.431	-2.000	0	3.449		

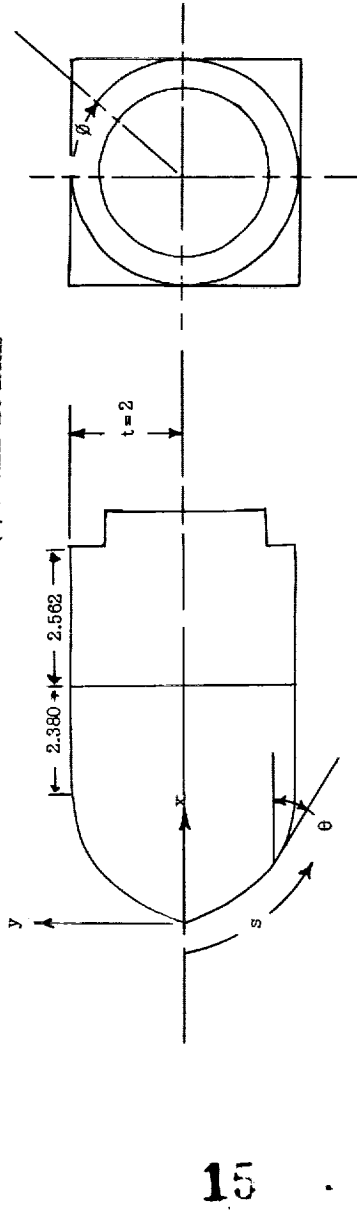
54° parabolic arc					
Orifice location	Slope θ, deg	s/t	θ/t	ϕ, deg	
x, in.	y, in.	x, in.	y, in.	x, in.	
0.036	-0.052	23.04	0.030	180	
.140	-1.180	50.39	.114		
.275	-1.332	47.21	.217		
.415	-1.416	44.12	.317		
.630	-1.554	40.21	.448		
1.227	-1.886	26.80	.755		
1.512	-1.035	26.80	.755		
1.861	1.199	23.88	1.130		
2.455	1.359	20.82	1.324		
2.698	1.512	17.66	1.558		
3.829	1.782	10.75	2.142		
4.306	1.875	8.26	2.385		
4.774	1.933	6.02	2.619		
5.241	1.975	3.97	2.854		
5.720	1.999	2.03	3.093		
6.999	2.000	0	3.133		
.172	-1.18	40.0	.114		
.282	-2.26	38.42	.185		
.412	-3.38	37.41	.268		
.571	-1.56	35.75	.320		
.730	-1.59	34.11	.464		
.968	-1.725	31.76	.606		
1.226	-1.877	29.44	.755		
1.518	-1.034	26.90	.921		
1.862	-1.197	23.87	1.111		
2.257	-1.359	20.81	1.325		
2.702	-1.512	17.64	1.560		
3.836	-1.794	10.71	2.113		
4.305	-1.873	8.26	2.383		
4.776	-1.932	6.01	2.620		
5.242	-1.972	3.97	2.854		
5.718	-1.994	2.05	3.092		
6.174	-2.000	.35	3.321		
6.431	-2.000	0	3.449		

66° parabolic arc					
Orifice location	Slope θ, deg	s/t	θ/t	ϕ, deg	
x, in.	y, in.	x, in.	y, in.	x, in.	
0.026	-0.058	64.19	0.021	180	
.102	-1.202	29.35	.114		
.293	-1.468	20.37	.278		
.660	-1.829	16.23	.360		
1.066	-1.051	21.22	.732		
1.446	-1.291	23.26	.992		
2.152	-1.521	16.54	1.359		
3.049	-1.761	10.35	1.829		
4.092	-1.910	5.90	2.355		
4.612	-1.98	4.16	2.616		
5.129	-1.967	2.69	2.854		
5.659	-1.98	1.967	3.093		
6.197	-1.98	1.38	3.150		
6.735	-1.98	0.76	3.156		
7.273	-1.98	0.25	3.159		
7.811	-1.98	0	3.162		
8.349	-1.98	0	3.165		
8.887	-1.98	0	3.168		
9.425	-1.98	0	3.171		
9.963	-1.98	0	3.174		
10.500	-1.98	0	3.177		
11.037	-1.98	0	3.180		
11.574	-1.98	0	3.183		
12.111	-1.98	0	3.186		
12.648	-1.98	0	3.189		
13.185	-1.98	0	3.192		
13.722	-1.98	0	3.195		
14.259	-1.98	0	3.198		
14.796	-1.98	0	3.201		
15.333	-1.98	0	3.204		
15.870	-1.98	0	3.207		
16.407	-1.98	0	3.210		
16.944	-1.98	0	3.213		
17.481	-1.98	0	3.216		
18.018	-1.98	0	3.219		
18.555	-1.98	0	3.222		
19.092	-1.98	0	3.225		
19.629	-1.98	0	3.228		
20.166	-1.98	0	3.231		
20.703	-1.98	0	3.234		
21.239	-1.98	0	3.237		
21.776	-1.98	0	3.240		
22.313	-1.98	0	3.243		
22.850	-1.98	0	3.246		
23.387	-1.98	0	3.249		
23.924	-1.98	0	3.252		
24.461	-1.98	0	3.255		
24.998	-1.98	0	3.258		
25.535	-1.98	0	3.261		
26.072	-1.98	0	3.264		
26.609	-1.98	0	3.267		
27.146	-1.98	0	3.270		
27.683	-1.98	0	3.273		
28.220	-1.98	0	3.276		
28.757	-1.98	0	3.279		
29.294	-1.98	0	3.282		
29.831	-1.98	0	3.285		
30.368	-1.98	0	3.288		
30.905	-1.98	0	3.291		
31.442	-1.98	0	3.294		
31.979	-1.98	0	3.297		
32.516	-1.98	0	3.300		
33.053	-1.98	0	3.303		
33.590	-1.98	0	3.306		
34.127	-1.98	0	3.309		
34.664	-1.98	0	3.312		
35.201	-1.98	0	3.315		
35.738	-1.98	0	3.318		
36.275	-1.98	0	3.321		
36.812	-1.98	0	3.324		
37.349	-1.98	0	3.327		
37.886	-1.98	0	3.330		
38.423	-1.98	0	3.333		
38.960	-1.98	0	3.336		
39.497	-1.98	0	3.339		
40.034	-1.98	0	3.342		
40.571	-1.98	0	3.345		
41.108	-1.98	0	3.348		
41.645	-1.98	0	3.351		
42.182	-1.98	0	3.354		

78° parabolic arc					
Orifice location	Slope θ, deg	s/t	θ/t	ϕ, deg	
x, in.	y, in.	x, in.	y, in.	x, in.	
0.015	-0.069	73.95	0.031	180	
.052	-1.164	66.82	-.086		
.108	-1.267	59.79	-.148		
.206	-1.615	59.79	-.375		
.277	-1.862	58.87	-.599		
.339	-1.701	51.104	-.215		
.401	-1.309	41.74	1.272		
.463	-1.224	40.61	1.48		
.525	-1.147	39.53	1.725		
.587	-1.074	38.46	1.974		
.650	-1.007	37.39	2.120		
.713	-1.040	36.32	2.265		
.776	-1.073	35.25	2.410		
.839	-1.104	34.18	2.555		
.892	-1.135	33.11	2.699		
.945	-1.166	32.04	2.844		
.998	-1.197	30.97	3.089		
1.050	-1.228	29.90	3.234		
1.113	-1.260	28.83	3.379		
1.177	-1.291	27.76	3.524		
1.241	-1.322	26.69	3.669		
1.305	-1.353	25.62	3.814		
1.369	-1.384	24.55	3.959		
1.433	-1.415	23.48	4.104		
1.497	-1.446	22.41	4.249		
1.561	-1.477	21.34	4.393		
1.625	-1.508	20.27	4.538		
1.689	-1.539	19.20	4.682		
1.753	-1.570	18.13	4.821		
1.817	-1.601	17.06	4.959		
1.881	-1.632	15.99	5.098		
1.945	-1.663	14.92	5.238		
2.009	-1.704	13.85	5.377		
2.073	-1.735	12.78	5.516		
2.137	-1.766	11.71	5.655		
2.191	-1.807	10.64	5.794		
2.255	-1.848	9.57	5.933		
2.319					

TABLE I. - MODEL DIMENSIONS AND ORIFICE LOCATIONS - Continued

(b) Circular arc models



42° circular arc			
Orifice location x_1 , in.	Y, in.	Slope θ , deg	s/t
x_1 , in.	y_1 , in.	x_2 , in.	y_2 , in.
0.082	-0.075	41.19	0.056
.203	-1.179	40.01	0.040
.278	-2.259	59.30	.136
.461	-3.99	51.41	.180
.675	-5.42	35.63	.197
.979	-7.51	32.91	.195
1.226	-9.06	30.77	.164
1.488	-1.053	28.76	.913
1.979	-1.425	26.51	1.188
2.27	-1.425	22.19	1.345
3.036	-1.490	16.21	1.752
3.567	-1.823	12.18	2.022
4.082	-1.918	8.35	2.289
4.609	-1.980	4.42	2.575
5.121	-1.997	0.66	2.719
6.212	-1.998	0	3.293
1.162	-1.39	10.15	0
.287	-2.43	39.24	.887
.363	-3.05	38.51	.236
.592	-4.80	36.39	.380
.747	-5.92	34.99	.416
.979	-7.49	32.92	.616
1.233	-9.10	30.71	.758
1.383	-1.104	27.76	.967
1.979	-1.298	24.51	1.188
2.273	-1.424	22.16	1.347
3.037	-1.690	16.20	1.751
3.567	-1.823	12.18	2.022
4.083	-1.919	8.32	2.282
4.609	-1.982	4.42	2.586
5.127	-1.997	0.66	2.718
5.410	-1.999	0	2.879

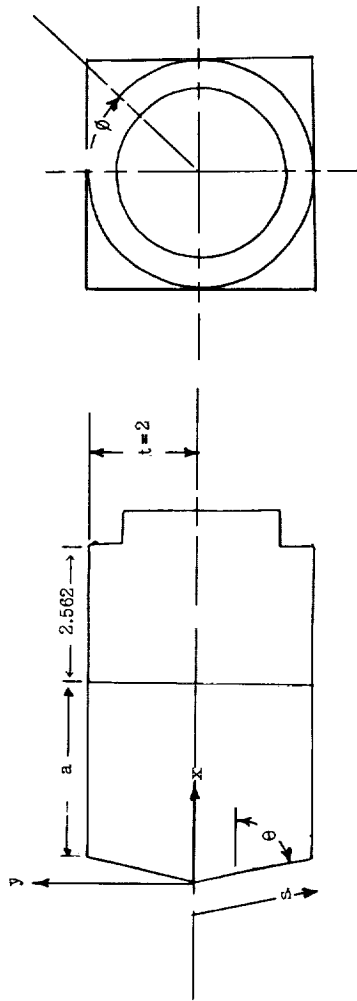
54° circular arc			
Orifice location x_1 , in.	Y, in.	Slope θ , deg	s/t
x_1 , in.	y_1 , in.	x_2 , in.	y_2 , in.
0.046	-0.064	53.07	0.040
.117	-1.154	51.71	.136
.195	-2.47	50.29	.180
.302	-3.70	48.36	.237
.422	-5.20	46.27	.356
.538	-6.19	44.31	.409
.721	-7.89	41.56	.525
1.149	-9.73	37.96	.679
1.979	-1.27	34.91	.880
2.27	-1.425	22.19	1.345
3.036	-1.490	16.21	1.752
3.567	-1.823	12.18	2.022
4.082	-1.918	8.35	2.289
4.609	-1.980	4.42	2.575
5.121	-1.997	0.66	2.719
6.212	-1.998	0	3.293
1.162	-1.39	10.15	0
.287	-2.43	39.24	.887
.363	-3.05	38.51	.236
.592	-4.80	36.39	.380
.747	-5.92	34.99	.416
.979	-7.49	32.92	.616
1.233	-9.10	30.71	.758
1.383	-1.104	27.76	.967
1.979	-1.298	24.51	1.188
2.273	-1.424	22.16	1.347
3.037	-1.690	16.20	1.751
3.567	-1.823	12.18	2.022
4.083	-1.919	8.32	2.282
4.609	-1.982	4.42	2.586
5.127	-1.997	0.66	2.718
5.410	-1.999	0	2.879

90° circular arc			
Orifice location x_1 , in.	Y, in.	Slope θ , deg	s/t
x_1 , in.	y_1 , in.	x_2 , in.	y_2 , in.
0.001	-0.003	89.91	0.001
.002	-0.073	87.90	.036
.011	-1.10	84.53	.095
.028	-3.23	80.71	.162
.056	-4.61	76.64	.232
.089	-5.82	73.06	.295
.134	-7.14	59.05	.365
.185	-8.97	53.31	.465
.279	-1.014	39.47	.532
.375	-1.156	34.59	.616
.503	-1.322	24.44	.722
.611	-1.538	14.00	.802
.822	-1.614	36.11	.939
1.523	-1.910	13.80	1.326
1.929	-1.996	2.04	1.307
3.004	-2.000	0	2.045
3.470	-1.999	0	2.207
3.790	-1.952	42.90	.722
.907	-1.506	36.39	.917
1.174	-1.644	30.85	1.042
2.012	-1.968	9.06	1.521
2.366	-1.997	1.89	1.665
3.470	-1.999	0	2.207
3.094	-2.024	75.11	.044
.056	-2.18	72.59	.114
.167	-3.19	70.46	.138
.457	-4.56	67.10	.241
.584	-5.91	51.11	.261
.205	-2.96	71.44	.648
.351	-3.85	71.44	.716
.098	-1.24	75.11	.461
.544	-4.45	57.11	.489
.544	-1.076	65.13	.085
.597	-1.190	53.40	.637
.042	-2.75	87.75	.196
.505	-1.322	48.51	.722
.071	-5.18	74.05	.261
.112	-1.39	44.02	.803
.826	-1.614	36.02	.939
1.152	-1.638	31.47	1.324
2.039	-1.964	9.82	1.324
2.573	-1.997	2.17	1.503
2.678	-1.999	0	1.643

78° circular arc			
Orifice location x_1 , in.	Y, in.	Slope θ , deg	s/t
x_1 , in.	y_1 , in.	x_2 , in.	y_2 , in.
0.004	-0.042	77.04	0.023
.022	-1.28	75.05	.068
.047	-2.14	73.02	.112
.089	-3.59	70.27	.173
.208	-5.99	63.57	.319
.271	-7.22	60.59	.389
.302	-8.99	55.10	.493
.493	-1.051	51.43	.588
.597	-1.171	47.83	.667
.790	-1.325	42.90	.722
.907	-1.506	36.39	.802
1.174	-1.644	30.85	1.042
2.012	-1.968	9.06	1.521
2.366	-1.997	1.89	1.665
3.470	-1.999	0	2.207
3.094	-2.024	75.11	.044
.056	-2.18	72.59	.114
.167	-3.19	70.46	.138
.457	-4.56	67.10	.241
.584	-5.91	51.11	.261
.205	-2.96	71.44	.648
.351	-3.85	71.44	.716
.098	-1.24	75.11	.461
.544	-4.45	57.11	.489
.544	-1.076	65.13	.085
.597	-1.190	53.40	.637
.042	-2.75	87.75	.196
.505	-1.322	48.51	.722
.071	-5.18	74.05	.261
.112	-1.39	44.02	.803
.826	-1.614	36.02	.939
1.152	-1.638	31.47	1.324
2.039	-1.964	9.82	1.324
2.573	-1.997	2.17	1.503
2.678	-1.999	0	1.643

TABLE I. - MODEL DIMENSIONS AND ORIFICE LOCATIONS - Concluded

(c) Wedge models



45° wedge						
Orifice location		Slope θ, deg	s/t	ϕ, deg	Orifice location	
x, in.	y, in.	x, in.	y, in.	θ, deg	x, in.	y, in.
0.054	-0.048	42.00	0.036	180	0.046	-0.063
.203	-1.183		1.136		.251	-1.181
.357	-1.321	2.00			.251	-1.318
.439	-1.413		1.008		.270	-1.438
.573	-1.516		.586		.410	-1.565
.761	-1.684		.512		.560	-1.711
.944	-1.850		.635		.704	-1.970
1.125	-1.012		.756		.934	-1.285
1.320	-1.188		.888		1.037	-1.428
1.498	-1.319		1.008		1.146	-1.579
1.667	-1.518		1.134		1.406	-1.936
2.145	-1.931		1.443		2.448	-2.000
3.216	-2.000	0	1.992	0	.099	-1.957
4.149	-1.134	42.00	.100		.164	.226
5.296	-1.290		.172		.231	.318
6.641	-1.358		.245		.321	.416
7.476	-1.488		.320		.417	.514
7.775	-1.517		.386		.564	.777
7.65	-1.689		.514		.714	.982
9.119	-1.955		.638		.932	1.284
1.141	-1.027		.767		1.042	1.435
1.326	-1.192		.891		1.146	1.531
1.510	-1.358		1.015		1.412	1.944
1.691	-1.523		1.015		2.159	1.941
2.417	-2.000	0	1.592		2.417	2.000

60° wedge						
Orifice location		Slope θ, deg	s/t	ϕ, deg	Orifice location	
x, in.	y, in.	x, in.	y, in.	θ, deg	x, in.	y, in.
0.025	-0.057	66.00	0.031	180	0.025	-0.011
.077	-1.172		.169		.061	-1.258
.138	-1.309		.198		.255	-1.574
.270	-1.445		.255		.359	-1.865
.410	-1.565		.349		.512	-2.177
.560	-1.711		.411		.653	-2.449
.704	-1.970		.493		.757	-2.768
.934	-1.285		.572		.822	-3.030
1.037	-1.428		.632		.874	-3.297
1.146	-1.579		.691		.923	-3.551
1.406	-1.936		.748		1.422	-2.000
2.448	-2.000	0	1.592		.062	.102
.046	-1.995	0	1.592		.094	.210
1.876	-2.000	0	1.592		.115	.320
.046	-1.922	0	1.592		.164	.418
1.422	-2.000	0	1.592		.200	.533
.046	-1.915	0	1.592		.200	.677
.995	-2.000	0	1.592		.112	.790
.000	.112	0	1.592		.200	.938

75° wedge						
Orifice location		Slope θ, deg	s/t	ϕ, deg	Orifice location	
x, in.	y, in.	x, in.	y, in.	θ, deg	x, in.	y, in.
0.025	-0.057	78.00	0.005	180	0.025	-0.011
.067	-1.172		.169		.061	-1.258
.117	-1.411		.198		.255	-1.768
.219	-1.530		.314		.359	-2.045
.371	-1.829		.411		.457	-2.322
.526	-2.000		.493		.589	-2.595
.676	-2.000	0	1.592		.727	-2.888
.779	-2.000	0	1.592		.822	-3.224
.874	-2.000	0	1.592		.923	-3.584
.968	-2.000	0	1.592		1.022	-3.945
1.062	-2.000	0	1.592		1.120	-4.200
1.155	-2.000	0	1.592		1.214	-4.561
.106	.106	0	1.592		.200	.533
.094	.210	0	1.592		.200	.677
.136	.304		1.592		.200	.822
.190	.403		1.592		.200	.968
.234	.506		1.592		.200	1.120
.286	.597		1.592		.200	1.274
.335	.696		1.592		.200	1.428
.386	.796		1.592		.200	1.582
.436	.895		1.592		.200	1.736
.482	.995		1.592		.200	1.889
.526	.1095		1.592		.200	2.042
.576	.1195		1.592		.200	2.196
.622	.1295		1.592		.200	2.349

90° wedge						
Orifice location		Slope θ, deg	s/t	ϕ, deg	Orifice location	
x, in.	y, in.	x, in.	y, in.	θ, deg	x, in.	y, in.
0.000	0.000	90.00	0.000	180	0.000	0.000
.109	-1.109		.169		.109	-1.000
.218	-1.218		.255		.218	-1.100
.314	-1.314		.359		.314	-1.157
.419	-1.419		.457		.419	-1.224
.516	-1.516		.564		.516	-1.248
.612	-1.612		.660		.612	-1.296
.714	-1.714		.757		.714	-1.348
.812	-1.812		.854		.812	-1.472
.911	-1.911		.951		.911	-1.595
.995	-2.000	0	1.592		.995	-2.000
.109	.109	0	1.592		.109	.109

a = 3.515

a = 2.625

a = 1.438

15

TABLE II. - MEASURED AND THEORETICAL VALUES OF PRESSURE COEFFICIENTS FOR
TWO-DIMENSIONAL AERODYNAMICALLY BLUNT BODIES

(a) Parabolic arc bodies - lower surface

a, deg	b, deg	$\theta_{le} = 42^\circ$				$\theta_{le} = 54^\circ$				$\theta_{le} = 66^\circ$									
		C_p , meas		C_p	C_p , meas - C_p	C_p , meas - C_p		C_p	C_p	C_p , meas - C_p	C_p , meas - C_p	C_p	C_p , meas - C_p						
		(a)	(b)	(a)	(b)	(a)	(b)	(a)	(b)	(a)	(b)	(a)	(b)						
0	41.232	1.2822	1.2822	1.2441	0	0.02971	0	53.041	1.8182	1.8178	1.7734	0.00022	0.02464						
39.441	1.1226	1.1908	1.1951	-0.06075	-0.02913	50.391	1.6148	1.5897	1.6484	-0.04638	59.336	1.6746	1.6600						
55.800	0.93906	1.0099	0.97988	-0.07543	-0.04347	44.120	1.2832	1.3799	1.3462	-0.07536	50.375	1.3699	1.3303						
59.332	0.65852	0.70248	0.68158	-0.06676	-0.03502	40.217	1.0888	1.1872	1.1581	-0.09058	46.236	1.1989	1.1697						
26.800	5.7012	6.0001	5.8214	-0.05243	-0.02108	36.920	0.94213	1.0273	1.0022	-0.09040	38.334	0.9165	0.86261						
23.884	1.6761	1.8380	1.46940	-0.04642	-0.00783	31.892	0.73125	0.79519	0.77575	-0.08744	31.229	0.6833	0.63035						
10.752	1.1409	1.0268	0.99961	-0.07339	-0.03070	27.229	0.55603	0.59362	0.58173	-0.07246	23.969	0.44057	0.37007						
3.976	0.5815	0.0426	0.01582	-0.74777	-0.76334	17.108	0.27568	0.36260	0.24018	-0.10694	16.548	0.28111	0.18199						
0	0.01764	0	1.0000	1.0000	0	9.546	1.30404	0.07840	0.07647	-0.39939	5.907	0.08221	0.02301						
5	46.232	1.6314	1.6314	1.5906	0	0.02901	5	58.041	1.8181	1.8174	1.7805	0.00017	0.02047	5	69.196	1.8179	1.8177	1.7767	-0.00006
14.141	1.4099	1.5352	1.4949	-0.09210	-0.06882	55.391	1.6719	1.7303	1.6756	-0.02114	64.396	1.7371	1.6902	0.02700					
40.800	1.1608	1.3357	1.3022	-0.15067	-0.12181	55.391	1.4364	1.4134	1.4131	-0.05598	55.375	1.4719	1.4082	0.04388					
34.332	0.83187	0.99511	0.97021	-0.19623	-0.16630	49.120	1.3674	1.3434	1.3433	-0.04960	51.236	1.3232	1.2645	0.04436					
31.800	0.7230	0.86866	0.84692	-0.20590	-0.17972	45.218	1.1874	1.2721	1.2463	-0.07007	43.334	1.0450	0.97924	0.05690					
26.884	0.60192	0.72989	0.71163	-0.21260	-0.18227	41.920	0.9532	1.1270	1.1041	-0.07007	36.229	0.7946	0.71030	0.08488					
15.753	0.22472	0.23048	0.24743	-0.02563	-0.00004	36.894	0.84881	0.91325	0.89185	-0.06267	28.969	0.55118	0.47896	0.11488					
8.979	0.10756	0.07627	0.07436	0.29091	0.30666	32.229	0.66266	0.71836	0.70578	-0.06002	15.534	0.20918	0.14917	0.26688					
5.000	0.05117	0.01523	0.01485	0.70236	0.70979	27.271	0.50222	0.55000	0.51926	-0.03393	9.165	0.10317	0.05278	0.09097					
10	46.232	1.8190	1.8190	1.7609	0	0.02995	10	49.120	1.8182	1.8182	1.7882	0.00016	0.01666	10	74.196	1.8187	1.8187	1.7885	-0.02250
19.141	1.5955	1.7367	1.6904	-0.08223	-0.05468	5.000	0.01534	0.19199	0.01880	-0.25098	69.356	1.8069	1.7528	1.6915	0.02994	0.08687			
45.800	1.3571	1.5379	1.5056	-0.15018	-0.12602	50.391	1.2056	1.2717	1.2674	-0.02059	60.375	1.5978	1.5123	1.4595	0.05351	0.08696			
39.332	0.86966	1.2021	1.1768	-0.21922	-0.19356	50.391	1.0908	1.1711	1.1674	-0.02059	56.236	1.4658	1.3833	1.3350	0.05199	0.08799			
36.800	0.86787	1.0737	1.0511	-0.23717	-0.21088	60.391	1.7524	1.7299	1.7013	-0.01284	48.334	1.1946	1.1171	1.0760	0.06488	0.09706			
33.384	0.7344	0.93000	0.92046	-0.23958	-0.21312	54.120	1.4905	1.5026	1.4777	-0.00812	50.217	1.3295	1.30745	1.2645	0.05167	0.11267			
27.567	0.50660	0.64511	0.63156	-0.23741	-0.21466	50.217	1.3295	1.3517	1.3294	-0.00670	45.229	1.2299	1.19483	1.16485	0.05054	0.10520			
16.029	0.23390	0.28285	0.23345	-0.06709	-0.04165	46.920	1.1924	1.2210	1.2008	-0.02399	41.229	0.9483	0.82124	0.76558	0.03535	0.09611			
10.000	0.09771	0.07321	0.07169	-0.25074	-0.26630	41.892	0.85124	0.9209	0.84753	-0.02853	10.000	0.03693	0.01581	0.05160	0.07189	0.22654			
15	56.232	1.8186	1.8186	1.7868	0	0.01749	15	63.041	1.8185	1.8182	1.7882	0.00016	0.01666	15	74.196	1.8187	1.8187	1.7885	-0.02163
54.141	1.5716	1.7113	1.7108	-0.04170	-0.02845	57.107	1.7119	1.7450	1.7119	-0.00747	64.396	1.8069	1.7528	1.6915	0.02994	0.08687			
50.800	1.1362	1.5804	1.5827	-0.10040	-0.08112	56.236	1.2056	1.2678	1.2093	-0.00920	50.375	1.5978	1.5123	1.4595	0.05351	0.08696			
44.332	0.9904	1.2052	1.2027	-0.17007	-0.14958	50.391	1.1871	1.2093	1.1871	-0.00920	56.236	1.4658	1.3833	1.3350	0.05199	0.08799			
41.800	0.98350	1.1691	1.1487	-0.16797	-0.14797	50.391	1.16797	1.2093	1.16797	-0.00920	50.375	1.3295	1.2576	1.2020	0.05160	0.08687			
38.884	0.86305	1.0188	0.20155	-0.21055	-0.16797	48.229	1.8176	1.7890	1.7236	-0.03955	48.334	1.6074	1.5402	1.4658	0.04688	0.08665			
32.667	0.62216	0.76667	0.73235	-0.25227	-0.21070	56.236	1.2056	1.2719	1.2153	-0.02059	56.236	1.4658	1.4323	1.38926	0.05008	0.08797			
29.753	0.40783	0.49670	0.48800	-0.21791	-0.19558	50.391	1.1658	1.2188	1.1658	-0.03431	50.375	1.3295	1.2576	1.1993	0.05126	0.11267			
18.978	0.24477	0.27848	0.27361	-0.13772	-0.11782	55.217	1.3219	1.3519	1.3140	-0.00683	54.334	1.2359	1.2516	1.1933	0.05141	0.10461			
15.000	0.15212	0.15133	0.15133	-0.01262	-0.00519	51.920	1.3319	1.3519	1.3140	-0.02629	51.920	1.2099	1.2299	1.1915	0.03535	0.09537			
20	61.232	1.8170	1.8170	1.7909	0	0.01436	20	68.041	1.8089	1.7936	1.7936	0.00846	0.01762	20	79.196	1.7931	1.7931	1.7936	-0.02163
59.441	1.7523	1.7532	1.7279	-0.00051	-0.01392	57.272	1.7761	1.7566	1.7279	-0.0172	64.396	1.8184	1.8038	1.7284	0.00803	0.04949			
55.800	1.5496	1.6176	1.5943	-0.04388	-0.03885	52.107	1.59270	1.6122	1.58888	-0.03125	66.236	1.6861	1.6074	1.5402	0.04688	0.08665			
49.332	0.23252	0.35051	0.34049	-0.10144	-0.08557	24.546	1.59243	1.59243	1.59243	-0.01425	61.236	1.4741	1.4323	1.38926	0.05008	0.08797			
46.800	0.1192	0.2966	0.2966	-0.12277	-0.10659	19.219	1.46511	1.46511	1.46511	-0.01406	50.375	1.3295	1.2576	1.1993	0.05126	0.11267			
43.884	0.06062	0.1363	0.1199	-0.12930	-0.11300	15.000	1.4102	1.4102	1.4102	-0.02629	50.375	1.2099	1.2299	1.1915	0.03535	0.09537			
37.667	0.75410	0.88297	0.87027	-0.17089	-0.15405	42.229	0.95199	0.97791	0.9217	-0.02917	42.229	0.83585	0.76935	0.73718	0.07956	0.11805			
30.753	0.52493	0.6818	0.60929	-0.15563	-0.13901	50.391	1.81771	1.81771	1.7454	-0.0172	56.236	1.8184	1.8038	1.7284	0.00803	0.04949			
26.026	0.39756	0.45550	0.44896	-0.14747	-0.12929	37.107	1.72789	1.74533	1.71577	-0.02396	56.236	1.6856	1.6000	1.5305	0.05078	0.09225			
20.000	0.24067	0.25064	0.24702	-0.04143	-0.02638	29.546	1.4774	1.48287	1.47847	-0.01428	50.375	1.3295	1.2576	1.1993	0.05126	0.11267			
25	66.232	1.8187	1.8187	1.7978	0	0.01149	25	78.041	1.7869	1.7854	1.7797	0.00011	0.02682	25	79.196	1.7868	1.7868	1.7864	-0.02163
64.441	1.8138	1.7902	1.7466	-0.01301	-0.03705	75.391	1.7817	1.7817	1.7454	-0.01712	75.391	1.7375	1.6871	1.6205	0.04103	0.08696			
60.800	1.6619	1.6763	1.6335	-0.08666	-0.01589	47.229	1.0883	1.1040	1.0502	-0.01713	58.334	1.4741	1.3833	1.3233	0.05126	0.10320			
54.332	1.3774	1.4526	1.4167	-0.08516	-0.02853	42.229	1.91303	1.9266	1.88989	-0.01942	50.375	1.3295	1.2576	1.1993	0.05126	0.11218			
51.800	1.2632	1.3786	1.3275	-0.07552	-0.04932	37.107	1.72789	1.74533	1.71577	-0.02396	50.375	1.2099	1.2299	1.1915	0.03535	0.09537			
48.800	1.1890	1.2486	1.2182	-0.06668	-0.06023	29.546	1.4774	1.48287	1.47847	-0.01428	50.375	1.1687	1.1887	1.1306	0.04222	0.07463			
42.667	0.88970	0.9105	0.95888	-0.11378	-0.10810	24.219	1.34337	1.34465</											

TABLE II. - MEASURED AND THEORETICAL VALUES OF PRESSURE COEFFICIENTS FOR
TWO-DIMENSIONAL AERODYNAMICALLY BIJNT BODIES - Continued

(a) Parabolic arc bodies - lower surface - Concluded

$\theta_{le} = 78^\circ$									$\theta_{le} = 90^\circ$									
α , deg	δ , deg	C_p ,meas	C_p	C_p	C_p ,meas - C_p		C_p ,meas - C_p		α , deg	δ , deg	C_p ,meas	C_p	C_p	C_p ,meas - C_p		C_p ,meas - C_p		
					C_p ,meas	C_p	C_p ,meas	C_p						C_p ,meas	C_p	C_p ,meas	C_p	
0	70.560	1.8192	1.8192	1.6909	0	0.07053	0	0.07053	0	89.633	1.8183	1.8182	0	0	0.00011	0	0.00011	
66.612	1.7205	1.7236	1.6018	-.00180	.06899	83.508	1.7951	1.7950	.00217	77.797	1.7330	1.7372	1.7371	1.7371	.00222	1.7371	.00222	
59.517	1.5597	1.5195	1.4122	.02577	.09457	77.797	1.7330	1.7372	1.7371	61.219	1.6129	1.6144	1.6144	1.6144	-.00242	1.6144	-.00237	
39.792	.95817	.83825	.77900	.12516	.18699	70.137	1.4225	1.3968	1.3967	61.219	1.4225	1.3968	1.3967	1.3967	-.00093	1.3967	-.00093	
28.875	.60391	.47732	.41358	.20962	.26549	44.181	1.0019	.89279	.89275	44.181	1.0019	.89279	.89275	.89275	.01807	.01814	.01814	
20.759	.38482	.25718	.23899	.33169	.37836	32.221	.63411	.51682	.51680	32.221	.63411	.51682	.51680	.51680	.18654	.18500	.18500	
14.743	.23748	.13260	.12323	.44164	.48109	25.646	.46671	.34073	.34073	19.168	.30430	.19599	.19599	.19599	.26993	.26993	.26993	
9.470	.13178	.05538	.02019	.57975	.84679	5.121	.06340	.01446	.01446	12.935	.18482	.09108	.09108	.09108	.50720	.50720	.50720	
6.172	.07668	.02361	.02194	.69210	.71388	0	1.0000	1.0000	1.0000	0	0	1.0000	1.0000	1.0000	.77192	.77192	.77192	
2.565	.02607	.00366	.00382	.85961	.85347	0	1.0000	1.0000	1.0000	0	0	1.0000	1.0000	1.0000	1.0000	1.0000	1.0000	
0	.00237	0	0	1.0000	1.0000	0	1.0000	1.0000	1.0000	0	0	1.0000	1.0000	1.0000	1.0000	1.0000	1.0000	
5	71.612	1.8185	1.8187	1.6623	-.00011	.08589	5	94.633	1.8180	1.8061	1.8061	0	0	0	.00655	0	.00655	
64.517	1.6917	1.6457	1.5043	.02719	.11078	88.508	1.8180	1.8180	1.8180	82.797	1.7992	1.7907	1.7904	1.7904	.00472	.00472	.00472	
44.792	1.1250	1.0027	.91651	.10871	.18532	23.201	1.5597	1.5238	1.5238	75.157	1.7161	1.7030	1.7030	1.7030	.00711	.00711	.00711	
33.875	.74707	.62727	.57374	.15982	.23201	30.588	1.2398	1.2398	1.2398	66.219	1.5597	1.5238	1.5238	1.5238	.02327	.02327	.02327	
25.759	.50109	.38161	.34882	.29844	.30388	49.181	1.1610	1.0518	1.0518	37.221	.79419	.66552	.66552	.66552	.16201	.16201	.16201	
19.743	.33110	.23046	.19072	.30396	.43506	30.648	.60297	.47281	.47281	24.168	.41550	.30490	.30490	.30490	.21557	.21557	.21557	
12.569	.15467	.09560	.08738	.36191	.45496	30.648	.60297	.47281	.47281	17.935	.26629	.17247	.17247	.17247	.35232	.35232	.35232	
7.565	.05873	.03502	.03201	.40317	.56331	10	10	10	10	10	10	10	10	10	.48905	.48905	.48905	
5.000	.02002	.01535	.01402	.30291	10	10	10	10	10	10	10	10	10	10	.51796	.51796	.51796	
10	76.612	1.8184	1.8184	1.7231	0	.05241	10	10	10	10	10	10	10	10	.00841	.00841	.00841	
69.517	1.7405	1.6862	1.5977	.03120	.08205	10	10	10	10	10	10	10	10	10	-.00111	-.00111	-.00111	
49.792	1.2537	1.1209	1.0621	.10593	.15293	10	10	10	10	10	10	10	10	10	.00148	.00148	.00148	
38.875	.88814	.75715	.71741	.14749	.19223	10	10	10	10	10	10	10	10	10	.00729	.00729	.00729	
30.759	.61804	.50281	.47642	.18644	.22914	10	10	10	10	10	10	10	10	10	.17170	.17170	.17170	
24.743	.42646	.33679	.31911	.21027	.25172	10	10	10	10	10	10	10	10	10	.13138	.13138	.13138	
15.207	.16201	.13207	.12514	.18480	.22758	10	10	10	10	10	10	10	10	10	.16004	.16004	.16004	
12.565	.10359	.09096	.08619	.12192	.16797	10	10	10	10	10	10	10	10	10	.19180	.19180	.19180	
10.000	.05209	.05793	.05490	.11211	10	10	10	10	10	10	10	10	10	10	.24737	.24737	.24737	
15	81.612	1.8182	1.8182	1.7795	0	.02128	15	99.633	1.7827	1.7677	1.7677	10	10	10	0	0	0	
74.520	1.7862	1.7254	1.6887	.03404	.05459	10	10	10	10	10	10	10	10	10	0	0	0	
54.792	1.3880	1.2405	1.2141	.10627	.01253	10	10	10	10	10	10	10	10	10	.00874	.00874	.00874	
43.875	1.0448	.89268	.87368	.14560	.16378	15	15	15	15	15	15	15	15	15	.11359	.11359	.11359	
35.759	.76556	.63464	.62113	.17101	.18866	15	15	15	15	15	15	15	15	15	.13355	.13355	.13355	
29.743	.55391	.45742	.44770	.17420	.19175	15	15	15	15	15	15	15	15	15	.15883	.15883	.15883	
17.565	.16819	.17173	.16807	.202105	.00071	15	15	15	15	15	15	15	15	15	.19063	.19063	.19063	
15.000	.10432	.12446	.12180	.19306	15	15	15	15	15	15	15	15	15	15	.24737	.24737	.24737	
20	86.612	1.8000	1.8125	1.7586	-.00694	20	104.633	1.7142	1.7023	1.7023	10	98.508	1.7648	1.7787	1.7787	1.7787	1.7787	1.7787
79.517	1.8188	1.7851	1.7586	.01853	.03310	20	92.797	1.7808	1.8118	1.8118	10	92.797	1.7808	1.8118	1.8118	1.8118	1.8118	1.8118
59.517	1.5289	1.3791	1.3586	.09798	.11139	20	59.181	1.4579	.3581	.3495	20	47.224	1.1050	.98572	.97948	.97948	.10795	.10795
48.875	1.1989	1.0478	1.0323	.12603	.13896	20	40.648	.89607	.77658	.77658	20	40.648	.89607	.77658	.77658	.77658	.11359	.11359
40.759	.91897	.78719	.77550	.14340	.15612	20	34.168	.67826	.57718	.57718	20	27.935	.47119	.39903	.39903	.39903	.14773	.14773
34.743	.69355	.59984	.59093	.13512	.14796	20	20.121	.25086	.21616	.21616	20	20.121	.25086	.21616	.21616	.21616	.15314	.15314
29.470	.48468	.44684	.44020	.07656	.09008	20	15.000	.12145	.12260	.12260	20	15.000	.12145	.12260	.12260	.12260	.13713	.13713
22.565	.24709	.27189	.26785	-.10037	-.08402	20	20.000	.19370	.21277	.21277	20	20.000	.19370	.21277	.21277	.21277	-.00947	-.00947
20.000	.17383	.21596	.21276	-.24236	-.22395	25	114.633	1.5031	1.5029	1.5029	25	108.508	1.6991	1.7198	1.7198	1.7198	.00585	.00585
25	114.633	1.8187	1.8023	.00913	.04403	25	97.797	1.7764	1.7854	1.7854	25	90.137	1.8189	1.8186	1.8186	1.8186	1.8186	1.8186
64.792	1.6607	1.5248	1.4892	.08183	.10327	25	81.219	1.8180	1.7861	1.7765	25	70.137	1.8189	1.8186	1.8186	1.8186	1.8186	1.8186
53.875	1.3812	1.2154	1.1870	.12004	.14060	25	64.181	1.5830	1.6894	1.6894	25	64.181	1.5830	1.6894	1.6894	1.6894	.02283	.02283
45.759	1.1029	.95616	.93379	.13305	.15333	25	54.648	1.2673	1.1423	1.1423	25	54.648	1.2673	1.1423	1.1423	1.1423	.06418	.06418
39.743	.86458	.76154	.76265	.07066	.09239	25	45.648	1.0574	.95510	.95510	25	39.168	.82781	.69831	.69831	.69831	.10353	.10353
32.569	.56252	.53965	.52703	.04066	.06309	25	39.168	.82781	.69831	.69831	25	39.168	.82781	.69831	.69831	.69831	.12041	.12041
30.207	.47497	.47126	.46024	.00781	.03101	25	27.206	.34969	.38210	.38210	25	27.206	.34969	.38210	.38210	.38210	.09456	.09456
29.079	.43369	.44005	.42975	-.01466	.00908	25	22.230	.23250	.26181	.26181	25	22.230	.23250	.26181	.26181	.26181	-.09268	-.09268
27.565	.37490	.39888	.38955	-.06396	-.03908	25	20.000	.19370	.21392	.21392	25	20.000	.19370	.21392	.21392	.21392	-.17141	-.17141
2																		

TABLE II.-- MEASURED AND THEORETICAL VALUES OF PRESSURE COEFFICIENTS FOR
TWO DIMENSIONAL AERODYNAMICALLY BIJET BODIES - Continued

(b) Parabolic arc bodies - upper surface

θ _{te} = 42°								θ _{te} = 54°								θ _{te} = 66°							
a, deg	δ, deg	C _p , meas	C _p	C _p , mean - C _p C _p , meas	C _p , mean - C _p (a)	α, deg	δ, deg	C _p , meas	C _p	C _p , mean - C _p C _p , meas	C _p , mean - C _p (a)	α, deg	δ, deg	C _p , meas	C _p	C _p , mean - C _p C _p , meas	C _p , mean - C _p (a)	α, deg	δ, deg	C _p , meas	C _p	C _p , mean - C _p C _p , meas	C _p , mean - C _p (a)
0	40.044	1.0974	1.0976	1.1854	-0.00018	-0.08019	0	50.839	1.6530	1.6701	0	-0.07034	0	61.215	1.7390	1.7390	1.6732	0	0.03764				
38.884	1.0518	1.0616	1.1256	0.00932	-0.07057	49.090	1.5514	1.5700	1.5863	-0.01023	-0.02072	57.757	1.6153	1.6193	1.5882	-0.00248		0.03535					
37.413	5.99003	5.97869	1.0571	0.01113	-0.06777	47.190	1.4446	1.4794	1.4947	-0.02409	-0.03469	54.654	1.5037	1.5061	1.4492	-0.01610		0.03624					
35.735	3.9783	3.90145	3.97681	0.03591	-0.04156	44.035	1.2682	1.3484	1.3421	-0.03212	-0.04184	50.129	1.3426	1.3537	1.2831	-0.00678		0.04446					
34.110	6.06264	6.31095	3.00055	0.03359	-0.04358	40.217	1.0988	1.1462	1.1581	-0.04219	-0.05301	46.096	1.1951	1.1754	1.1308	-0.01648		0.05380					
31.763	1.7587	1.7515	7.9348	0.03066	-0.04685	36.901	9.9879	9.9917	1.0015	-0.04511	-0.05600	38.256	1.0056	1.0056	1.0056	-0.01781		0.04178					
29.441	1.0689	1.0615	6.9187	0.03866	-0.04986	32.979	7.7525	7.7736	7.7936	-0.03189	-0.04259	31.171	6.6950	6.60537	6.58355	-0.00506		0.011516					
26.900	1.1676	1.1626	5.8617	0.04109	-0.03259	22.307	4.2712	3.9589	4.0000	-0.07512	-0.06350	23.941	4.4805	3.8729	3.8566	-0.01496		0.18117					
17.841	2.8897	2.9432	26.300	1.5822	-0.08087	17.101	2.7693	2.7772	2.8018	-14.159	-13.271	8.007	1.0593	0.9486	0.04226	-0.02626		0.2919		3.2625			
10.714	1.3724	0.9167	0.09898	3.3253	-0.27931	6.374	0.9608	0.3382	0.3417	-6.800	-6.4436	4.150	0.0094	0.001186	0.01141	-0.0141		0.80481		0.81221			
3.970	0.5086	0.02720	0.13735	1.7640	-0.74508	2.094	0.3725	0.03569	0.03372	-9.0094	-9.0013	0	1.0000	0.0000	0.0000	0		1.0000		1.0000			
0	0.02193	0	1.0000	0.00000	0	0.02266	0	0	1.0000	0.0000	0	0.01786	0	1.0000	0	0	1.0000	0	1.0000	0	1.0000		
5	35.044	.86132	.86110	.94122	-.00020	-.00625	5	45.736	1.3601	1.3598	1.4299	.00022	-.05132	5	56.215	1.5499	1.5499	1.5047	0	.02916			
33.824	.82310	.80605	.88725	.01706	-.00786	44.080	1.2741	1.2791	1.3410	-.00418	-.05552	52.757	1.4112	1.4216	1.3802	-.00737		0.2197					
32.413	1.75064	.82283	.03437	-.05849	-.0235	32.190	1.1825	1.1917	1.2527	-.00778	-.05937	49.651	1.2965	1.3031	1.2653	-.00509		0.0406					
30.735	7.73162	.68221	1.74797	0.06754	-.02235	39.035	1.0355	1.0482	1.1018	-.01226	-.06403	45.129	1.1485	1.1711	1.0911	0.01863		0.04737					
29.110	6.66491	6.1847	.67775	0.06673	-.02273	35.217	.88605	8.8877	9.2379	-.01718	-.06216	41.096	1.0035	9.9695	9.4118	0.03779		0.06210					
26.761	5.63707	5.2979	5.8059	0.06016	-.02996	31.901	7.7322	7.7800	7.7570	-.00787	-.06216	38.256	7.2095	7.6752	7.5373	0.03343		0.09113					
24.441	1.8855	1.4634	1.9027	0.08632	-.00360	26.979	.56201	5.9408	5.7186	-.03190	-.01753	26.171	5.0418	5.1841	5.1822	0.02768		0.15840					
21.900	1.0204	1.36340	5.9840	0.06911	-.00505	17.507	2.8947	2.7371	2.4571	-.02017	-.01717	15.207	3.7025	3.6465	12.110	0.01708		0.17678	0.10372	0.10060	0.17291	0.08877	
12.641	1.1928	1.2493	1.3715	1.36205	-.02167	12.101	1.1867	1.1613	1.1207	-.00207	-.01701	10.847	2.906	3.0034	3.0041	0.02702		0.0890	0.00615	0.00599	0.01035	0.00391	
5.714	.08813	0.2591	0.02839	1.7600	-.02816	1.574	0.4505	0.00151	0.00159	-.96107	-.96532	5	5.000	0.0000	0.0000	0		0.00334	0	0	0	0	
-1.030	0.0248	-0.00000	0.02283	0	0	5.000	0.02284	0	0	0	0	5.000	0.0000	0.0000	0	0	0	0	0	0	0	0	
-5.000	0	0	0	0	0	0	0	0	0	0	0	0	0	0	0	0	0	0	0	0	0	0	
10	30.044	.66342	.66355	.71782	-.00020	-.08200	10	40.839	1.1025	1.1023	1.1881	.00018	-.07764	10	51.215	1.3739	1.3739	1.3236	0	.03661			
28.824	.61483	.61481	.66657	0.04210	-.03714	39.060	1.0290	1.0247	1.1037	-.00418	-.07259	47.757	1.2912	1.2986	1.1937	-.00625		0.2046					
27.413	5.9295	6.1016	6.0703	0.05378	-.02375	37.190	.95804	.94107	1.0148	-.01704	-.05927	44.246	1.1246	1.1167	1.0759	0.00526		0.04160					
25.735	5.34194	5.19887	5.33992	0.09154	-.01679	34.035	8.83930	8.8078	8.87020	-.03779	-.05682	40.129	1.2966	1.3033	1.2654	0.01647		0.07195					
24.110	1.9517	1.44180	1.7784	0.07078	-.03500	30.217	1.6785	1.6530	1.70361	-.05822	-.05632	36.096	1.8423	1.8625	1.7682	0.01687		0.14987					
21.761	1.14702	1.36389	3.9962	1.11402	0.04163	26.901	5.7124	5.2774	5.6867	-.07615	-.06600	28.256	5.7421	5.6066	5.6818	0.01786		0.10290					
19.441	1.45496	1.29294	3.1724	1.3525	0.08302	21.979	4.2331	3.6124	3.8922	1.46169	0.08160	21.171	5.9040	5.9804	2.8940	0.02437		0.14667		0.26213			
16.900	2.27803	2.28564	2.4200	1.9963	1.2959	12.307	2.0995	1.1700	1.2624	1.41666	1.39804	13.941	2.9615	1.3081	1.2641	0.01467		0.14662		0.17411			
12.641	1.21210	1.04688	0.05603	1.62080	1.58871	7.101	1.2587	0.9393	0.04247	0.68201	0.65733	17.410	1.3132	0.03767	0.05623	0.1314		0.17401		0.17241			
-6.030	0.00518	0.00042	0.00041	0.99140	0.99999	-7.009	0.00937	0.00000	0.00000	0.00000	0.00000	-10.000	0.01138	0.00000	0.00000	0		0.00582					
-10.000	0.00071	0.00000	0.00000	0.00000	0	0	0	0	0	0	0	0	0	0	0	0	0	0	0	0	0	0	
15	25.044	5.0172	.50187	.51515	-.00030	-.02278	15	35.839	.81574	.81574	.95246	-.01610	-.16760	15	46.215	1.1758	1.1758	1.1353	0	.03444			
23.824	1.56653	1.45648	1.67626	0.00033	-.02328	34.080	8.8929	8.8578	8.7020	-.01610	-.02906	39.654	9.6823	9.4108	8.8705	0.02804		0.03584					
22.413	1.1957	1.40710	1.61630	0.02972	-.00779	32.190	7.5379	7.5379	7.54504	-.01041	-.04565	35.129	10.8078	7.8678	7.6153	0.02874		0.10723					
20.735	1.88709	1.85085	3.5897	0.09591	0.07499	29.035	6.9408	6.9131	6.9133	-.04586	-.06068	32.190	10.8078	7.8678	7.6153	0.02874		0.10723					
19.110	3.5101	3.0028	.50693	1.1464	1.2558	25.217	.53507	4.77177	5.00424	1.0802	0.05762	31.096	1.6166	1.6166	1.58104	0.03573		0.13665					
16.761	2.29603	2.3297	2.2061	1.29144	1.2558	21.901	1.4913	1.36580	1.36369	1.47556	0.06660	22.207	1.7458	1.70936	1.67814	0.03576		0.23556					
14.441	1.21065	1.1944	1.70128	0.04848	1.33977	20.217	3.7310	3.60609	3.33176	1.17960	1.11080	20.292	1.2102	1.2102	1.1896	0.03576		0.23556					
11.761	2.10776	1.36508	1.1886	1.35231	1.35231	11.7979	2.2121	1.1100	1.11969	1.17904	1.17904	11.7979	1.43572	1.43572	1.43572	0.03576		0.23556					
9.441	1.17046	0.88769	0.07655	1.48440	1.55092	2.307	0.06765	0.00413	0.00450	0.95288	0.94666	2.307	1.0777	1.0777	1.0777	0.03576		0.23556					
6.900	1.33646	1.04133	0.04133	0.65192	0.65194	-13.626	0.01266	0.00000	0.00000	0.00000	0.00000	-13.626	0.00000	0.00000	0.00000	0		0.03576					
-2.559	.05968	-0.00000	0	0	0	-17.956	0.01947	0.00000	0.00000	0.00000	0.00000	-17.956	0.00000	0.00000	0.00000	0		0.03576					
-9.266	0.01905	-0.00000	0	0	0	-16.936	0.02418	0.00000	0.00000	0.00000	0.00000	-16.936	0.00000	0.00000	0.00000	0		0.03576					
-16.030	0.00135	-0.00000	0	0	0	-22.906	0.00503	0.00000	0.00000	0.00000	0.00000	-22.906	0.00000	0.00000	0.00000	0		0.03576					
-20.000	-0.00209	-0.00000	0	0	0	-25.000	-0.00502	0.00000	0.00000	0.00000	0.00000	-25.000	0.00000	0.00000	0.00000	0		0.03576					
25	15.044	.20452	.34618	.19293	-.69265	.05667	25.839	.24103	.24103	.52777													

^{a, b} See footnotes at end of table.

TABLE II.- MEASURED AND THEORETICAL VALUES OF PRESSURE COEFFICIENTS FOR
TWO-DIMENSIONAL AERODYNAMICALLY BLUNT BODIES - Continued

(b) Parabolic arc bodies - upper surface - Concluded

$\theta_{le} = 78^\circ$										$\theta_{le} = 90^\circ$									
a_x deg	δ , deg	C_p , meas	C_p	C_p	$C_p, \text{meas} - C_p$		$C_p, \text{meas} - C_p$		a_x deg	δ , deg	C_p , meas	C_p	C_p	$C_p, \text{meas} - C_p$		$C_p, \text{meas} - C_p$			
					(a)	(c)	(a)	(c)						(a)	(c)	(a)	(c)		
0	70.560	1.8192	1.8192	1.6908	0	0.07058			0	83.900	1.7990	1.7978	1.7978	0	0.000667				
	65.353	1.6853	1.6899	1.5707	-.00273	.06800				77.532	1.7348	1.7336	1.7336	.00721	.00790				
	60.192	1.5546	1.5405	1.4316	.00907	.07912				70.540	1.6279	1.6175	1.6165	.00639	.00700				
	40.864	1.0113	.8758	.81393	.13395	.19516				61.096	1.4314	1.3946	1.3935	.02775	.02851				
	28.773	.60519	.47381	.44053	.21709	.27208				44.922	.99129	.90713	.90666	.08490	.08537				
	20.678	.38354	.25522	.23709	.33457	.38184				32.279	.63784	.51907	.51858	.18621	.18697				
	14.680	.24004	.13144	.12211	.45242	.49129				25.692	.46547	.34219	.34175	.26485	.26584				
	9.350	.13306	.05399	.05019	.59424	.62820				19.131	.31799	.19544	.19530	.38539	.38583				
	6.168	.07860	.02361	.02195	.69962	.72074				12.938	.19416	.09114	.09115	.53059	.53054				
	2.563	.02735	.00411	.00380	.89173	.86106				7.217	.09459	.02871	.02870	.69618	.69659				
	0	.00237	0	0	1.0000	1.0000				3.497	.04357	.00666	.00676	.84714	.84485				
										0	.00250	0	1.0000						
5	65.560	1.7451	1.7451	1.5760	0	.09690			5	78.900	1.7522	1.7522	1.7509	0	.00074				
	60.353	1.5739	1.5902	1.4362	-.01036	.08749				72.532	1.6563	1.6557	1.6545	.00036	.00109				
	55.192	1.4155	1.4197	1.2818	-.00297	.09445				65.540	1.5152	1.5075	1.5066	.00508	.00568				
	35.864	.85203	.72279	.65261	.15168	.23405				56.096	1.2945	1.2536	1.2525	.03160	.03244				
	25.773	.48178	.34199	.30897	.29015	.55869				39.922	.84121	.74922	.74883	.10935	.10982				
	15.678	.29118	.15385	.13885	.47163	.52315				27.279	.51394	.38235	.38195	.25604	.25682				
	9.680	.17656	.05956	.05376	.66266	.69551				20.692	.36347	.22735	.22702	.37450	.37541				
	4.350	.08384	.01211	.01094	.85556	.86951				14.131	.23745	.10844	.10838	.54331	.54357				
	1.168	.04198	.00086	.000790	.97951	.98118				7.932	.13275	.03466	.03463	.73891	.73913				
	-2.437	.00399								2.217	.05626	.00273	.00272	.95148	.95165				
	-5.000	-.00824								-1.503	.01739								
10	60.560	1.5646	1.5646	1.4421	0	.07829			-5.000	-.01145									
	55.353	1.3718	1.3961	1.2668	-.01771	.06196													
	50.192	1.2003	1.2177	1.1220	-.01450	.06523													
	30.864	.66515	.54299	.50039	.18366	.24770													
	18.773	.35673	.21352	.19693	.40145	.44796													
	10.678	.20786	.07091	.06528	.65886	.68594													
	4.680	.11490	.01375	.01266	.88033	.88982													
	-.650	.06463																	
	-3.832	.01655																	
	-7.437	-.01010																	
	-10.000	-.01450																	
15	55.560	1.3955	1.3955	1.2914	0	.07460			-10.000	-.01816									
	50.353	1.1863	1.2163	1.1273	-.02529	.04973													
	45.192	1.0167	1.0330	.95706	-.01603	.05866													
	25.864	.52699	.39053	.36185	.2894	.31336													
	13.773	.26274	.11619	.10777	.55776	.58982													
	5.678	.14126	.02012	.01861	.85757	.86826													
	-.320	.06988																	
	-5.650	.02041																	
	-8.832	-.00150																	
	-12.437	-.01653																	
	-15.000	-.01841																	
20	50.560	1.2277	1.2277	1.1341	0	.07624			-15.000	-.02186									
	45.353	1.0217	1.0418	.96241	-.01967	.05803													
	40.192	.84446	.85757	.79189	-.01552	.06225													
	20.864	.40457	.26116	.24117	.35448	.40389													
	8.773	.18015	.04782	.04423	.73455	.75448													
	.678	.09217	.000266	.000266	.99696	.99711													
	-5.320	.03519																	
	-10.650	.00263																	
	-13.832	-.01151																	
	-17.437	-.01810																	
	-20.000	-.02203																	
25	45.560	1.0266	1.0266	.96929	0	.05583													
	40.353	.83832	.84420	.79718	-.00701	.04907													
	35.192	.66946	.66914	.63153	-.00048	.05666													
	15.864	.29398	.15053	.14207	.48796	.51674													
	3.773	.12925	.00469	.00823	.96371	.93652													
	-.322	.05808																	
	-10.320	.01315																	
	15.650	-.00870																	
	-18.832	-.01821																	
	-22.437	-.02119																	
	-25.000	-.01838																	

^{b, c} See footnotes at end of table.

TABLE II. - MEASURED AND THEORETICAL VALUES OF PRESSURE COEFFICIENTS FOR
TWO-DIMENSIONAL AERODYNAMICALLY BLUNT BODIES - Continued

(c) Circular arc bodies - lower surface

$\theta_{le} = 42^\circ$								$\theta_{le} = 54^\circ$								$\theta_{le} = 66^\circ$											
a, deg	δ_1 , deg	Cp, meas		Cp		Cp, meas - Cp		Cp, meas - Cp		α_1 , deg	δ_2 , deg	Cp, meas		Cp		Cp, meas - Cp		Cp, meas - Cp		α_1 , deg	δ_2 , deg	Cp, mean		Cp		Cp, meas - Cp	
		(a)	(b)	(a)	(b)	Cp, meas	Cp	Cp, meas	Cp			Cp, meas	Cp	Cp, meas	Cp	Cp, meas	Cp	Cp, meas	Cp			Cp, meas	Cp	Cp, meas	Cp	Cp, meas	Cp
0.	41.19	1.2802	1.2798	1.2397	0.00031	0.03164	0	53.07	1.8182	1.8181	1.7749	0.00005	0.02381	0	65.28	1.8182	1.8182	1.7977	-0.00011	1.7977	-0.00011	0.01127	0.00980				
40.01	1.1786	1.2205	1.1822	-0.03555	-0.03035	51.71	1.6971	1.7532	1.7117	-0.03678	-0.02680	61.74	1.7647	1.7994	1.7474	-0.00513	1.6900	-0.00513	0.00571	0.00569							
39.30	1.1341	1.1842	1.1470	-0.04148	-0.01137	50.29	1.6008	1.6831	1.6437	-0.05172	-0.02823	59.45	1.6255	1.6343	1.6157	-0.00535	1.5318	-0.00183	0.01348	0.00183							
37.41	1.0375	1.0898	1.0561	-0.05041	-0.00508	48.36	1.5092	1.5891	1.5518	-0.05321	-0.02823	58.67	1.5986	1.5933	1.5318	-0.00183	1.2803	-0.02941	0.01773	0.01773							
35.65	9674.9	1.0019	9704.7	-0.03557	-0.00939	47.36	1.5802	1.4856	1.4504	-0.0826	-0.01895	50.05	1.2981	1.2981	1.2955	-0.02941	1.2803	-0.02941	0.01773	0.01773							
52.91	1.0532	1.0713	8441.32	-0.02271	-0.01023	37.96	1.1218	1.2128	1.2133	-0.10319	-0.01319	47.10	1.1668	1.1825	1.1691	-0.03113	1.0945	-0.03113	0.01945	0.01945							
50.71	1.0425	1.0724	7481.9	-0.01347	-0.0175	34.91	1.8213	1.9323	1.9102	-0.13497	-0.01805	40.12	1.8837	1.9148	1.9052	-0.03518	1.0848	-0.03518	0.02348	0.02348							
28.56	1.0621	1.0746	65377	-0.04761	-0.00526	31.71	1.6970	1.7863	1.7677	-0.12766	-0.01090	35.71	1.7487	1.7597	1.7426	-0.05050	1.0859	-0.05050	0.02859	0.02859							
24.51	1.0971	1.0826	49251	-0.03581	-0.00846	28.77	1.5810	1.6501	1.6371	-0.10602	-0.01290	31.04	1.5708	1.5866	1.5790	-0.02697	1.0533	-0.02697	0.01533	0.01533							
16.21	23.93	23.0201	22295	-0.05275	-0.00726	17.96	1.2818	1.2707	1.2613	-0.04726	-0.05985	18.18	1.2604	1.2158	1.2125	-0.17609	1.0854	-0.17609	0.1854	0.1854							
12.18	1.6663	1.3148	12734	-0.02618	-0.00607	6.52	1.0808	0.9365	0.9378	-0.06690	-0.06895	9.79	1.1440	1.0636	1.06289	-0.05942	1.06289	-0.05942	0.06447	0.06447							
8.33	1.1162	1.06201	1.06007	-0.04253	-0.00000	1.0000	1.0000	1.0000	1.0000	0	0	0	1.0000	1.0000	1.0000	1.0000	0	1.0000	1.0000	1.0000	1.0000						
0	0.0926	0	0	1.0000	1.0000	0	0	0	0	0	0	0	0	0	0	0	0	0	0	0	0	0	0	0			
5.	46.19	1.6295	1.6892	1.5862	0.00018	0.02657	58.07	1.8181	1.8181	1.7826	0.00005	0.01974	56.71	1.7330	1.7644	1.7296	-0.01812	1.00196	-0.01812	1.00196	0.00875						
45.01	1.1691	1.1656	1.1564	-0.06555	-0.03744	55.29	1.6500	1.7058	1.6723	-0.03582	-0.02147	66.45	1.7746	1.7528	1.7165	-0.01059	1.03835	-0.01059	1.03835	0.02769							
44.30	1.1045	1.5214	1.4861	-0.08323	-0.01506	52.36	1.5603	1.6228	1.5938	-0.04198	-0.02147	61.98	1.6242	1.6214	1.5819	-0.01267	1.01924	-0.01267	1.01924	0.03806							
42.41	1.2767	1.4236	1.3861	-0.11506	-0.08569	51.27	1.4457	1.5363	1.5060	-0.06267	-0.02721	56.10	1.2905	1.2954	1.2663	-0.03530	1.03530	-0.03530	1.03530	0.01924							
40.63	1.1796	1.3270	1.2919	-0.12496	-0.09520	49.31	1.3542	1.4519	1.4233	-0.07215	-0.05103	52.10	1.2909	1.2954	1.2663	-0.03549	1.03549	-0.03549	1.03549	0.01906							
35.77	9016.0	1.0690	1.0407	-0.18757	-0.00010	18.70	1.2020	1.2325	1.2106	-0.09718	-0.07424	52.10	1.0930	1.0710	1.0210	-0.0378	1.0378	-0.0378	1.0378	0.00903							
33.56	78296	95660	93134	-0.21020	-0.00000	12.46	1.2069	1.3225	1.2965	-0.10778	-0.08433	52.10	1.0930	1.0710	1.0210	-0.0378	1.0378	-0.0378	1.0378	0.00903							
29.51	61.828	75923	73947	-0.23738	-0.00000	12.46	1.1947	1.1748	1.1497	-0.10778	-0.08433	52.10	1.0930	1.0710	1.0210	-0.0378	1.0378	-0.0378	1.0378	0.00903							
27.19	56373	65304	65880	-0.23980	-0.00000	12.46	1.1748	1.1448	1.1297	-0.10778	-0.08433	52.10	1.0930	1.0710	1.0210	-0.0378	1.0378	-0.0378	1.0378	0.00903							
21.21	33399	34092	33900	-0.20752	-0.00000	12.46	1.1448	1.1148	1.0997	-0.10778	-0.08433	52.10	1.0930	1.0710	1.0210	-0.0378	1.0378	-0.0378	1.0378	0.00903							
17.18	24415	27310	26590	-0.11857	-0.00805	12.46	1.1064	1.0532	1.0464	-0.10671	-0.08433	52.10	1.0930	1.0710	1.0210	-0.0378	1.0378	-0.0378	1.0378	0.00903							
15.33	1.7961	1.6640	1.6200	-0.07355	-0.00500	12.46	1.0532	1.0464	1.0433	-0.10671	-0.08433	52.10	1.0930	1.0710	1.0210	-0.0378	1.0378	-0.0378	1.0378	0.00903							
5.00	0.0567	0.02377	0.02316	-0.05711	-0.00000	12.46	1.0433	1.0280	1.0260	-0.10671	-0.08433	52.10	1.0930	1.0710	1.0210	-0.0378	1.0378	-0.0378	1.0378	0.00903							
10.	51.19	1.8178	1.8174	1.7772	.00002	0.02333	63.07	1.8175	1.8174	1.7883	.00002	0.01607	61.71	1.7914	1.7721	.01027	0.02612	1.0172	.01027	1.0172	-0.03005						
50.01	1.6617	1.7576	1.7187	-0.05711	-0.03430	60.29	1.7334	1.7246	1.6970	-0.05058	-0.02100	61.74	1.8178	1.8123	1.7765	-0.01718	1.01718	-0.01718	1.01718	0.02266							
49.30	1.5900	1.7207	1.6826	-0.08220	-0.03624	58.36	1.6372	1.6975	1.6310	-0.06018	-0.02157	60.45	1.7459	1.7299	1.7163	-0.01718	1.01718	-0.01718	1.01718	0.02266							
47.41	1.4529	1.6230	1.5870	-0.11708	-0.09230	56.27	1.5973	1.5814	1.5560	-0.08148	-0.02862	60.05	1.5231	1.5088	1.4946	-0.01924	1.01924	-0.01924	1.01924	0.02266							
45.63	1.3424	1.5200	1.4960	-0.13907	-0.09230	54.31	1.4745	1.5085	1.4844	-0.02306	-0.02862	59.10	1.4268	1.4216	1.4152	-0.01924	1.01924	-0.01924	1.01924	0.02266							
44.77	1.2765	1.3521	1.3272	-0.18577	-0.09230	52.36	1.3547	1.3793	1.3521	-0.04514	-0.02862	59.10	1.3815	1.3793	1.3521	-0.01924	1.01924	-0.01924	1.01924	0.02266							
43.56	1.0425	1.2510	1.2279	-0.20000	-0.09230	50.31	1.2010	1.2561	1.2212	-0.06360	-0.02862	59.10	1.3160	1.3084	1.2937	-0.01924	1.01924	-0.01924	1.01924	0.02266							
39.51	87.661	1.0661	1.0467	-0.22912	-0.09230	47.91	1.2011	1.2561	1.2212	-0.06360	-0.02862	59.10	1.3160	1.3084	1.2937	-0.01924	1.01924	-0.01924	1.01924	0.02266							
37.19	77032	96203	94244	-0.24887	-0.09230	45.77	1.0653	1.0287	0.9917	-0.06360	-0.02862	59.10	1.3160	1.3084	1.2937	-0.01924	1.01924	-0.01924	1.01924	0.02266							
31.21	55342	70746	66949	-0.21376	-0.09230	43.21	1.0281	1.0748	0.96357	-0.06360	-0.02862	59.10	1.3160	1.3084	1.2937	-0.01924	1.01924	-0.01924	1.01924	0.02266							
27.18	42.268	54.9667	53.9511	-0.26980	-0.09230	37.25	1.0468	1.0826	0.98666	-0.06360	-0.02862	59.10	1.3160	1.3084	1.2937	-0.01924	1.01924	-0.01924	1.01924	0.02266							
19.42	42.268	29.2069	28.069	-0.20107	-0.09230	26.52	1.0304	1.0792	0.96523	-0.06360	-0.02862	59.10	1.3160	1.3084	1.2937	-0.01924	1.01924	-0.01924	1.01924	0.02266							
15.00	0.15271	1.17643	1.17317	-0.15533	-0.01340	20.00	1.06616	1.14375	1.13975	-0.15590	-0.02862	20	85.26	1.5702	1.8100	-0.00582	1.01736	-0.00582	1.01736	-0.15501							
20.	61.19	1.8176	1.8174	1.7897	.00011	0.01529	73.07	1.7619	1.8007	1.7739	.00402	0.02202	73.07	1.7387	1.8029	.00781	1.01736	-0.00582	1.01736	-0.15501							
60.01	1.7128	1.7761	1.7429	-0.08186	-0.01331	70.29	1.8138	1.8065	1.7436	.00402	0.02202	79.45	1.8171	1.8171	1.7648	-0.02878	1.01736	-0.00582	1.01736	-0.15501							
59.30	1.7335	1.7503	1.7238	-0.09699	-0.00560	75.29	1.8174	1.7615	1.7002	.01117	0.04558	79.45	1.7882	1.7882	1.7348	-0.02878	1.01736	-0.00582	1.01736	-0.15501							
57.41	1.6668	1.6808	1.6553	-0.03319	-0.01752	66.27	1.7259	1.7085	1.6940	.00108	0.04556	73.19	1.7681	1.7681	1.7168	-0.02878	1.01736	-0.00582	1.01736	-0.15501							
55.63	1.5599	1.6130	1.5885	-0.05132	-0.02830	61.36	1.5609	1.5704	1.5157	.00609	0.04558	76.98	1.8178	1.8178	1.7584	-0.02878	1.01736	-0.00582	1.01736	-0.15501							
50.77	1.2762	1.4203	1.3988	-0.09899	-0.00560	57.96	1.4563	1.4650	1.4140	.00198	0.04553	73.19	1.6339	1.6339	1.5949	-0.02878	1.01736	-0.00582	1.01736	-0.15501							
48.56	1.1743																										

^{a,b}See footnotes at end of table.

TABLE II.- MEASURED AND THEORETICAL VALUES OF PRESSURE COEFFICIENTS FOR
TWO-DIMENSIONAL AERODYNAMICALLY BLUNT BODIES - Continued

(c) Circular arc bodies - lower surface - Concluded

$\theta_{le} = 70^\circ$									$\theta_{le} = 90^\circ$								
α , deg	δ , deg	C_p , meas	C_p	C_p	C_p , meas - C_p	C_p , meas - C_p	C_p , meas	C_p	α , deg	δ , deg	C_p , meas	C_p	C_p	C_p , meas - C_p	C_p , meas - C_p		
		(a)	(b)		(a)	(b)					(a)	(b)		(a)	(b)		
0	77.04	1.8190	1.8189	1.8055	0.00005	0.00742	0	89.91	1.8176	1.8179	1.8176	-0.00017	0	.00132	.00132		
	75.05	1.7967	1.7879	1.7747	.00190	.01224		87.90	1.8176	1.8152	1.8152	.00112		.00172			
	73.02	1.7657	1.7519	1.7390	.00782	.01512		81.53	1.8042	1.8011	1.8011	.00172					
	66.70	1.6364	1.6157	1.6037	.01265	.01988		76.61	1.7181	1.7204	1.7204	.00134		.00134			
	60.39	1.4588	1.4523	1.4416	.00446	.01179		73.06	1.6582	1.6634	1.6634	.00314		.00314			
	55.70	1.3029	1.3071	1.2974	-.00322	.00422		69.05	1.5685	1.5852	1.5852	-.01065		.01065			
	51.43	1.1981	1.1709	1.1623	-.01105	-.00365		63.31	1.4311	1.4511	1.4511	-.01398		.01398			
	47.83	1.0442	1.0522	1.0445	-.00766	-.00029		59.47	1.3424	1.3485	1.3485	-.01835		.01835			
	42.90	.88394	.88753	.88098	-.00406	.00335		54.59	1.1845	1.2072	1.2072	-.01916		.01916			
	36.49	.68695	.67714	.67214	.01811	.02536		44.00	.87192	.87708	.87708	-.00592		.00592			
	30.85	.53554	.50366	.49993	.05953	.06649		36.11	.62711	.63149	.63149	-.00698		.00698			
	9.06	.14198	.04757	.04720	.66195	.66756		13.80	.17350	.10342	.10342	.40392		.40392			
	0	.04235	0	0	1.0000	1.0000		0	.04591	0	0	1.0000		1.0000			
5	82.04	1.8105	1.8104	1.8056	.00006		5	94.91	1.7989	1.8044	1.8044	-.00306					
	80.05	1.8185	1.8185	1.7908	0	.01523		92.90	1.8117	1.8131	1.8131	-.00077					
	78.02	1.8123	1.7937	1.7663	.01026	.02538		89.52	1.8178	1.8177	1.8177	.00006		.00006			
	71.70	1.7289	1.6897	1.6639	.02267	.03760		85.71	1.8062	1.8077	1.8077	-.00083		.00083			
	65.39	1.5193	1.5492	1.5256	.01906	.03400		81.64	1.7800	1.7793	1.7793	.00059		.00059			
	60.70	1.4406	1.4259	1.4038	.01069	.02575		74.05	1.6648	1.6805	1.6805	-.00943		.00943			
	56.43	1.3055	1.3014	1.2916	.00314	.01831		68.31	1.5491	1.5697	1.5697	-.01350		.01350			
	52.83	1.1986	1.1903	1.1722	.00692	.02203		64.47	1.4540	1.4801	1.4801	-.01795		.01795			
	47.90	1.0348	1.0319	1.0162	.00280	.01701		59.59	1.3279	1.3519	1.3519	-.01807		.01807			
	41.49	.83891	.82249	.80994	.01957	.03453		49.00	1.0288	1.0354	1.0354	-.01133		.01133			
	35.85	.66595	.64259	.63315	.04288	.05458		41.11	.76661	.78607	.78607	-.02358		.02358			
	31.06	.18934	.11073	.10904	.11518	.42410		18.80	.25046	.18880	.18880	.24619		.24619			
	5.00	.07747	.01424	.01402	.81619	.81903		5.00	.08288	.01382	.01382	.83325		.83325			
10	87.04	1.7380	1.8163	1.8076	-.04505		10	99.91	1.7530	1.7738	1.7738	-.01187					
	85.05	1.7992	1.8185	1.8076	-.00467			97.99	1.7775	1.7832	1.7832	-.03207					
	83.02	1.8190	1.8312	1.7943	-.00671	.01358		90.71	1.8175	1.8172	1.8172	.00017					
	80.27	1.8172	1.8095	1.7692	.00644	.02611		86.84	1.8101	1.8110	1.8110	-.00050		.00050			
	76.70	1.7675	1.7713	1.7386	.00738	.02736		83.06	1.7898	1.7910	1.7910	-.00067		.00067			
	70.39	1.6743	1.6942	1.6159	.01150	.03488		79.05	1.7394	1.7519	1.7519	-.00719		.00719			
	65.70	1.5612	1.5439	1.5128	.01108	.03100		73.51	1.6522	1.6677	1.6677	-.00938		.00938			
	57.83	1.3373	1.3319	1.3050	.00404	.02415		69.47	1.5742	1.5939	1.5939	-.01251		.01251			
	52.90	1.1814	1.1824	1.1586	-.00085	.01930		64.59	1.4560	1.4827	1.4827	-.01555		.01555			
	46.49	.99343	.97744	.95774	.01610	.03593		54.00	1.1663	1.1896	1.1896	-.01998		.01998			
	40.85	.81038	.79518	.787021	.01876	.07383		46.11	.92740	.94415	.94415	-.01806		.01806			
	19.03	.26369	.19834	.19434	.24783	.26300		23.80	.33772	.29598	.29598	.12359		.12359			
	10.00	.12392	.05604	.05492	.54777	.55681		10.00	.13256	.05480	.05480	.58660		.58660			
15	92.04	1.6225	1.8162	1.8056	-.11938		15	104.91	1.6839	1.6984	1.6984	-.00861					
	92.05	1.7374	1.8185	1.8056	-.04668			102.90	1.7167	1.7282	1.7282	-.00670					
	88.02	1.7911	1.8163	1.8056	-.01407			99.53	1.7613	1.7690	1.7690	-.00437					
	81.70	1.8185	1.8016	1.7806	.00929	.02061		91.64	1.8189	1.8174	1.8174	.00082		.00082			
	76.57	1.7948	1.7671	1.7471	.01510	.02658		88.06	1.8189	1.8168	1.8168	-.00115		.00115			
	75.39	1.7511	1.7228	1.7027	.01616	.02764		84.05	1.7985	1.7933	1.7933	-.00044		.00044			
	70.70	1.6675	1.6390	1.6198	.01709	.02861		76.31	1.7477	1.7443	1.7443	.00195		.00195			
	62.83	1.4740	1.4564	1.4394	.01194	.02347		74.17	1.6895	1.6884	1.6884	.00065		.00065			
	57.90	1.3291	1.3204	1.3050	.00655	.01813		69.51	1.5947	1.5976	1.5976	-.00182		.00182			
	51.49	1.1419	1.1264	1.1133	.01357	.02050		59.00	1.3248	1.3364	1.3364	-.00876		.00876			
	45.85	.96148	.94726	.93622	.01479	.02627		51.11	1.0913	1.1022	1.1022	-.00999		.00999			
	24.06	.35818	.30958	.30242	.14645	.15638		28.80	.45582	.42215	.42215	.07305		.07305			
	15.00	.17059	.12362	.121282	.27745	.26589		15.00	.17617	.12185	.12185	.30834		.30834			
20	97.04	1.4640	1.7911	1.7747	-.02234		20	109.91	1.5903	1.6076	1.6076	-.01088					
	95.05	1.6404	1.8043	1.8134	-.09991			107.90	1.6327	1.6468	1.6468	-.00868					
	93.02	1.7303	1.8184	1.8124	-.04805			100.71	1.7568	1.7557	1.7557	.00057					
	86.70	1.8181	1.8093	1.7956	.00500	.01254		93.06	1.8186	1.8134	1.8134	.00286		.00286			
	80.39	1.7940	1.7812	1.7676	.00713	.01472		89.05	1.8136	1.8181	1.8181	-.00248		.00248			
	75.70	1.7390	1.7205	1.7075	.01064	.01811		83.31	1.7899	1.7939	1.7939	-.00223		.00223			
	67.83	1.5846	1.5715	1.5595	.00827	.01584		79.47	1.7550	1.7578	1.7578	-.00160		.00160			
	62.90	1.4615	1.4521	1.4410	.00643	.01403		74.59	1.6864	1.6901	1.6901	-.00219		.00219			
	56.49	1.2809	1.2736	1.2640	.00570	.01319		64.00	1.4599	1.4691	1.4691	-.00626		.00626			
	50.85	1.1065	1.1120	1.0936	.00407	.01166		56.11	1.2411	1.2534	1.2534	-.00742		.00742			
	29.06	.46776	.43249	.42920	.02771	.03024		33.80	.57656	.56278	.56278	.00656		.00656			
	20.00	.25463	.21435	.21272	.15819	.16459		22.04	.33389	.25588	.25588	.23364		.23364			
25	102.04	1.2941	1.7389	1.7167	-.34371		25	114.91	1.4797	1.4952	1.4952	-.01048					
	100.05	1.5237	1.7625	1.7482	-.15672			112.90	1.5272	1.5425	1.5425	-.00992					
	98.02	1.6442	1.7825	1.7682	-.08411			109.53	1.6009	1.6146	1.6146	-.00856					
	91.70	1.7954	1.8163	1.8168	.01164	.01747		101.64	1.7477	1.7439	1.7439	.00446					
	88.57	1.8179	1.8168	1.8168	.00651	.01405		94.05	1.8084	1.8087	1.8087	-.00017					

TABLE II.- MEASURED AND THEORETICAL VALUES OF PRESSURE COEFFICIENTS FOR
 TWO-DIMENSIONAL AERODYNAMICALLY BLUNT BODIES - Continued
 (d) Circular arc bodies - upper surface

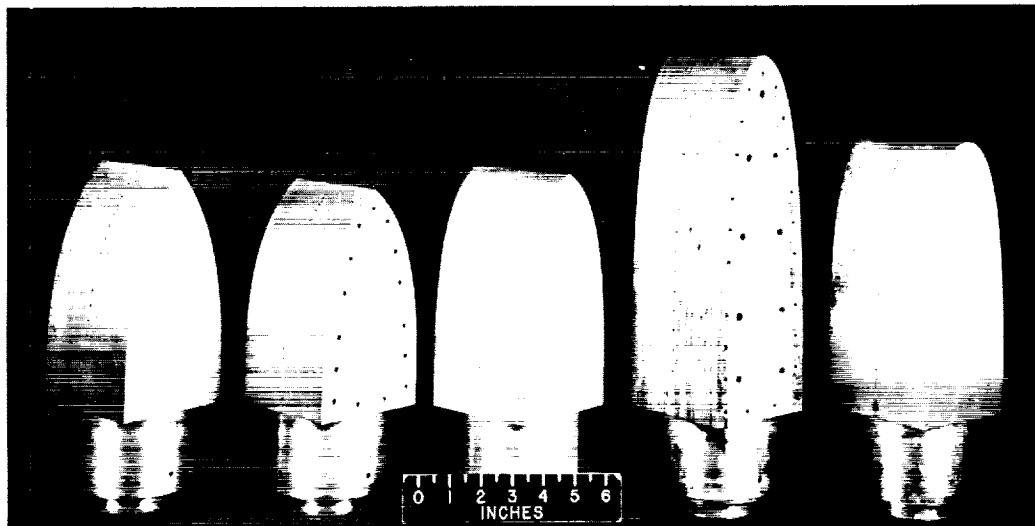
^{a, c} See footnotes at end of table.

TABLE II.- MEASURED AND THEORETICAL VALUES OF PRESSURE COEFFICIENTS FOR

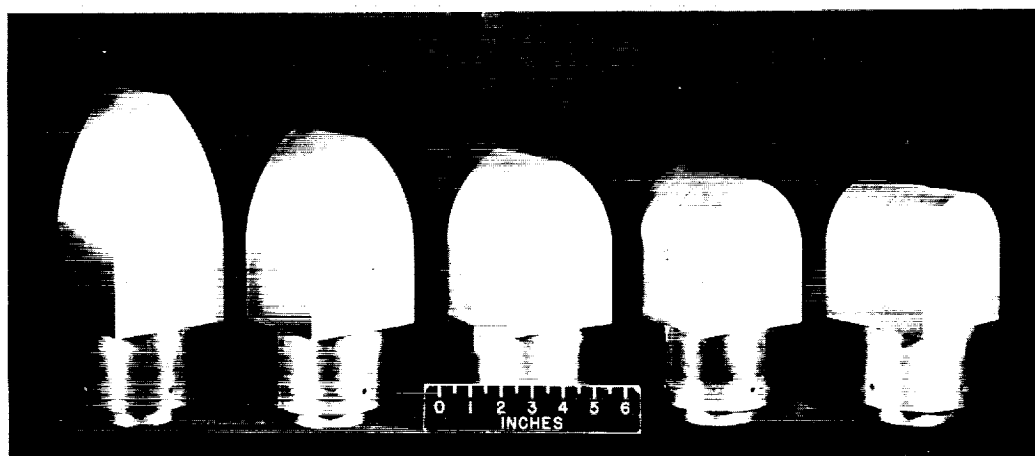
TWO-DIMENSIONAL AERODYNAMICALLY BLUNT BODIES - Concluded

(d) Circular arc bodies - upper surface - Concluded

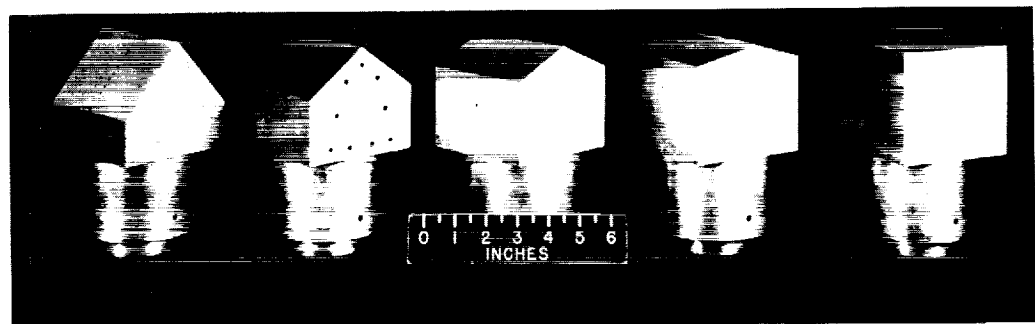
$\theta_{le} = 76^\circ$								$\theta_{le} = 90^\circ$								
α , deg	δ , deg	C_p, meas	C_p	C_p	$\frac{C_p, \text{meas} - C_p}{C_p, \text{meas}}$	$C_p, \text{meas} - C_p$	$\frac{C_p, \text{meas} - C_p}{C_p, \text{meas}}$	α , deg	δ , deg	C_p, meas	C_p	C_p	C_p	$\frac{C_p, \text{meas} - C_p}{C_p, \text{meas}}$	$C_p, \text{meas} - C_p$	$\frac{C_p, \text{meas} - C_p}{C_p, \text{meas}}$
(a)	(c)	(a)	(c)	(a)	(c)	(a)	(c)	(a)	(c)	(a)	(c)	(a)	(c)	(a)	(c)	
0	75.11	1.8010	1.8012	1.7758	-0.00011	0.01399	0.01620	0	87.45	1.8164	1.8164	1.8140	1.8140	0	0.00132	
	72.89	1.7651	1.7613	1.7365	.00215	.01711	.01784	85.15	1.8103	1.8069	1.8045	.00188	.00188	.00320		
	70.46	1.7181	1.7128	1.6887	.00308	.01411	.01441	82.07	1.7864	1.7853	1.7830	.00062	.00062	.00190		
	67.10	1.6488	1.6363	1.6133	.00758	.02153	.02018	78.73	1.7510	1.7505	1.7482	.00029	.00029	.00160		
	60.56	1.4718	1.4627	1.4421	.00618	.02018	.02018	71.05	1.6173	1.6281	1.6259	-.00668	-.00668	-.00532		
	57.11	1.3604	1.3599	1.3408	.00037	.01441	.01441	61.88	1.4006	1.4158	1.4138	-.01085	-.01085	-.00950		
	49.76	1.1135	1.1288	1.1080	-.00925	.00494	.00494	57.39	1.2767	1.2912	1.2897	-.01136	-.01136	-.01003		
	43.16	.92354	.90250	.88980	.02278	.03653	.03653	53.40	1.1546	1.1730	1.1715	-.01594	-.01594	-.01464		
	37.08	.72057	.70109	.69124	.02703	.04070	.04070	45.82	.86764	.87242	.87158	-.00551	-.00551	-.00418		
	31.47	.55906	.52544	.51805	.06014	.07336	.07336	36.02	.64176	.62931	.62858	.01940	.01940	.02071		
	9.82	.15683	.05607	.05256	.61248	.64764	.64764	14.27	.19121	.11053	.11043	.42194	.42194	.42273		
	0	.05349	0	1.0000	1.0000	1.0000	1.0000	0	0	0	1.0000	1.0000	1.0000	1.0000		
5	70.11	1.7279	1.6812	1.6812	-.00012	.02691	.02691	5	82.45	1.7782	1.7800	1.7863	-.00101	-.00101	-.01041	
	67.89	1.6757	1.6769	1.6518	-.00716	.02620	.02620	80.13	1.7520	1.7581	1.7642	-.00348	-.00348	-.00696		
	65.46	1.6127	1.5908	1.5733	.01358	.02443	.02443	77.07	1.7154	1.7205	1.7266	-.00297	-.00297	-.00652		
	62.10	1.5330	1.5260	1.4849	.00457	.03138	.03138	73.73	1.6624	1.6691	1.6749	-.00403	-.00403	-.00752		
	55.56	1.3352	1.3292	1.2931	.00449	.03153	.03153	66.05	1.4948	1.5128	1.5181	-.01203	-.01203	-.01559		
	52.11	1.2091	1.2171	1.1841	-.00662	.02068	.02068	60.96	1.3632	1.3846	1.3894	-.01570	-.01570	-.01922		
	44.76	.95943	.96988	.94265	-.00995	.017490	.017490	52.39	1.1219	1.1364	1.1406	-.01292	-.01292	-.01667		
	38.16	.76474	.74611	.72580	.02436	.05092	.05092	43.51	.85802	.85875	.86157	-.00085	-.00085	-.00414		
	32.08	.58303	.55122	.53629	.05456	.08017	.08017	36.82	.71603	.71167	.71426	.00509	.00509	.00244		
	26.47	.44088	.38809	.37774	.11974	.14321	.14321	31.02	.51311	.48093	.48085	.06272	.06272	.06287		
	4.82	.10467	.01377	.01342	.86844	.87179	.87179	9.27	.13712	.04696	.04717	.65753	.65753	.65672		
	-5.00	.02494						-5.00	.02499							
10	65.11	1.6038	1.6040	1.5644	-.00012	.02457	.02457	10	77.11	1.7143	1.7143	1.7318	0	0	-.01021	
	62.89	1.5132	1.5441	1.5064	-.00058	.02385	.02385	75.13	1.6756	1.6808	1.6979	-.00310	-.00310	-.01331		
	60.46	1.4740	1.4755	1.4391	-.00102	.02368	.02368	72.07	1.6166	1.6287	1.6453	-.00748	-.00748	-.01775		
	57.10	1.3948	1.3740	1.3402	.01491	.03915	.03915	68.73	1.5546	1.5626	1.5784	-.00515	-.00515	-.01551		
	50.56	1.1858	1.1627	1.1339	.01948	.04377	.04377	61.05	1.3555	1.3777	1.3917	-.01638	-.01638	-.02671		
	43.34	.93530	.91787	.89553	.01864	.04252	.04252	55.96	1.2192	1.2357	1.2481	-.01553	-.01553	-.02379		
	36.37	.70586	.68527	.66816	.02917	.05204	.05204	47.39	.97286	.97439	.98453	-.00157	-.00157	-.01200		
	33.16	.62237	.58333	.56883	.06273	.08063	.08063	43.40	.84447	.84942	.85809	-.00586	-.00586	-.01613		
	27.08	.46406	.40401	.39400	.12940	.15097	.15097	38.51	.71119	.69777	.70468	.01887	.01887	.00915		
	21.47	.34099	.26103	.25470	.23449	.25306	.25306	33.82	.57974	.57726	.56368	.00424	.00424	.02874		
	-18	.06435						26.02	.39855	.34615	.34978	.13143	.13143	.12232		
	-10.00	.00364						-10.00	.00431							
15	60.11	1.4596	1.4597	1.4290	-.00007	.02096	.02096	15	72.45	1.6341	1.6341	1.6524	0	0	-.01120	
	57.89	1.3997	1.3930	1.3641	.00479	.02443	.02443	70.13	1.5839	1.5899	1.6076	-.00379	-.00379	-.01496		
	55.46	1.3285	1.3178	1.2900	.00805	.02898	.02898	67.07	1.5139	1.5249	1.5417	-.00707	-.00707	-.01836		
	52.10	1.2517	1.2091	1.1837	.01403	.05133	.05133	63.73	1.4440	1.4455	1.4622	-.00104	-.00104	-.01260		
	45.56	1.0445	.99012	.96920	.05026	.07209	.07209	56.05	1.2297	1.2369	1.2507	-.00586	-.00586	-.01708		
	42.11	.91903	.87337	.85489	.01968	.06979	.06979	50.96	1.0879	1.0816	1.0966	-.00303	-.00303	-.00799		
	38.34	.79294	.74701	.73158	.05792	.07736	.07736	46.88	.96905	.95783	.96837	.01158	.01158	.00070		
	31.37	.57758	.52610	.51519	.08913	.10802	.10802	38.40	.71456	.69353	.70150	.02943	.02943	.01856		
	28.16	.50330	.43268	.42346	.11031	.15863	.15863	33.51	.58483	.54808	.55400	.06236	.06236	.05272		
	16.47	.25361	.15603	.15622	.38476	.39742	.39742	28.82	.41698	.41763	.42238	.11139	.11139	.10126		
	-5.18	.03451						21.02	.30960	.25121	.25305	.25320	.25320	.24467		
	-20.00	.01018						-20.00	-.00689							
20	55.11	1.2715	1.2717	1.2792	-.00016	-.00606	-.00606	20	67.45	1.5304	1.5304	1.5503	0	0	-.01300	
	52.89	1.2234	1.2017	1.2091	.01774	.01169	.01169	65.13	1.4686	1.4770	1.4961	-.00572	-.00572	-.01737		
	50.46	1.1515	1.1241	1.1307	.02380	.01806	.01806	62.07	1.3925	1.4005	1.4188	-.00575	-.00575	-.01889		
	47.10	1.0859	1.0414	1.0201	.06612	.06059	.06059	58.75	1.3158	1.3109	1.3279	-.00372	-.00372	-.00920		
	40.56	.88588	.79926	.80387	.09778	.09257	.09257	51.05	1.0881	1.0852	1.0993	-.00267	-.00267	-.01029		
	37.11	.76401	.66818	.69210	.12546	.09412	.09412	41.88	.81674	.79773	.81000	.02083	-.00825			
	33.34	.64526	.57065	.57428	.11563	.11000	.11000	37.39	.69885	.66114	.67021	.03983	.03983	.02706		
	29.76	.53588	.46580	.46943	.13078	.12857	.12857	33.40	.57843	.54372	.55080	.06001	.06001	.04777		
	23.16	.38838	.29248	.29409	.26692	.24278	.24278	28.51	.46240	.40895	.41410	.11560	.11560	.10446		
	11.47	.17651	.07469	.07518	.57685	.57407	.57407	16.02	.22410	.13660	.15660	.39045	.39045	.30120		
	-10.18	.01251						-5.73	.02759							
	-20.00	.01912						-20.00	-.02063							
25	50.11	1.0198	1.0200	1.1193	-.00020	-.09757	-.09757	25	62.45	1.4028	1.4028	1.4288	0	0	-.01853	
	47.89	.99127	.95316	1.0464	.03384	-.05562	-.05562	60.13	1.3384	1.3420	1.3668	-.00269	-.00269	-.02122		
	45.46	.92507	.88023	.96589	.04847	-.04413	-.04413	57.07	1.2522	1.2571	1.2605	-.00391	-.00391	-.02260		
	42.10	.86680	.77860	.85453	.08820	.01419	.01419	53.73	1.1722	1.1601	1.1815	-.01032	-.01032	-.00793		
	38.91	.79212	.68358	.75001	.13702	.05316	.05316	46.05	.93903	.92498	.94211	.01496	.01496	-.00322		
	35.56	.69194	.58606	.61503	.15302	.07068	.07068	40.96	.78965	.76708	.78108	.02858	.02858	.01085		
	32.11	.58690	.48963	.53719	.16574	.08470	.08470	32.39	.55715	.51191	.52155	.08120	.08120	.06390		
	28.34	.48732	.39020	.42840	.19929	.12091	.12091	28.40	.45715	.40371	.41117	.11590</td				



(a) Parabolic arc models.



(b) Circular arc models.



(c) Wedge models.

L-63-83

Figure 1.- Photograph of two-dimensional aerodynamically blunt bodies.
23

L-62-872

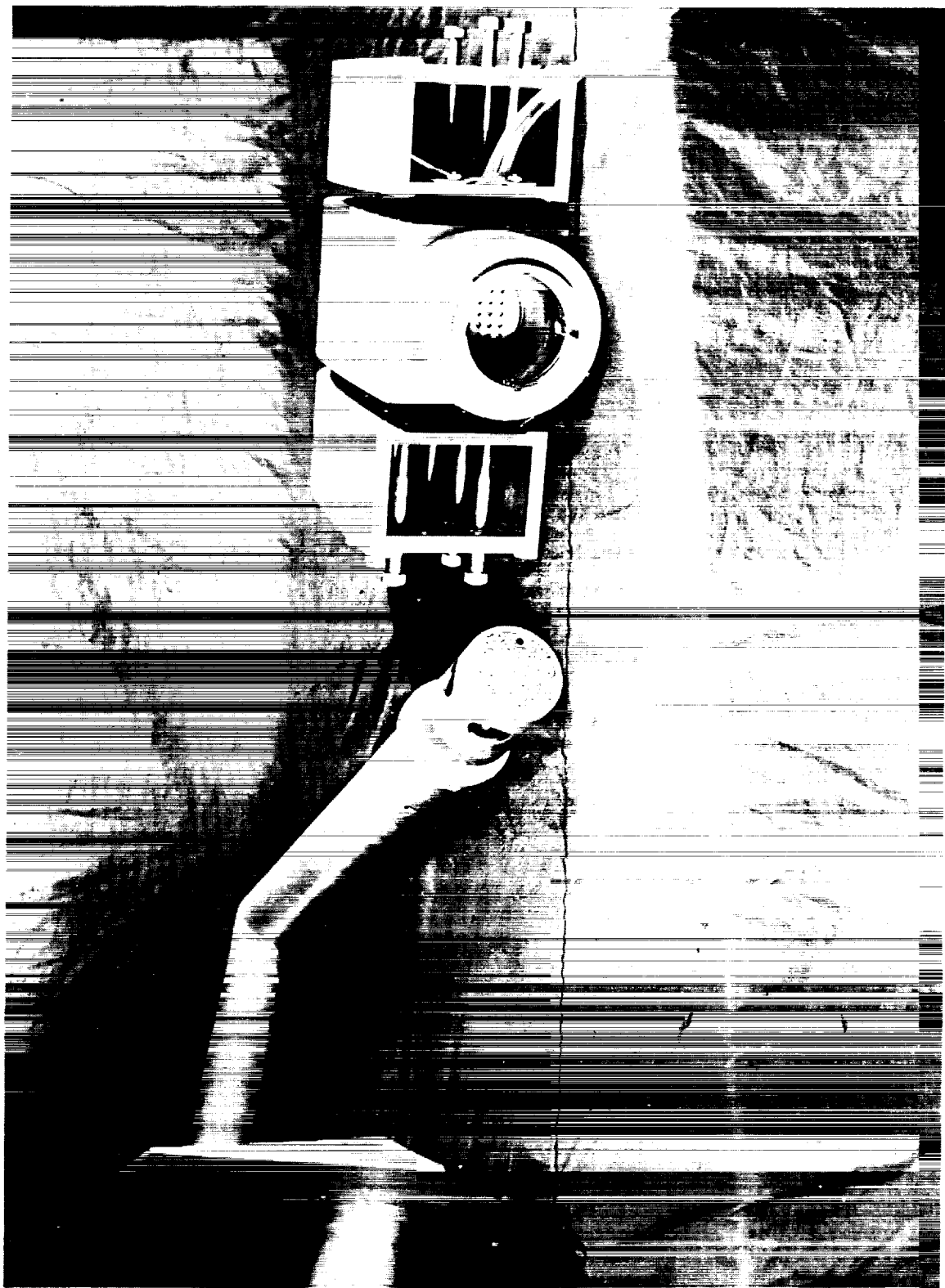


Figure 2.- Photograph of 78° parabola with extensions and support.

25

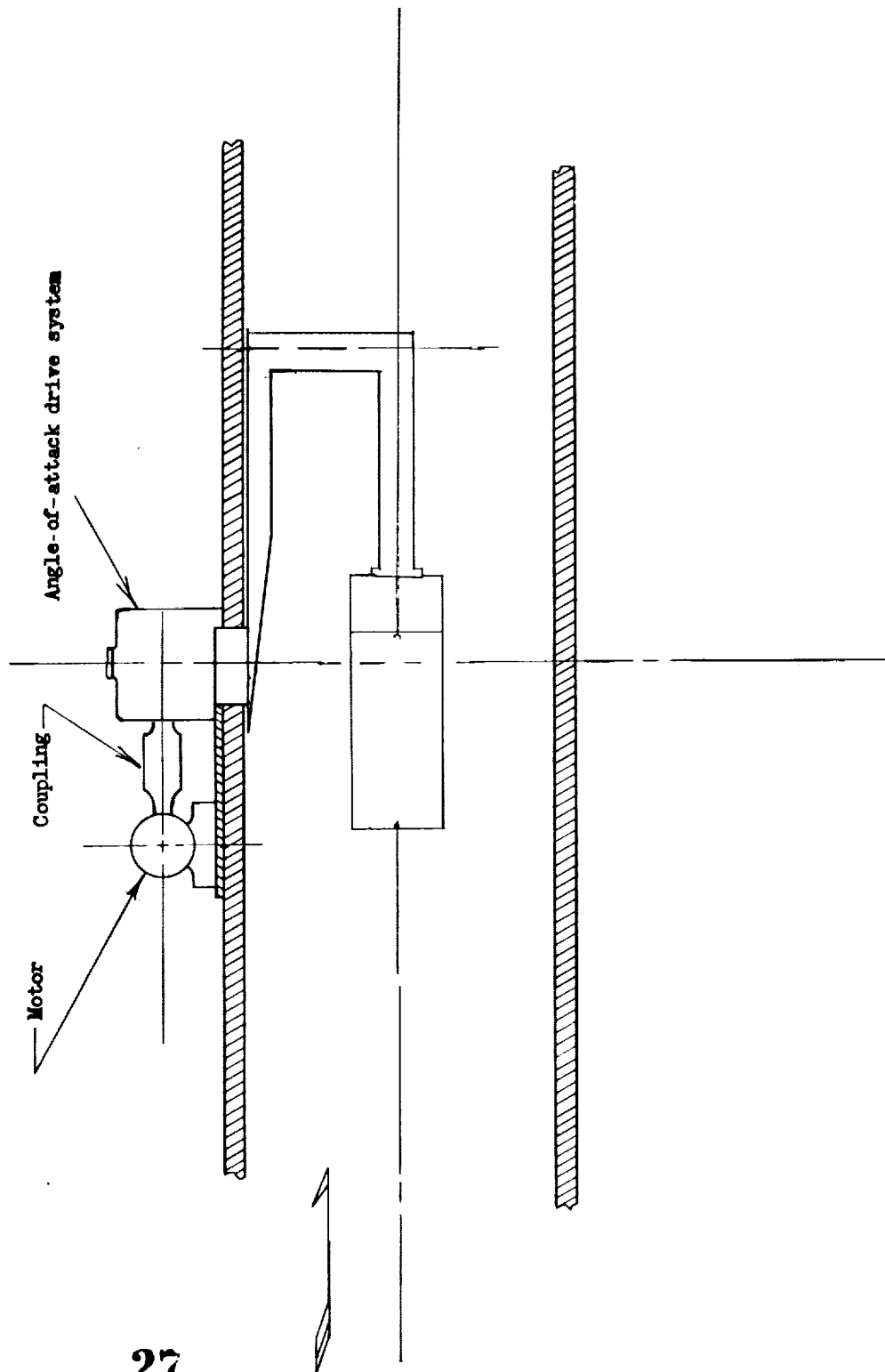


Figure 3.- Schematic diagram of model support system.

27

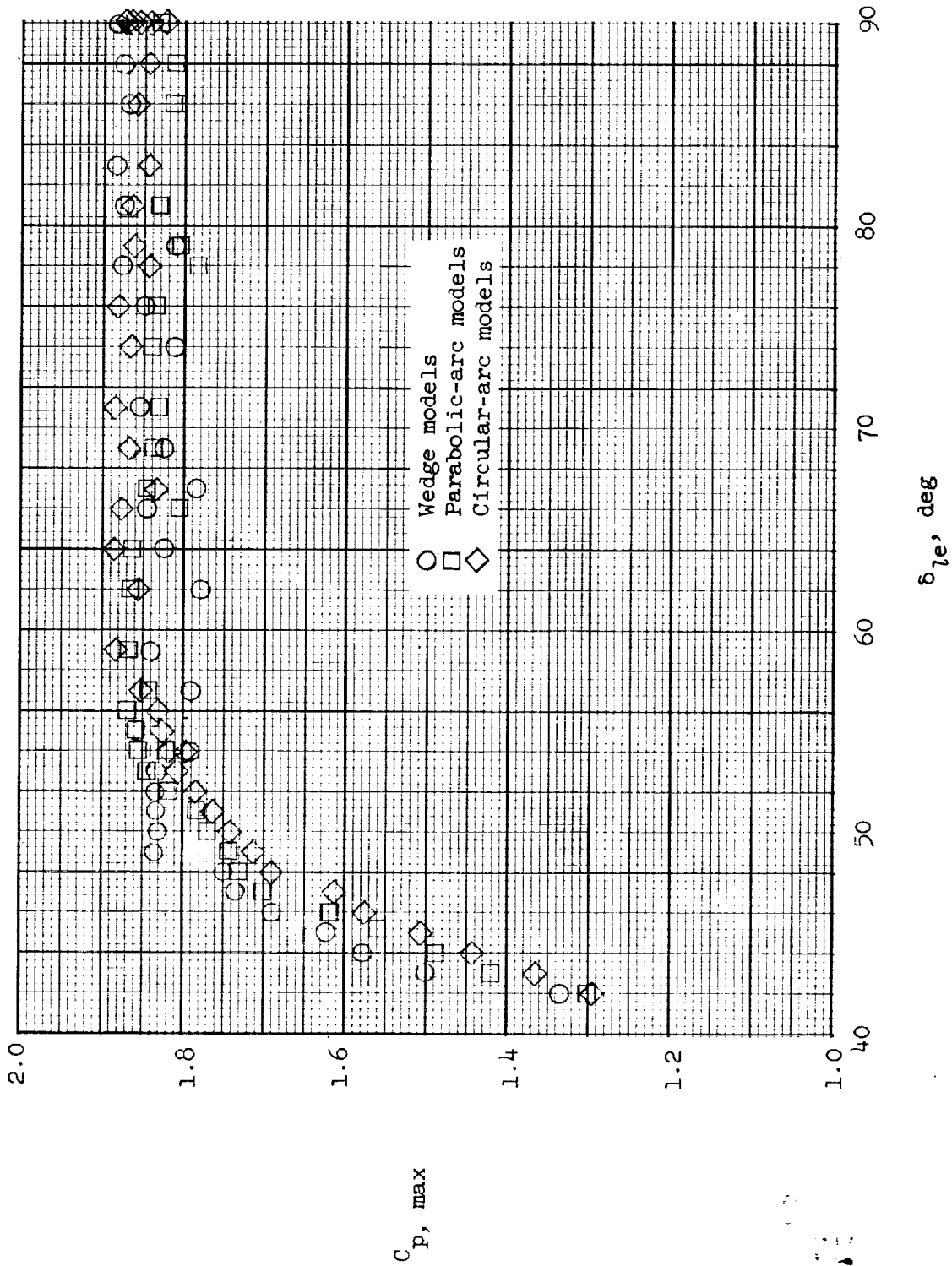


Figure 4.- Maximum pressure coefficients based upon an assumed Mach number of 6.

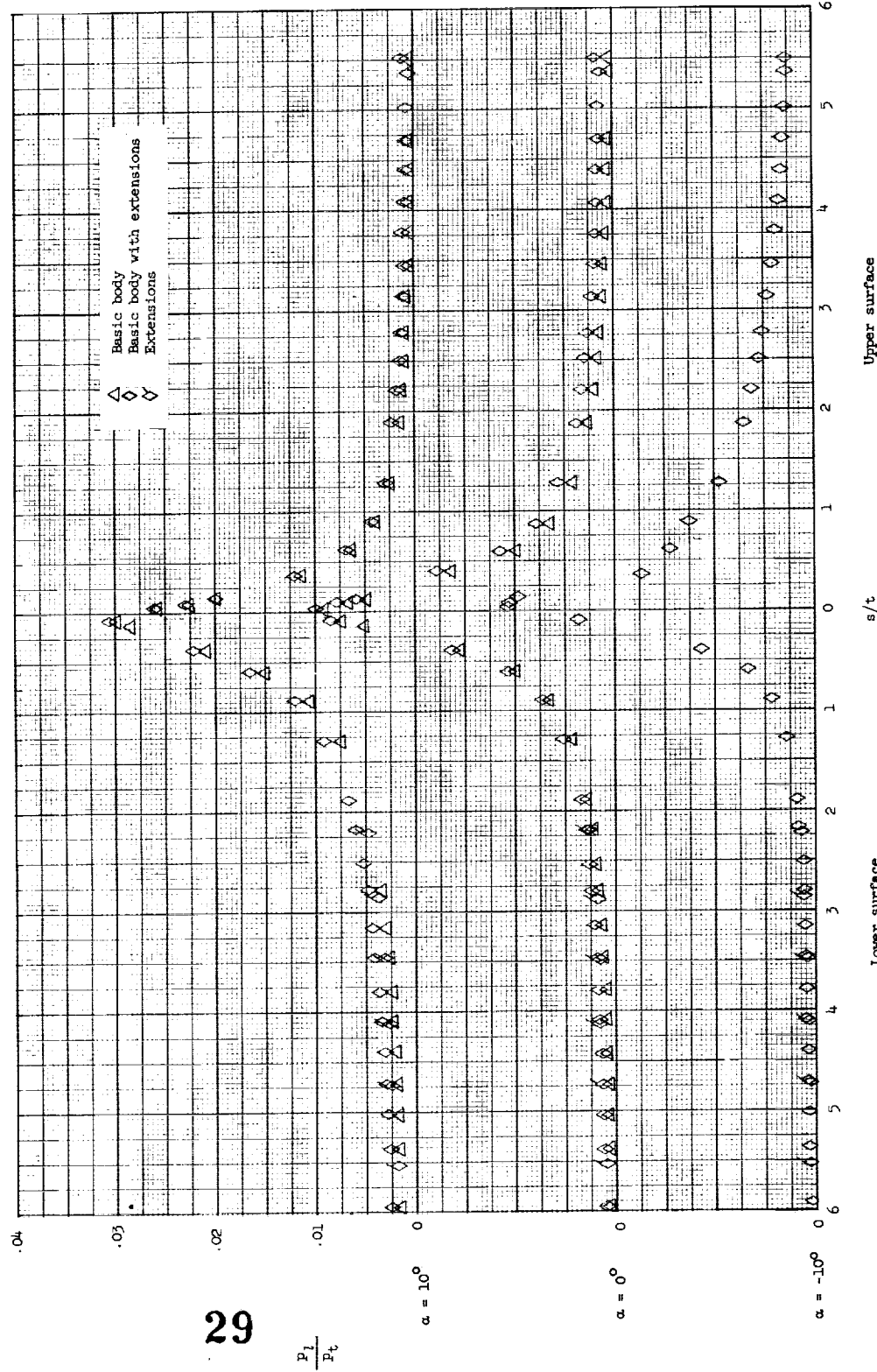
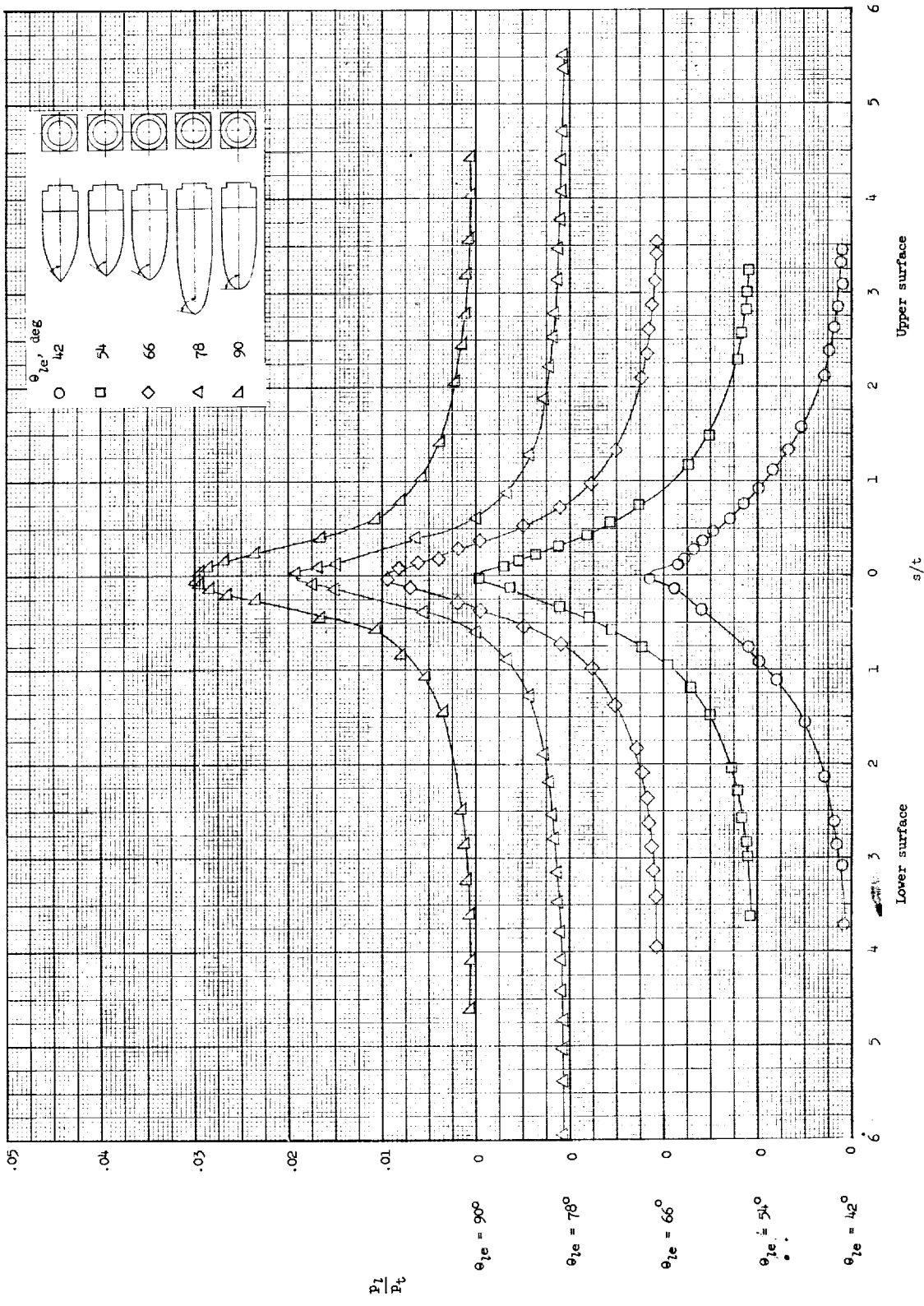
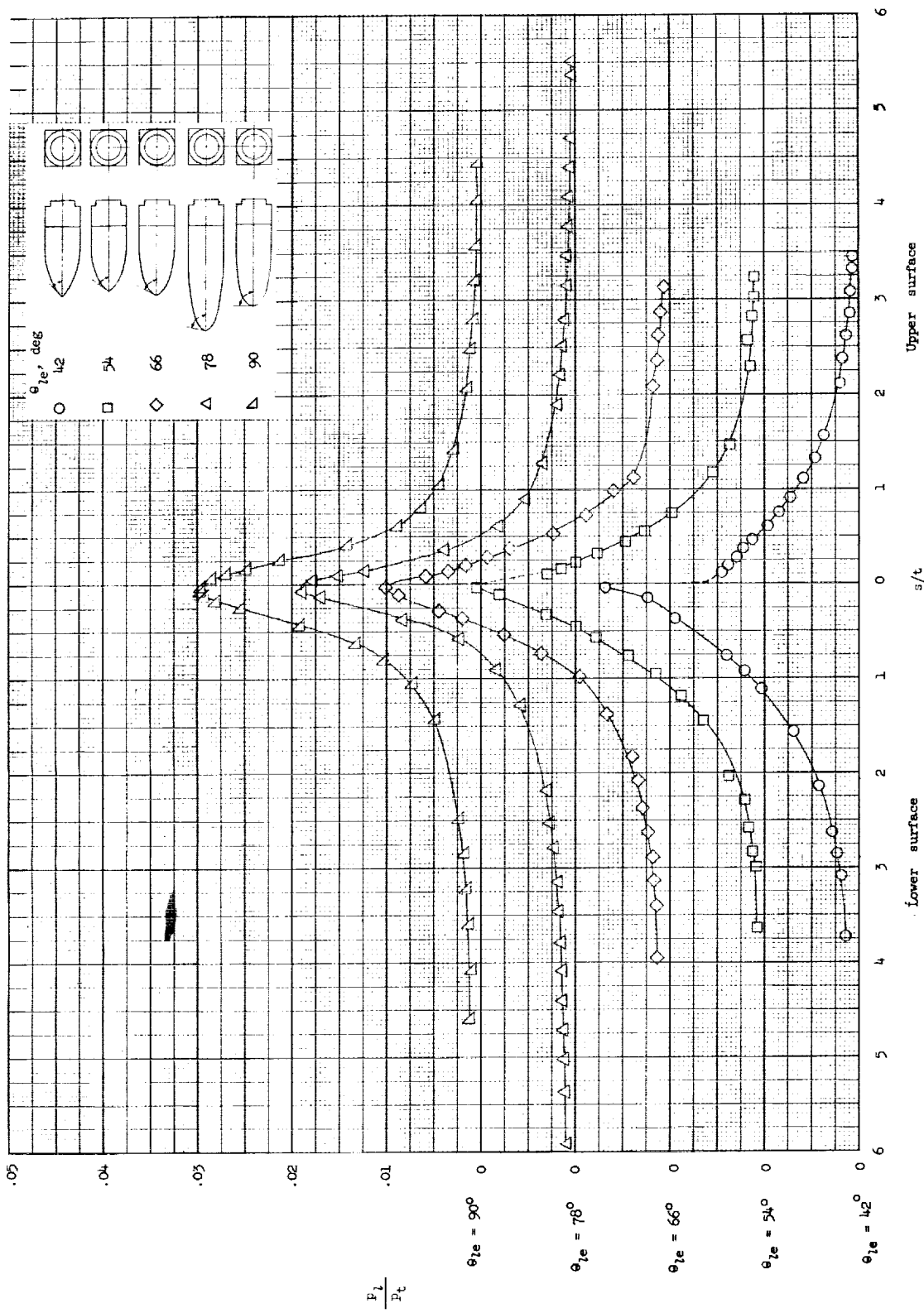


Figure 5.- Pressure distributions of two-dimensional 78° parabola with and without extensions.



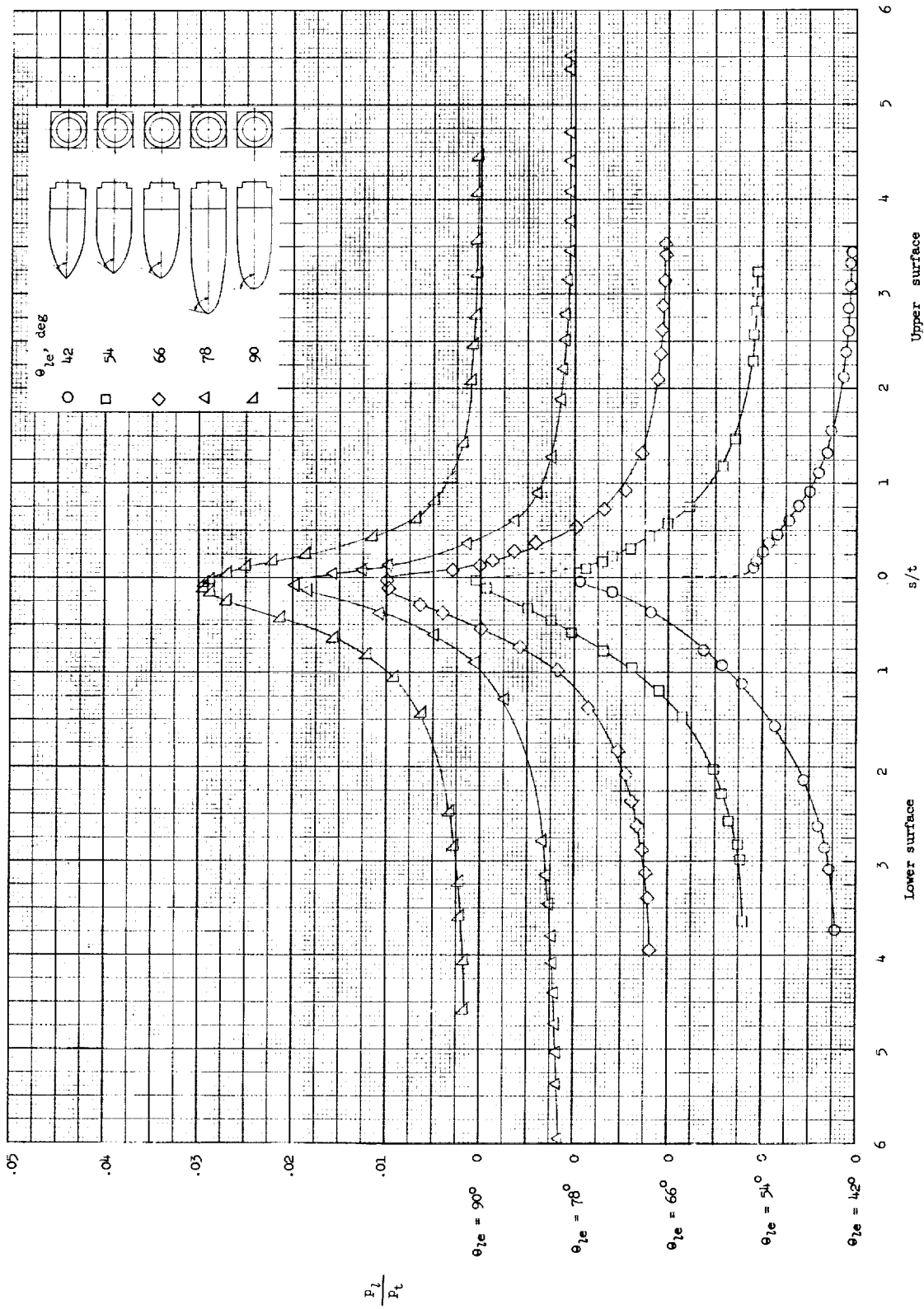
(a) $\alpha = 0^\circ$.

Figure 6.- Pressure distributions of two-dimensional parabolas.



(b) $\alpha = 5^\circ$.

Figure 6.- Continued.



(c) $\alpha = 10^\circ$.

Figure 6.- Continued.

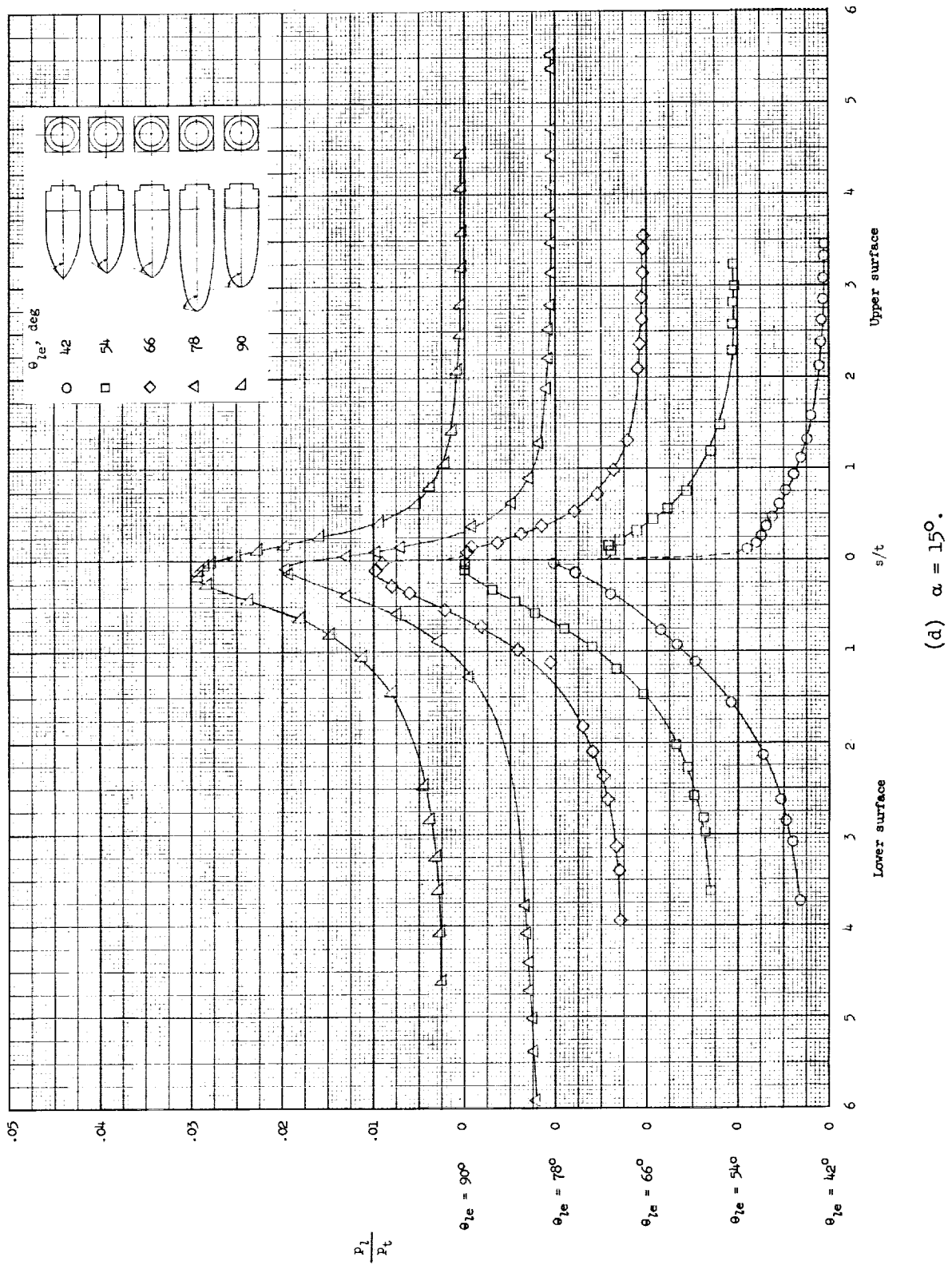
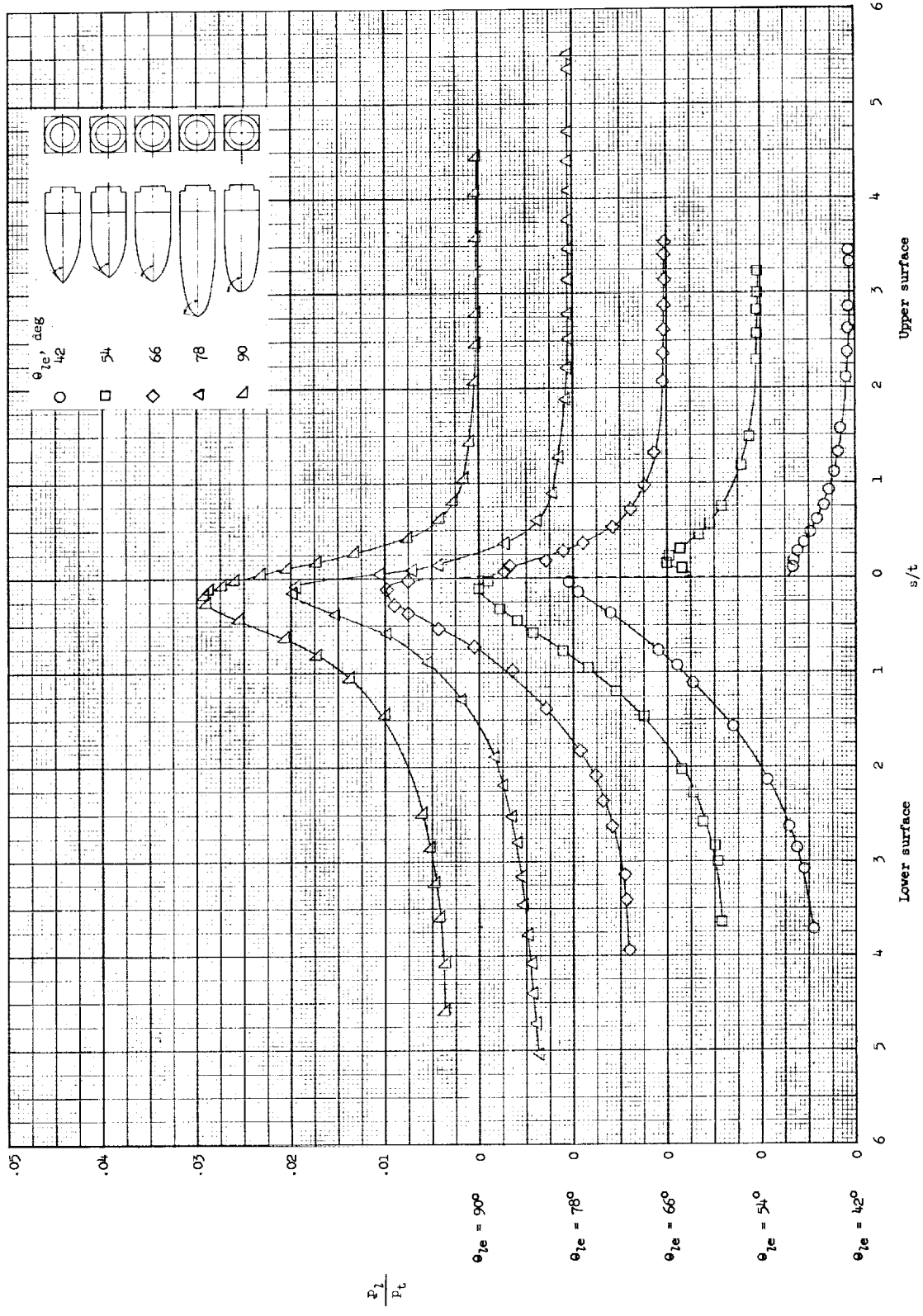
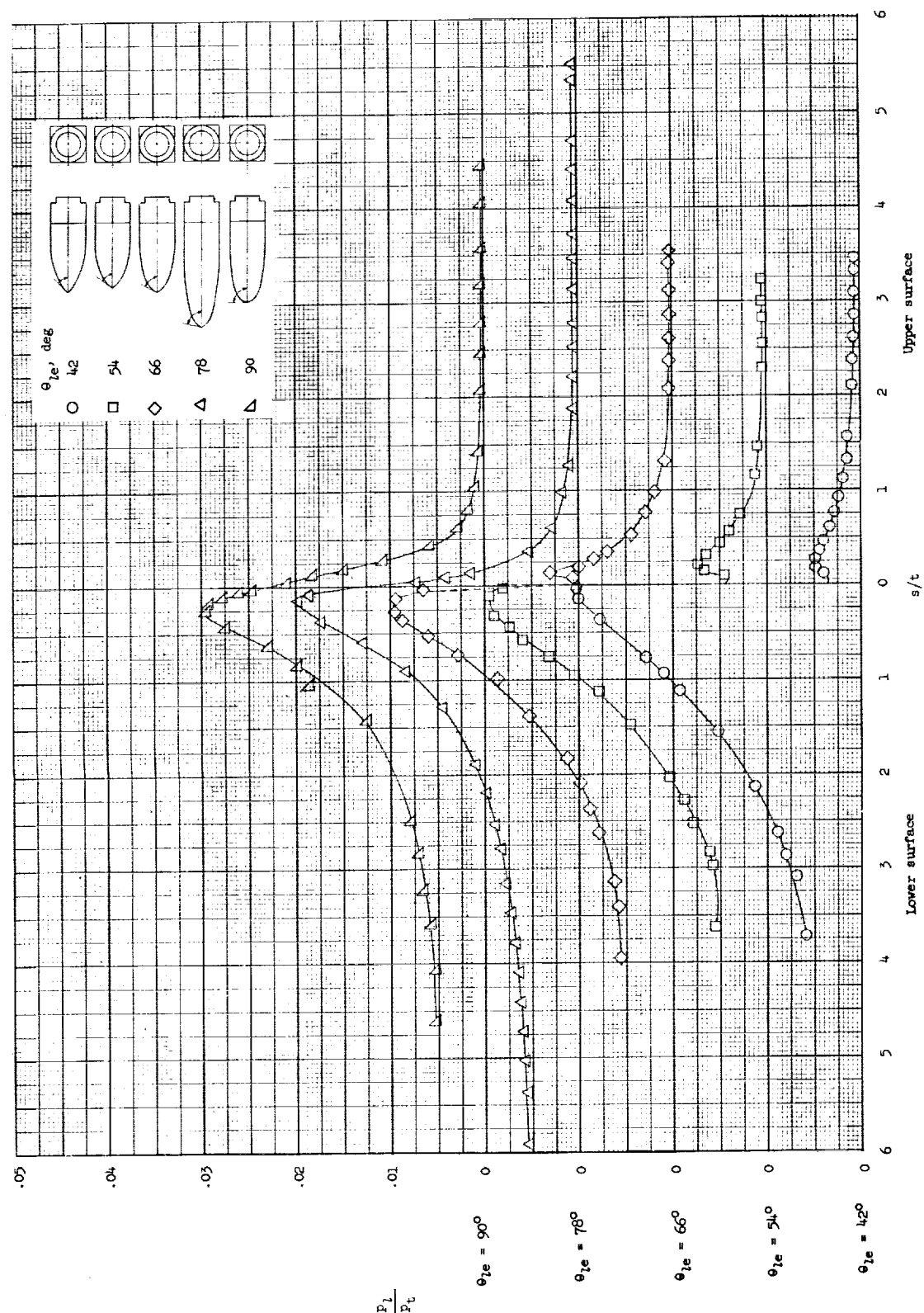
(d) $\alpha = 15^\circ$.

Figure 6.- Continued.



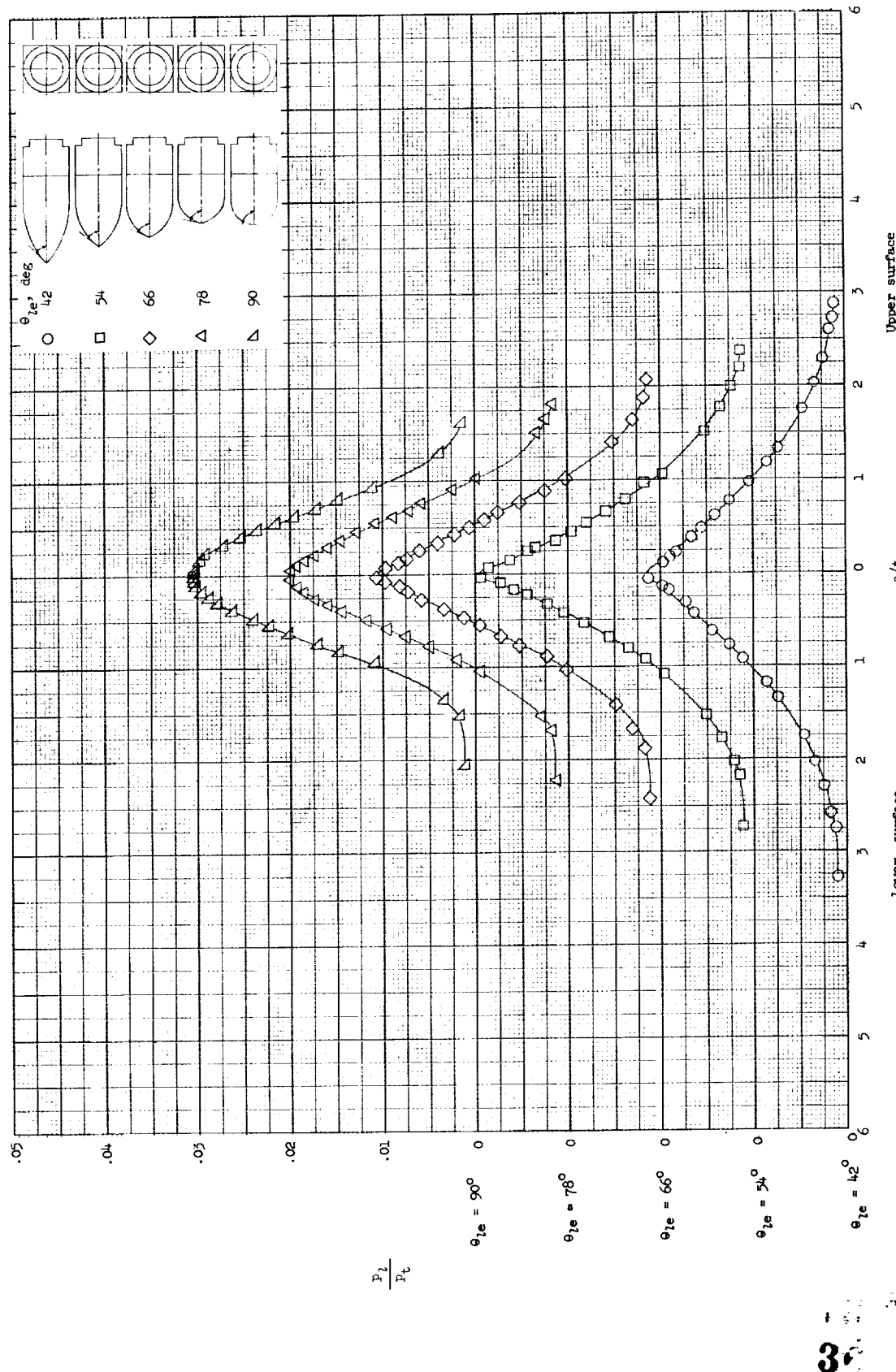
(e) $\alpha = 20^\circ$.

Figure 6.- Continued.



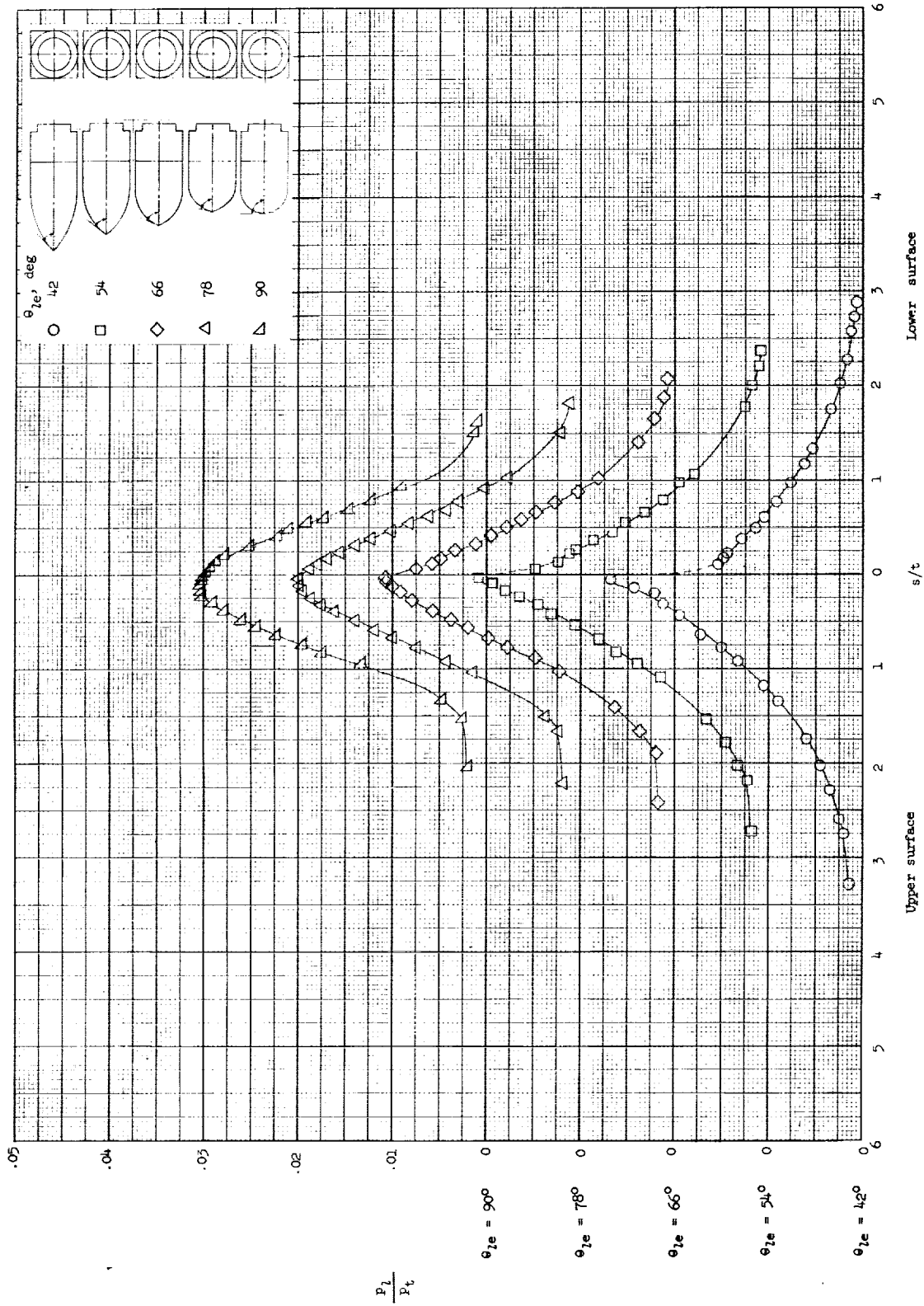
(f) $\alpha = 25^\circ$.

Figure 6.- Concluded.



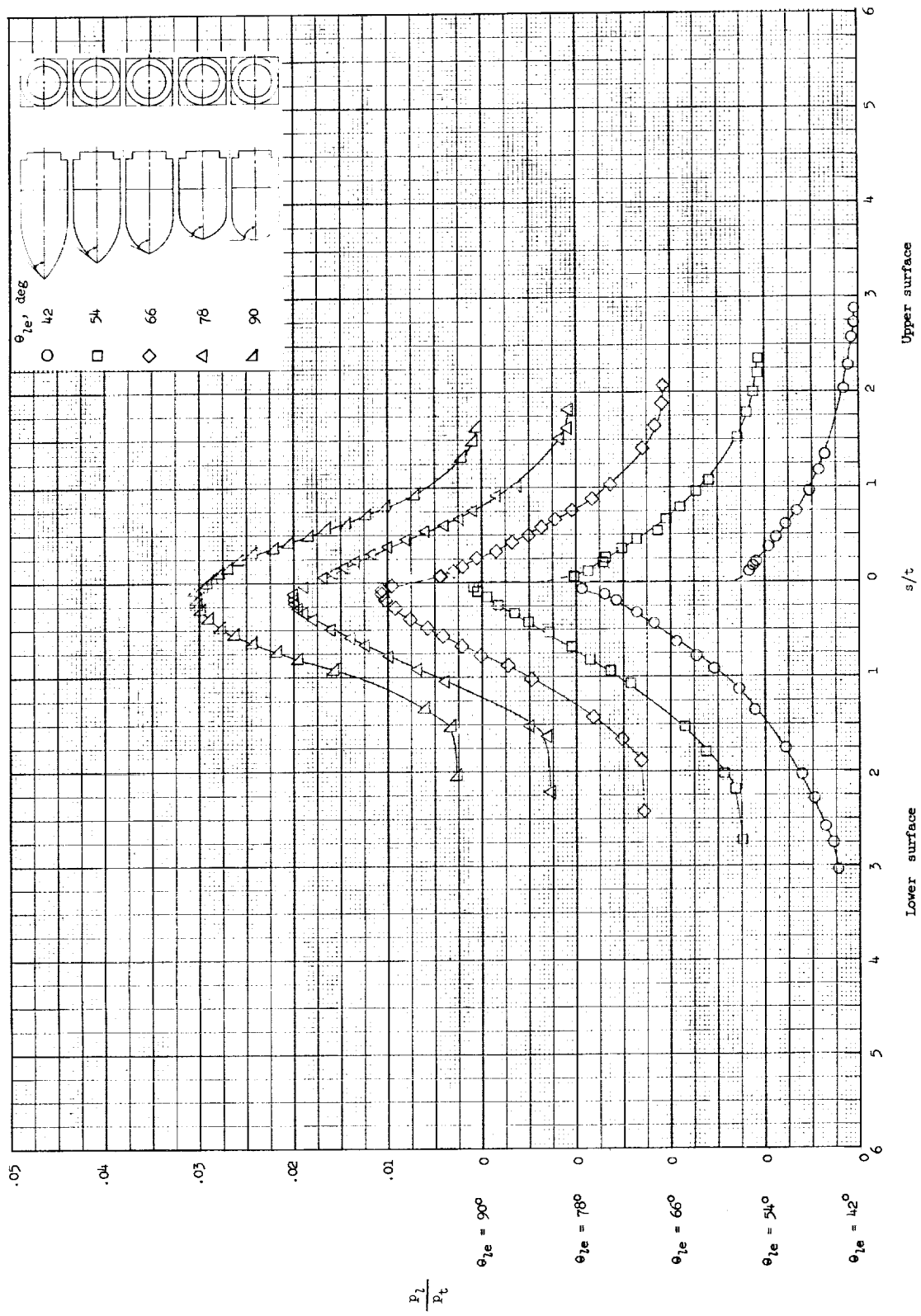
(a) $\alpha = 0^\circ$.

Figure 7.- Pressure distributions of two-dimensional circular arcs.



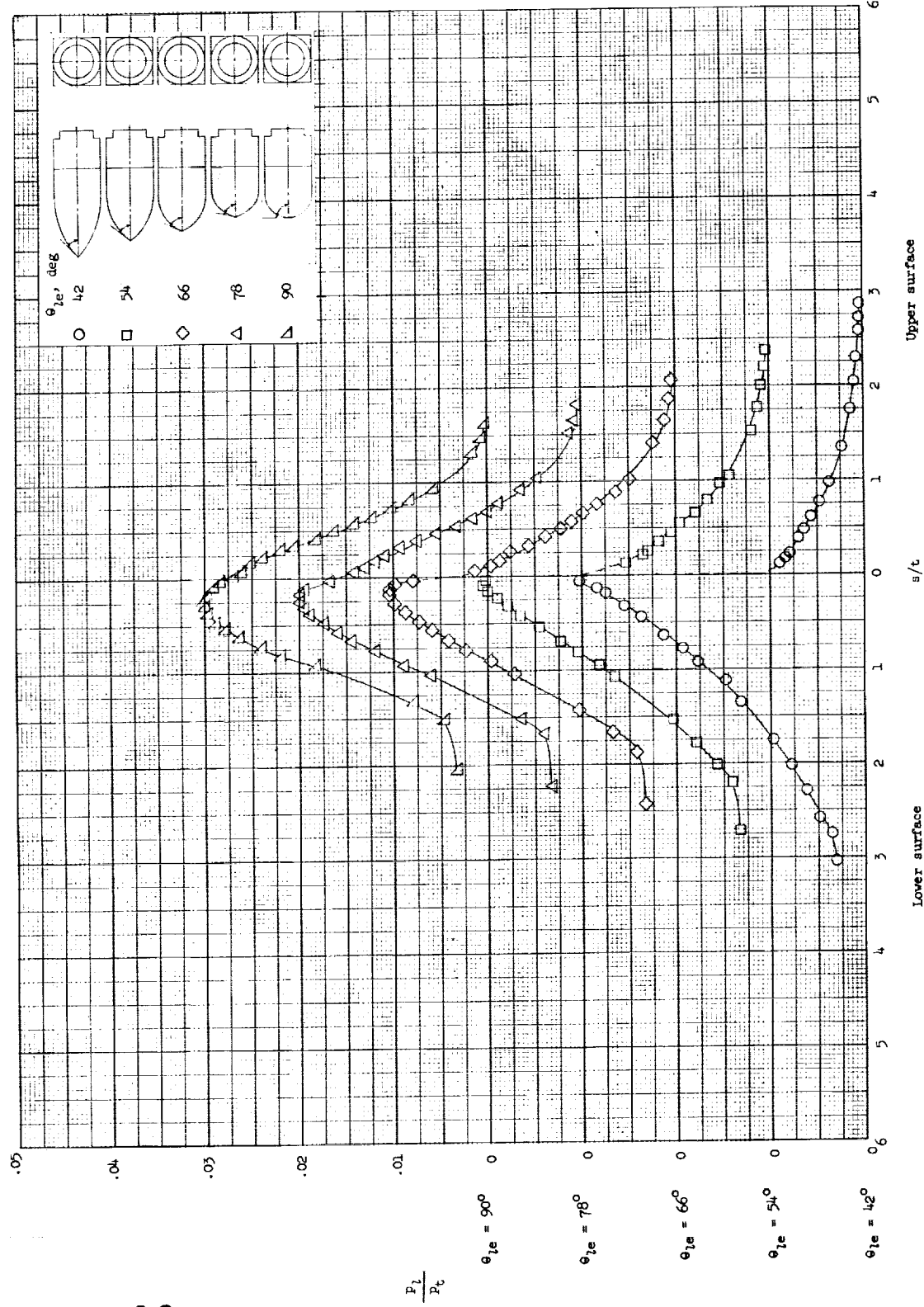
(b) $\alpha = 5^\circ$.

Figure 7. - Continued.



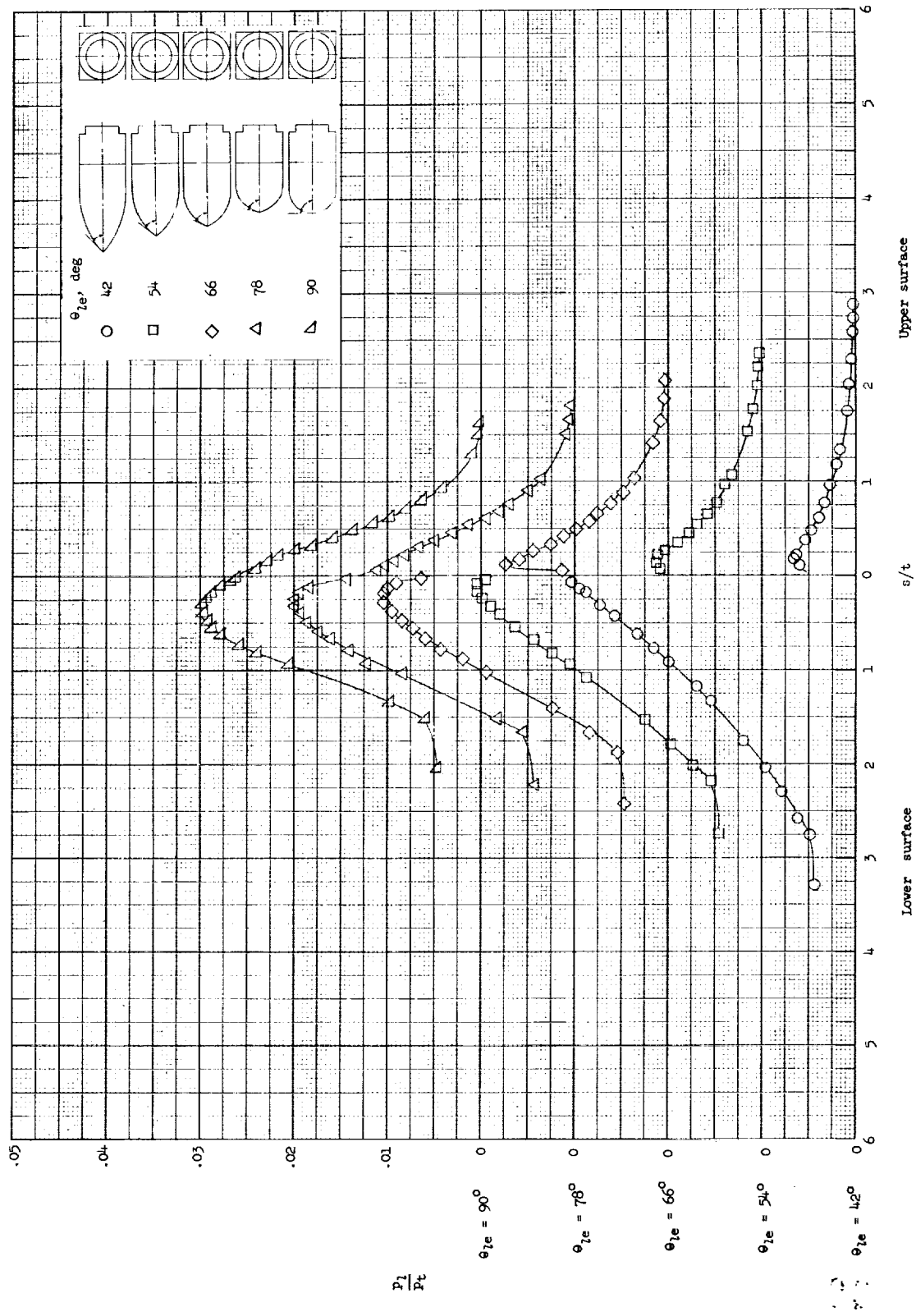
(c) $\alpha = 10^\circ$.

Figure 7.- Continued.



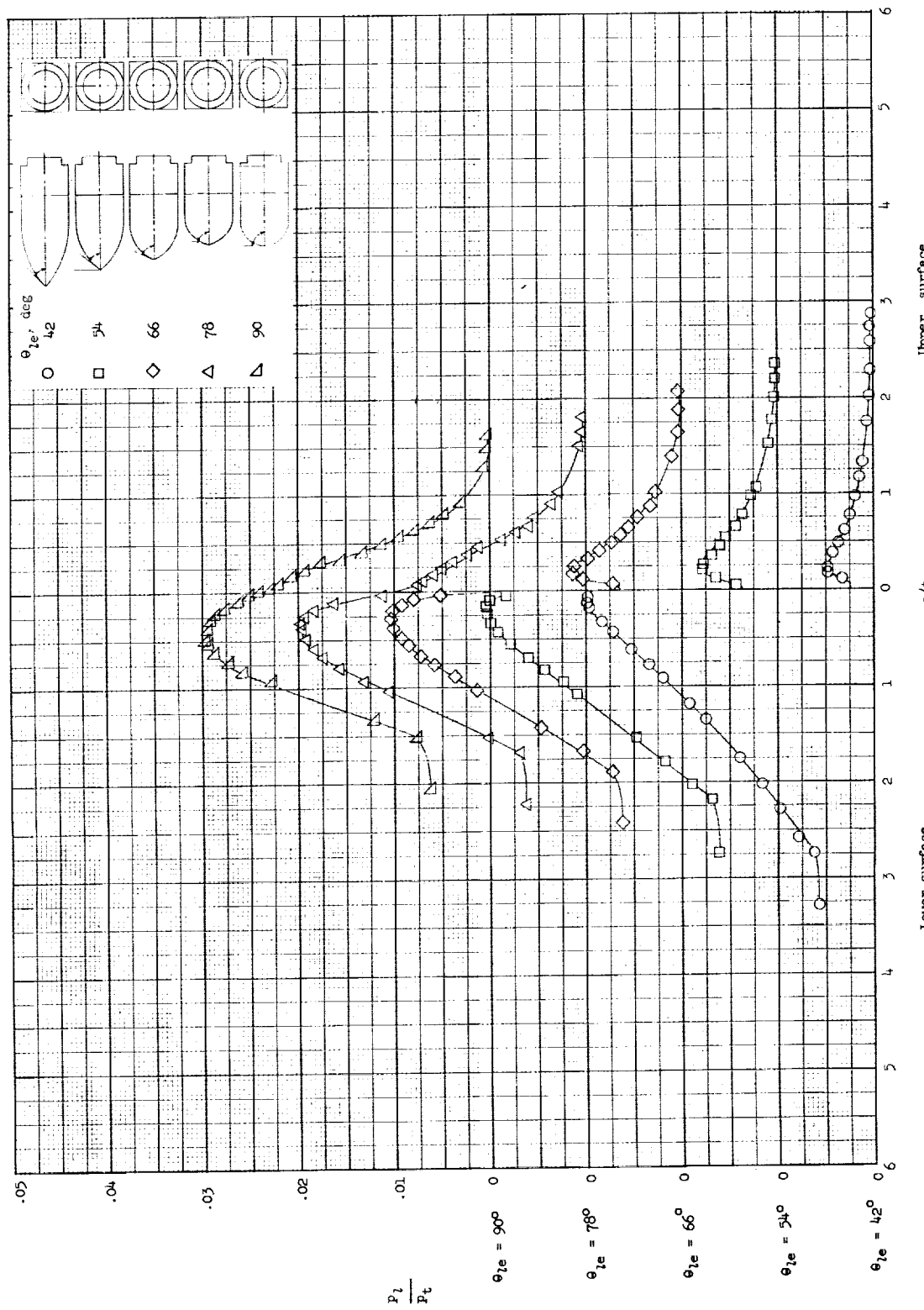
(d) $\alpha = 15^\circ$.

Figure 7.- Continued.



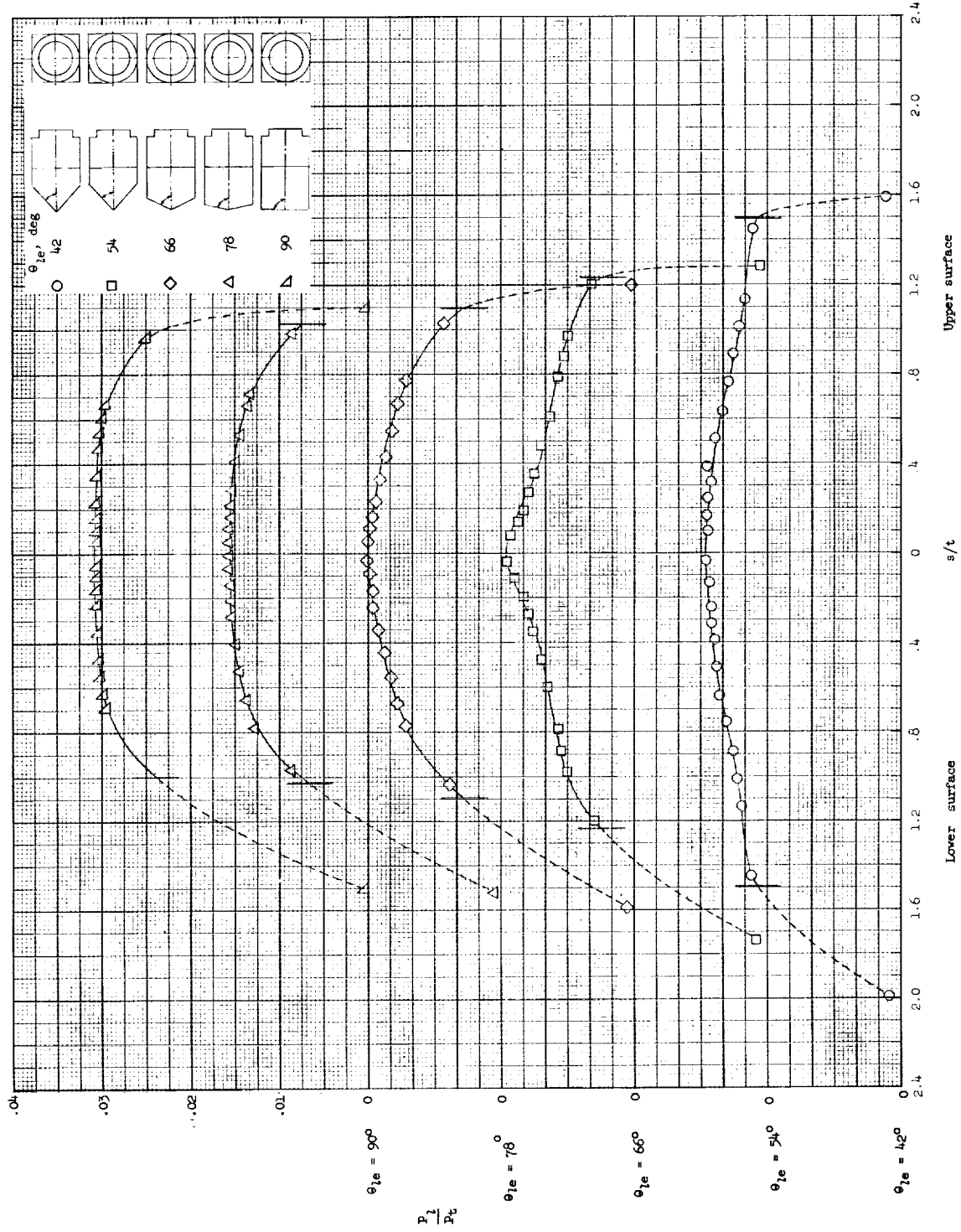
(e) $\alpha = 20^\circ$.

Figure 7.- Continued.



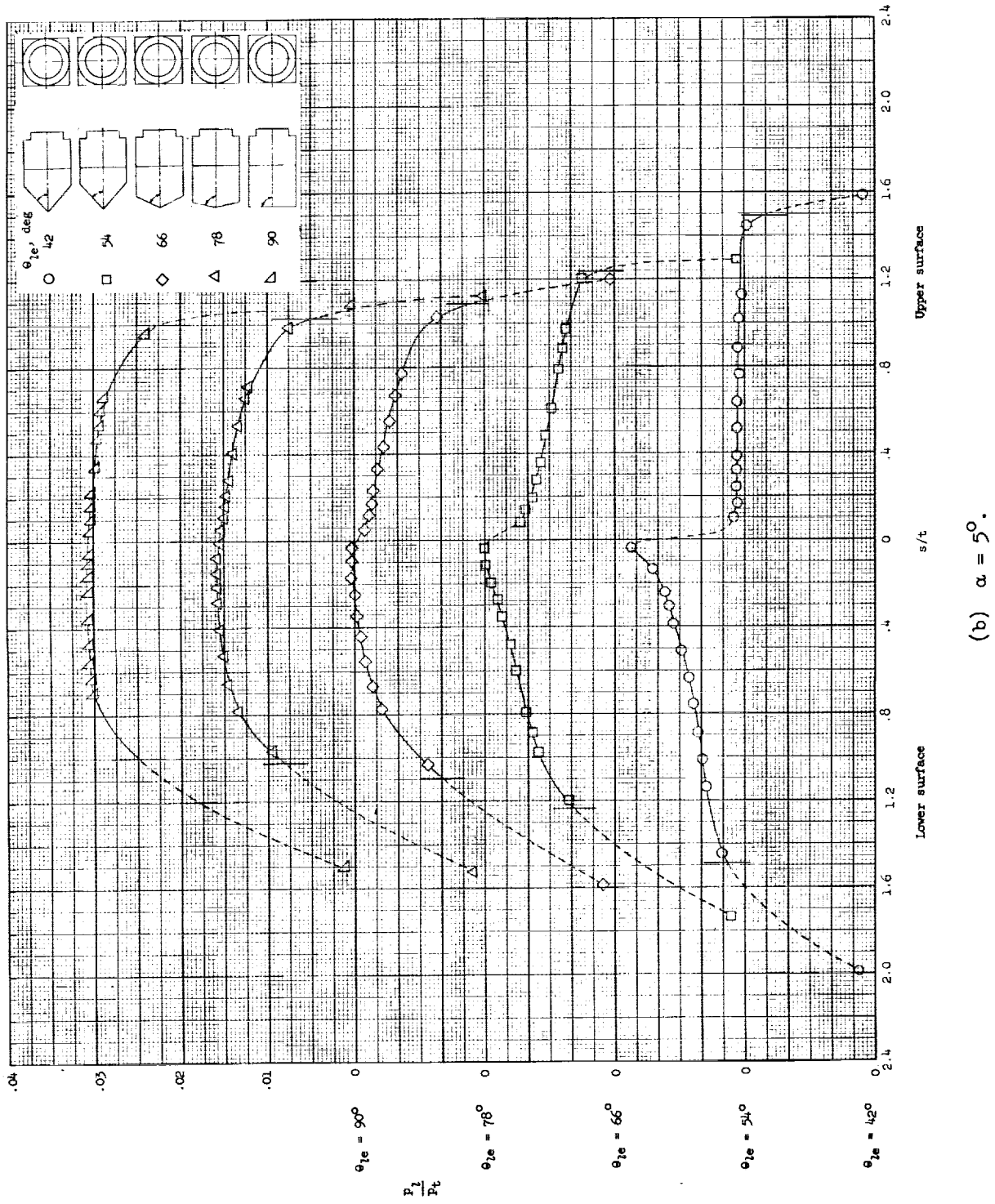
(f) $\alpha = 25^\circ$.

Figure 7.- Concluded.



(a) $\alpha = 0^\circ$.

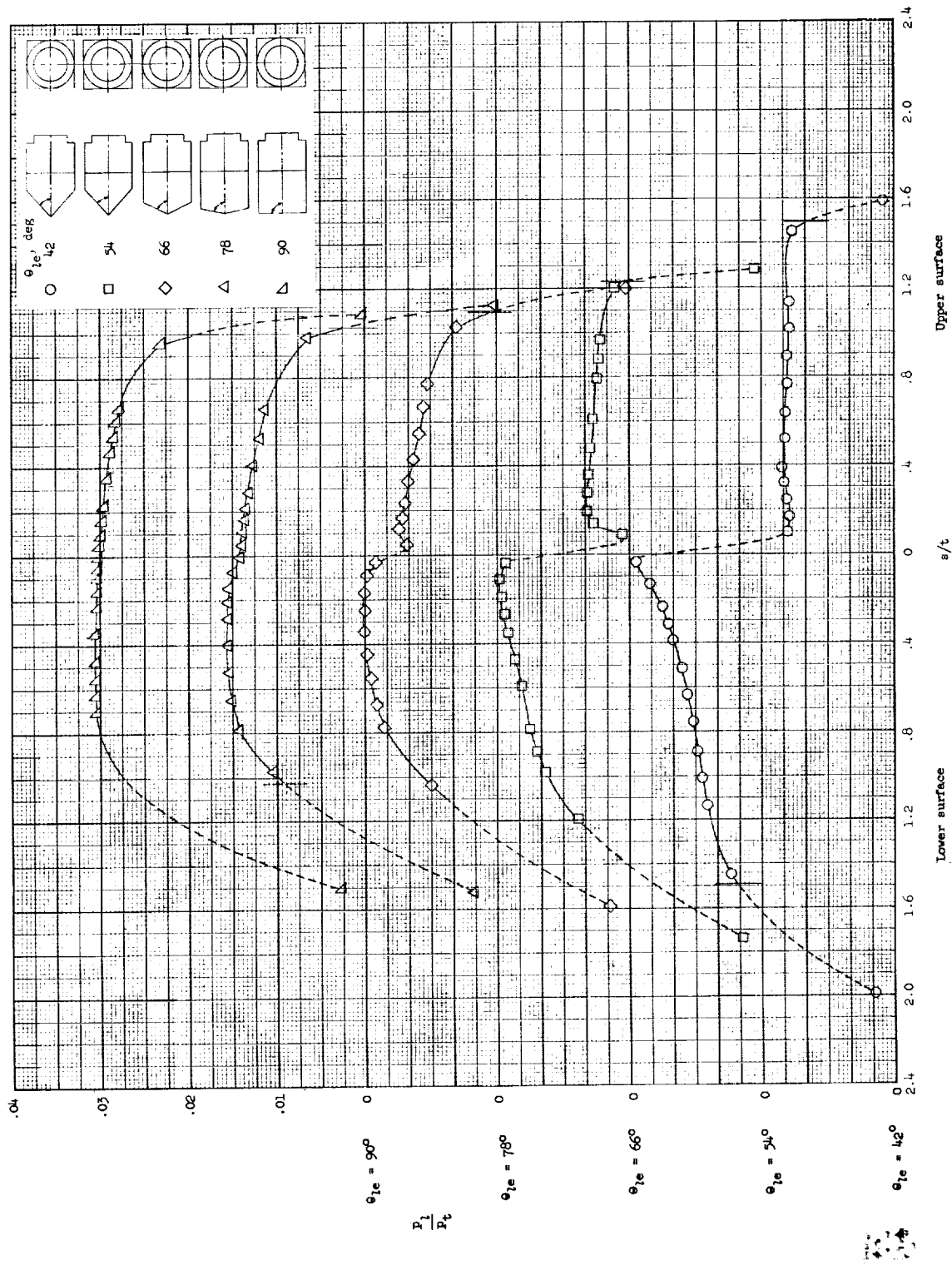
Figure 8.- Pressure distributions of wedges.



(b) $\alpha = 5^\circ$.

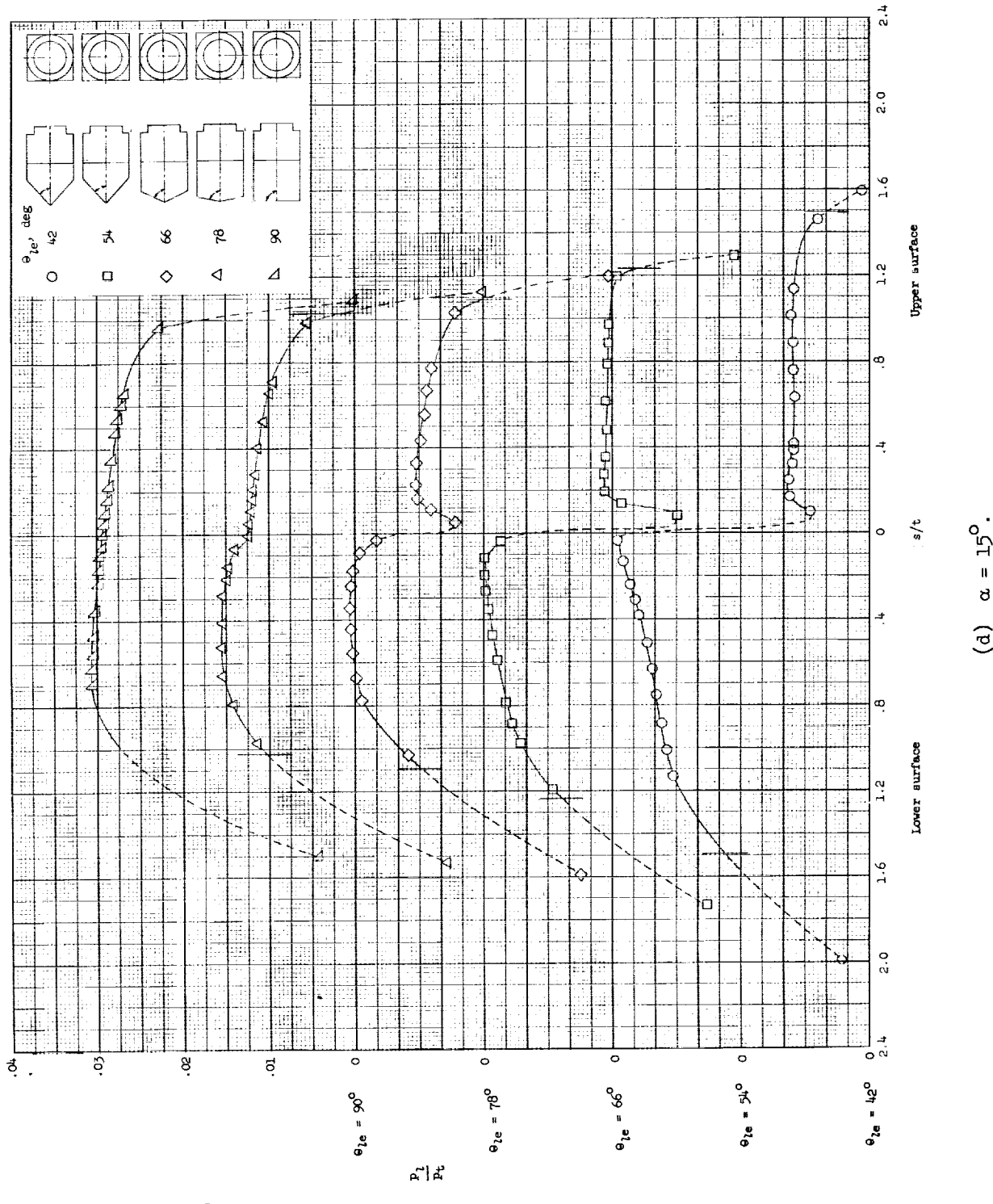
Figure 8.- Continued.

43



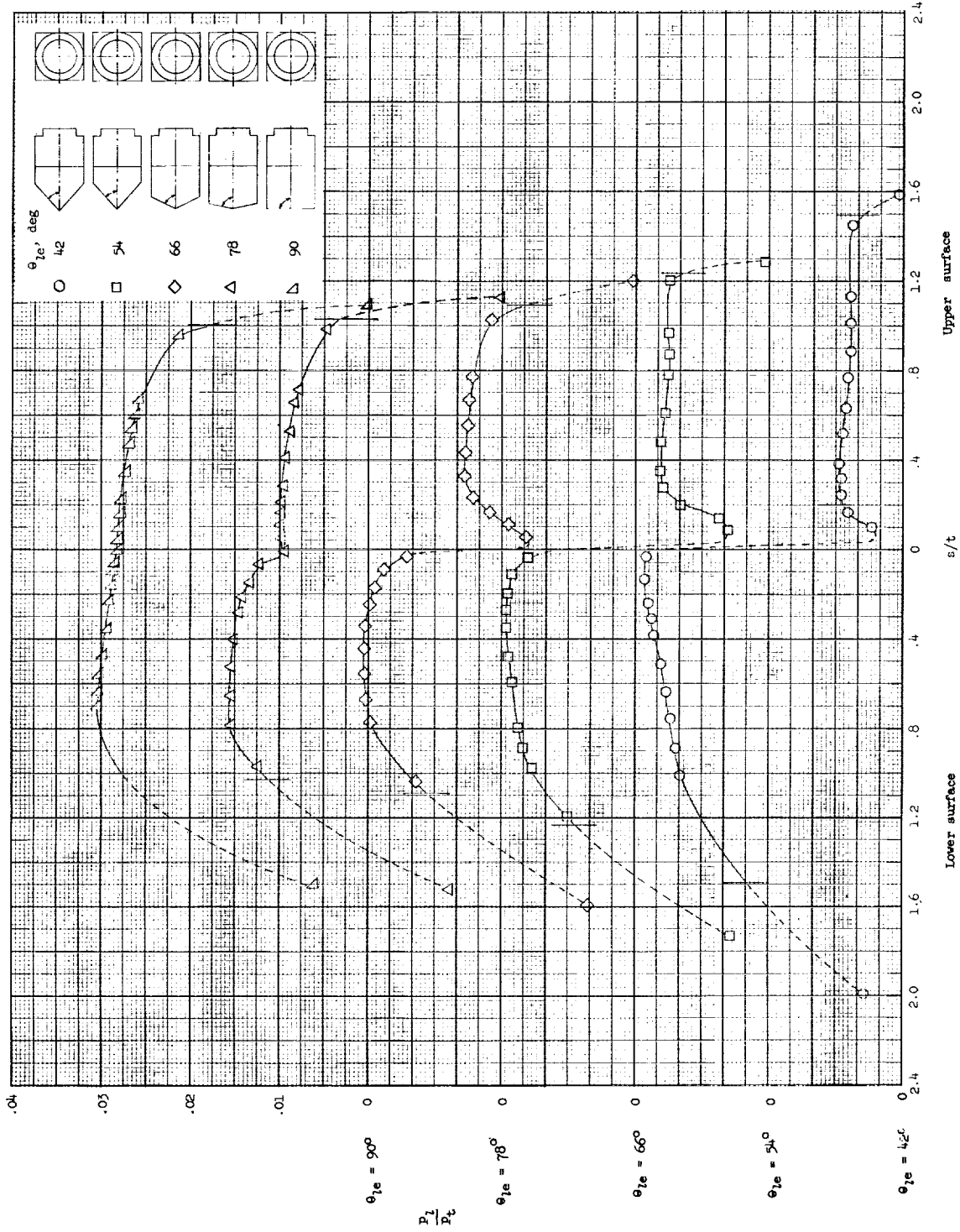
(c) $\alpha = 10^\circ$.

Figure 8.- Continued.



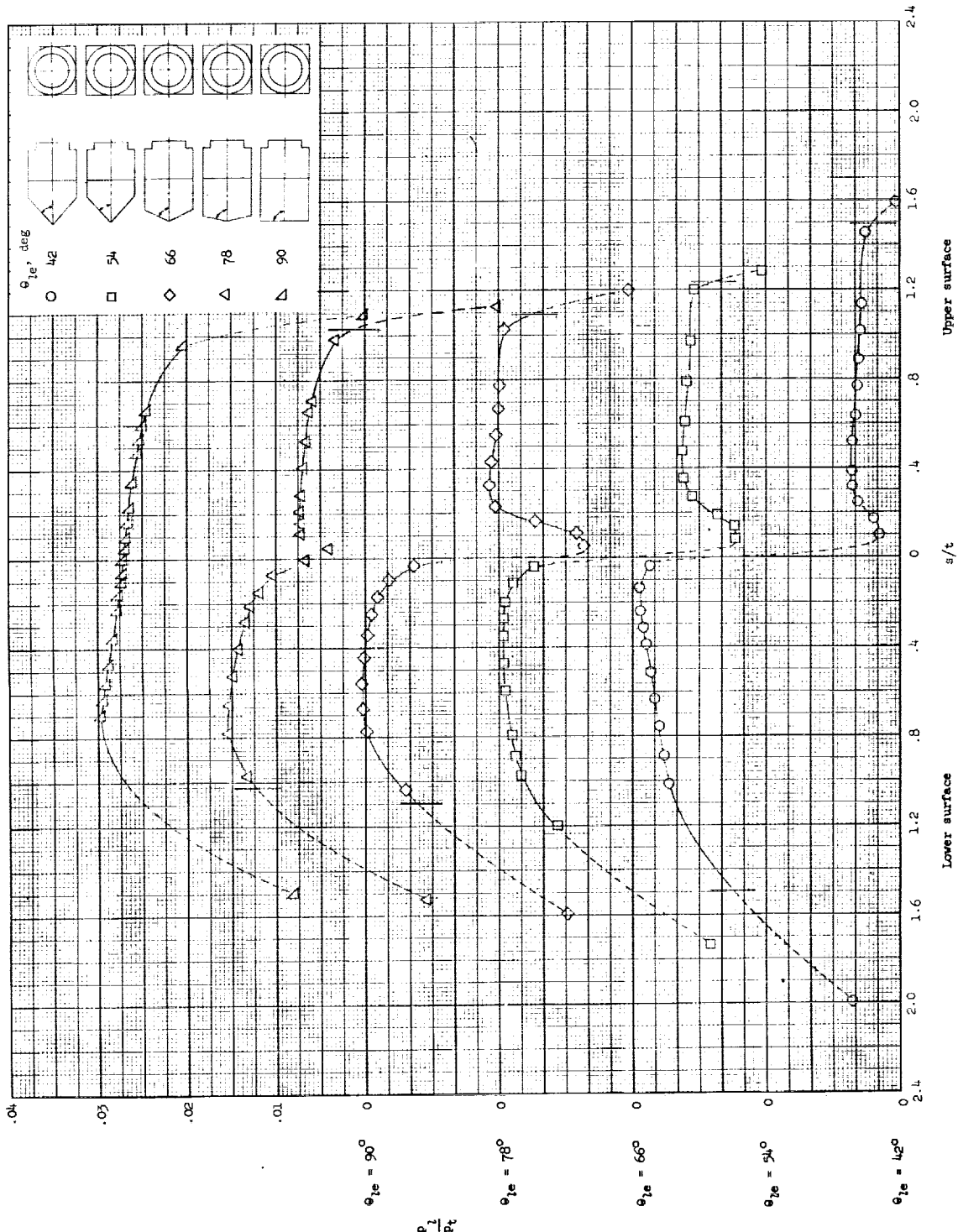
(d) $\alpha = 15^\circ$

Figure 8.- Continued.



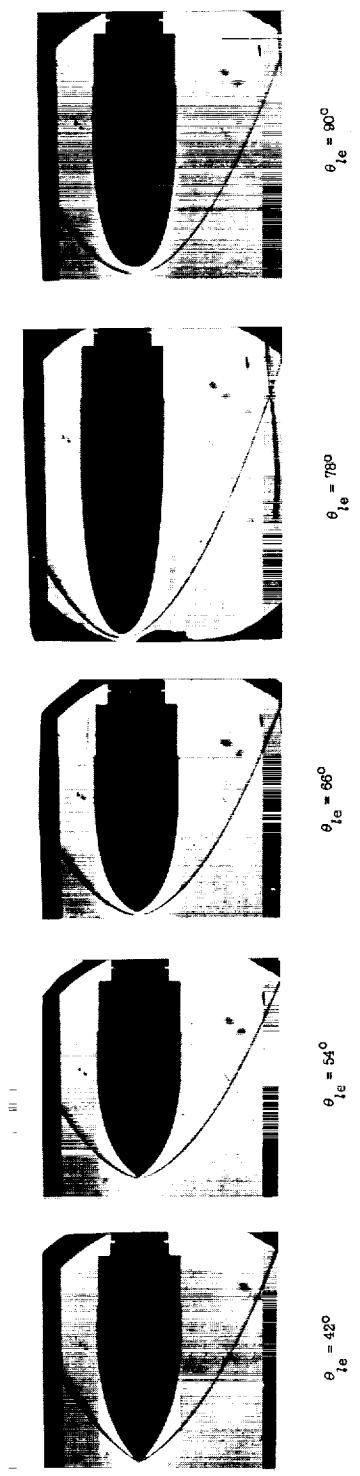
(e) $\alpha = 20^\circ$.

Figure 8.- Continued.

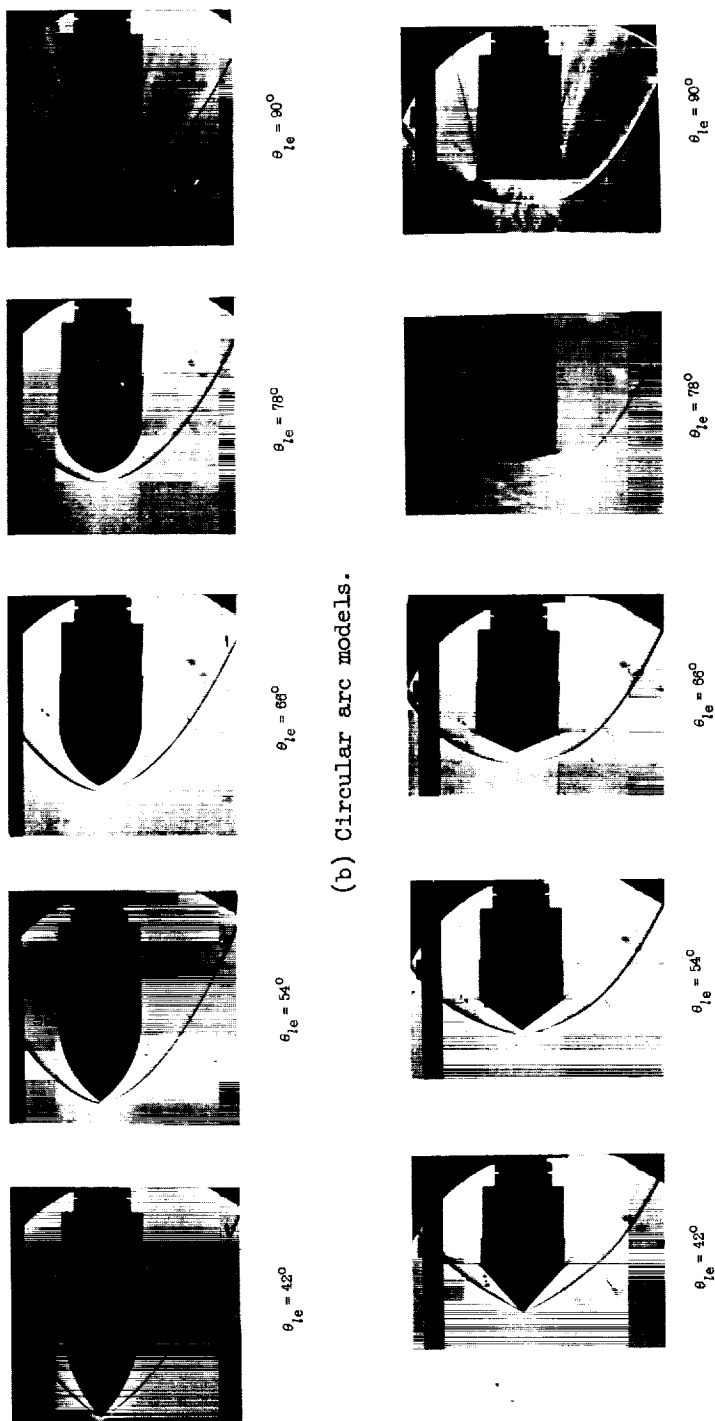


(f) $\alpha = 25^\circ$.

Figure 8.- Concluded.



(a) Parabolic arc models.



(c) Wedge models.
I-63-82

Figure 9. Schlieren photographs of aerodynamically blunt bodies near 0° angle of attack.

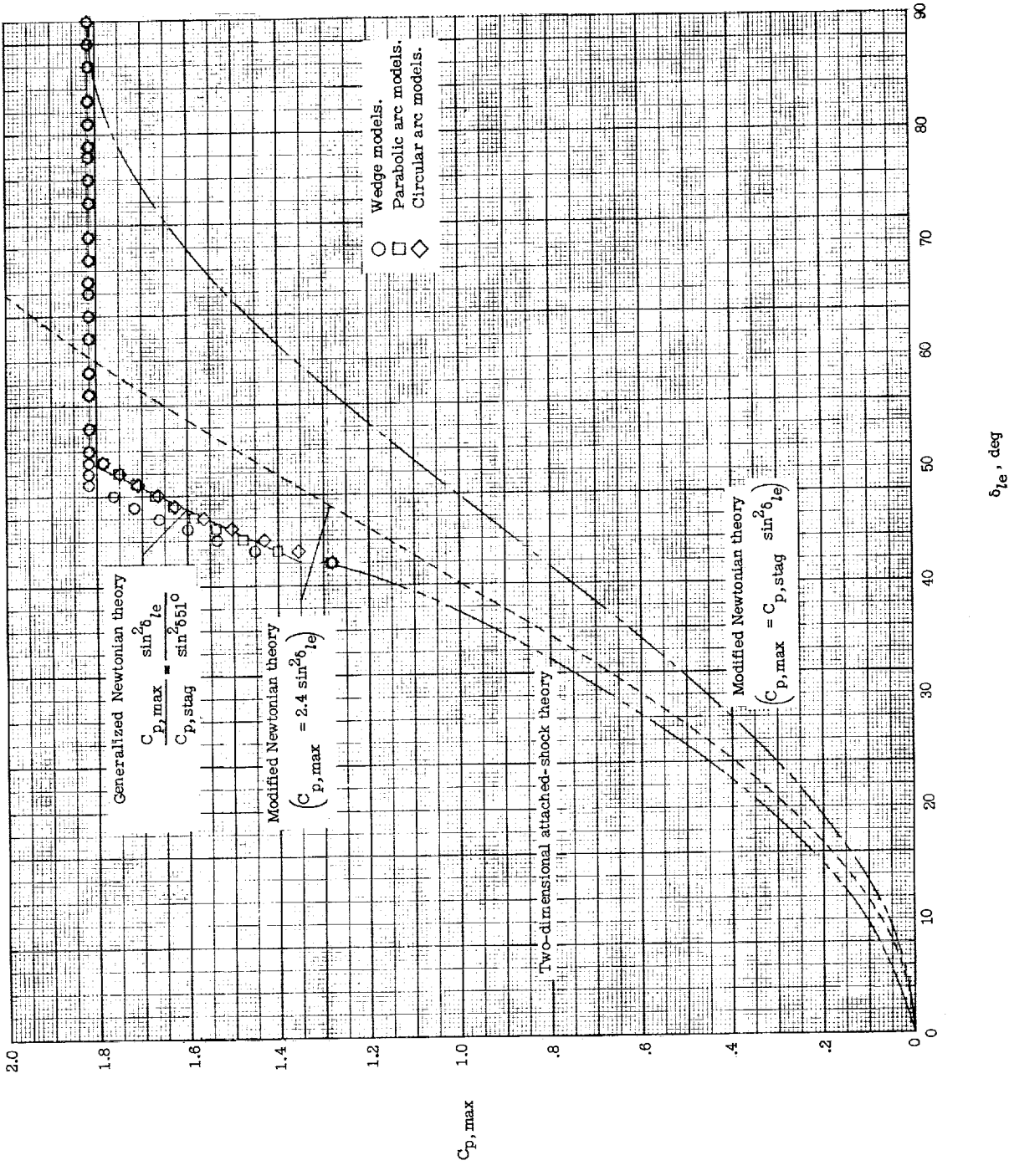
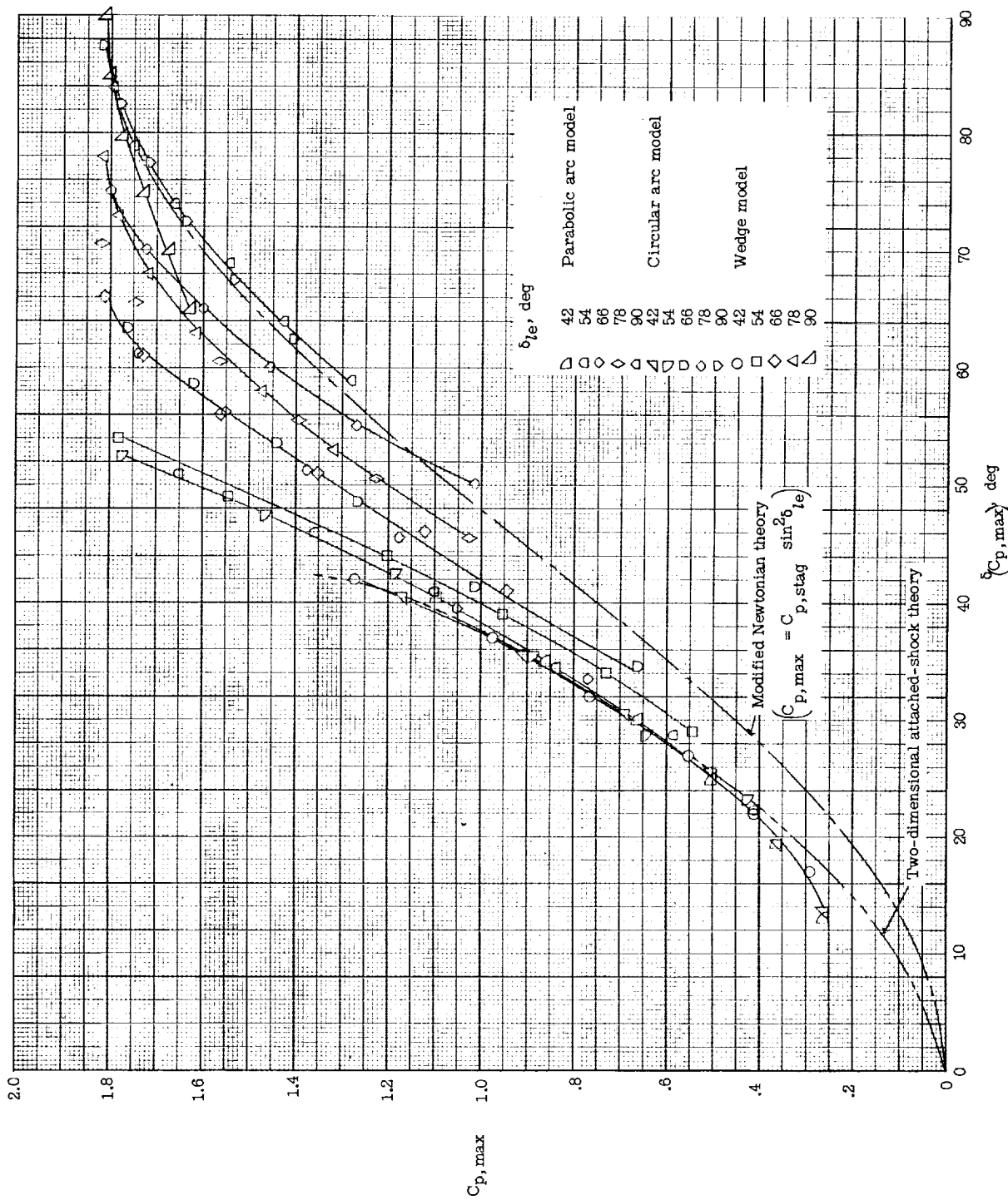


Figure 10.- Comparison of measured and predicted pressure coefficients on the lower surface for aerodynamically blunt bodies.

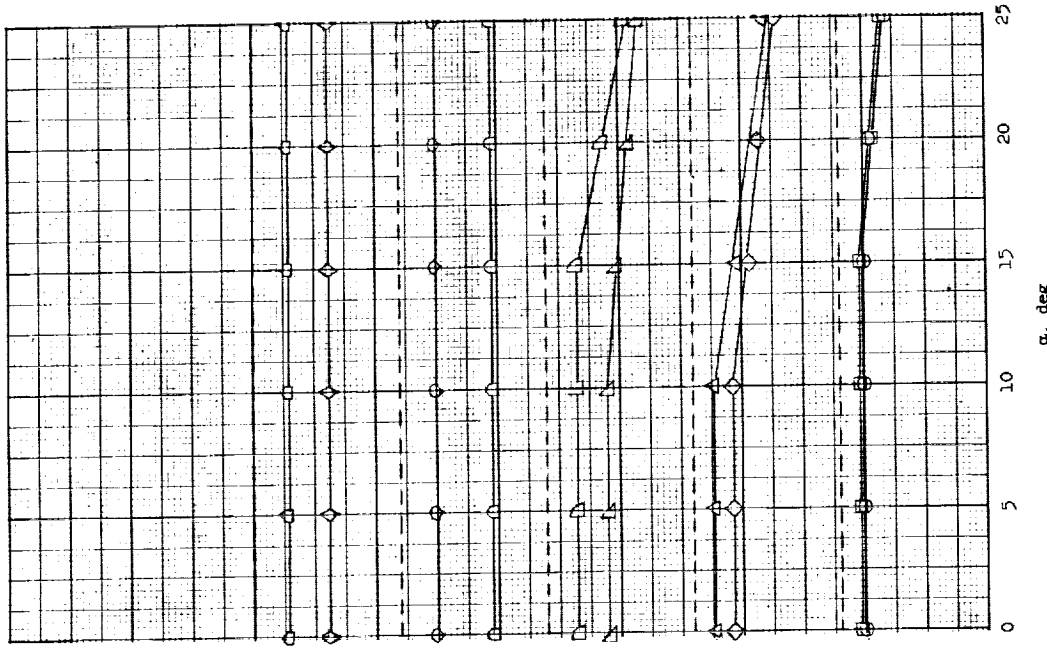


49

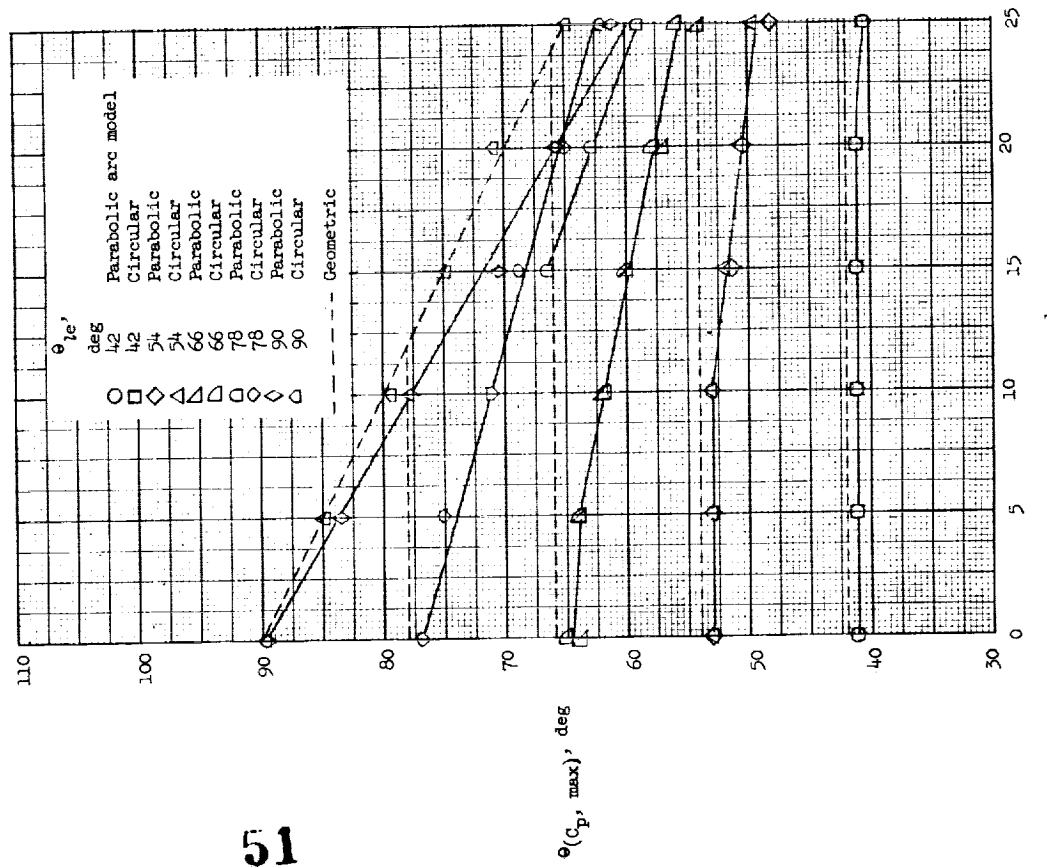
Figure 11.- Comparison

measured and predicted maximum pressure coefficients on the upper surface for aerodynamically blunt bodies.

50

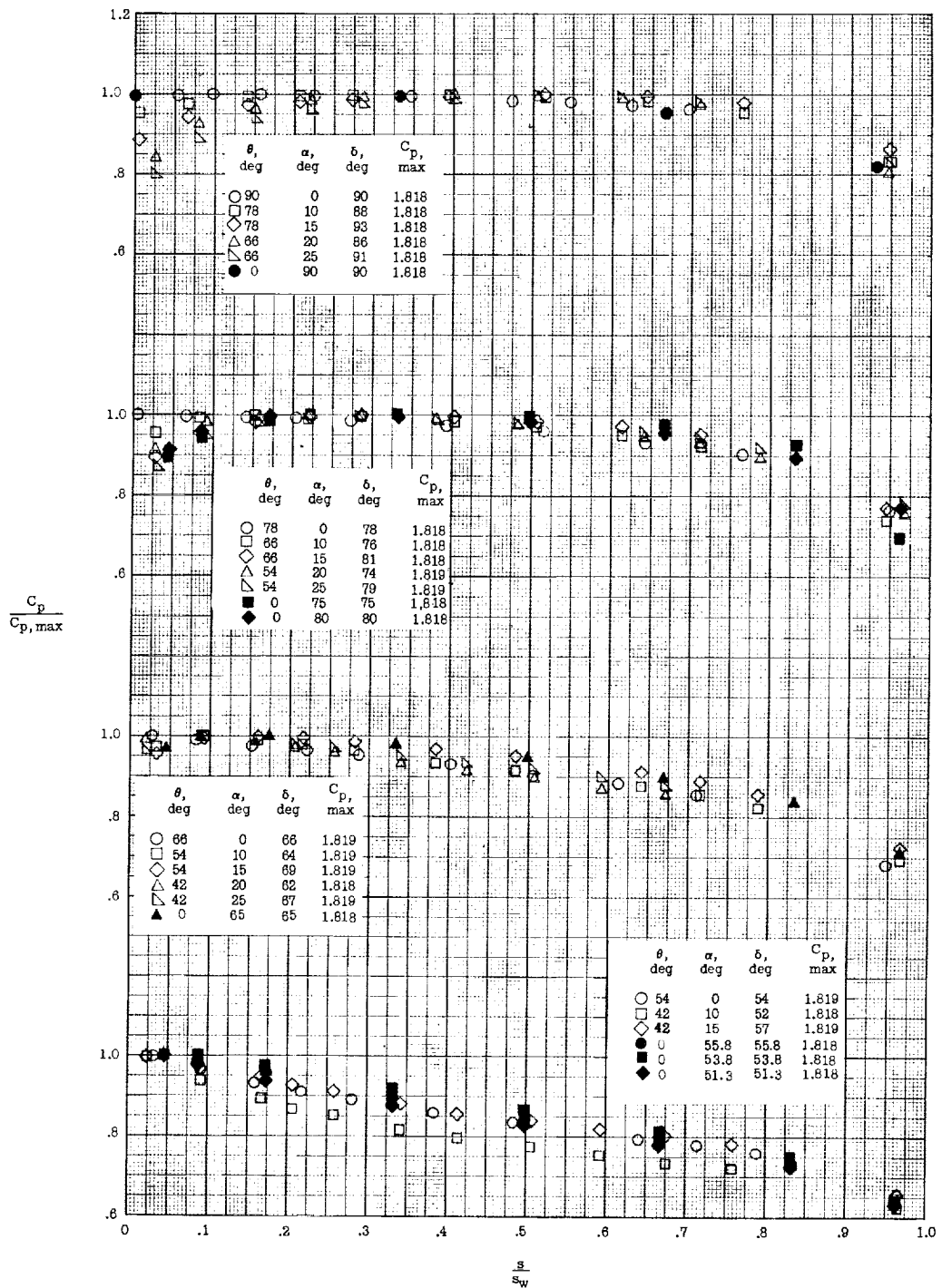


(b) Upper surface



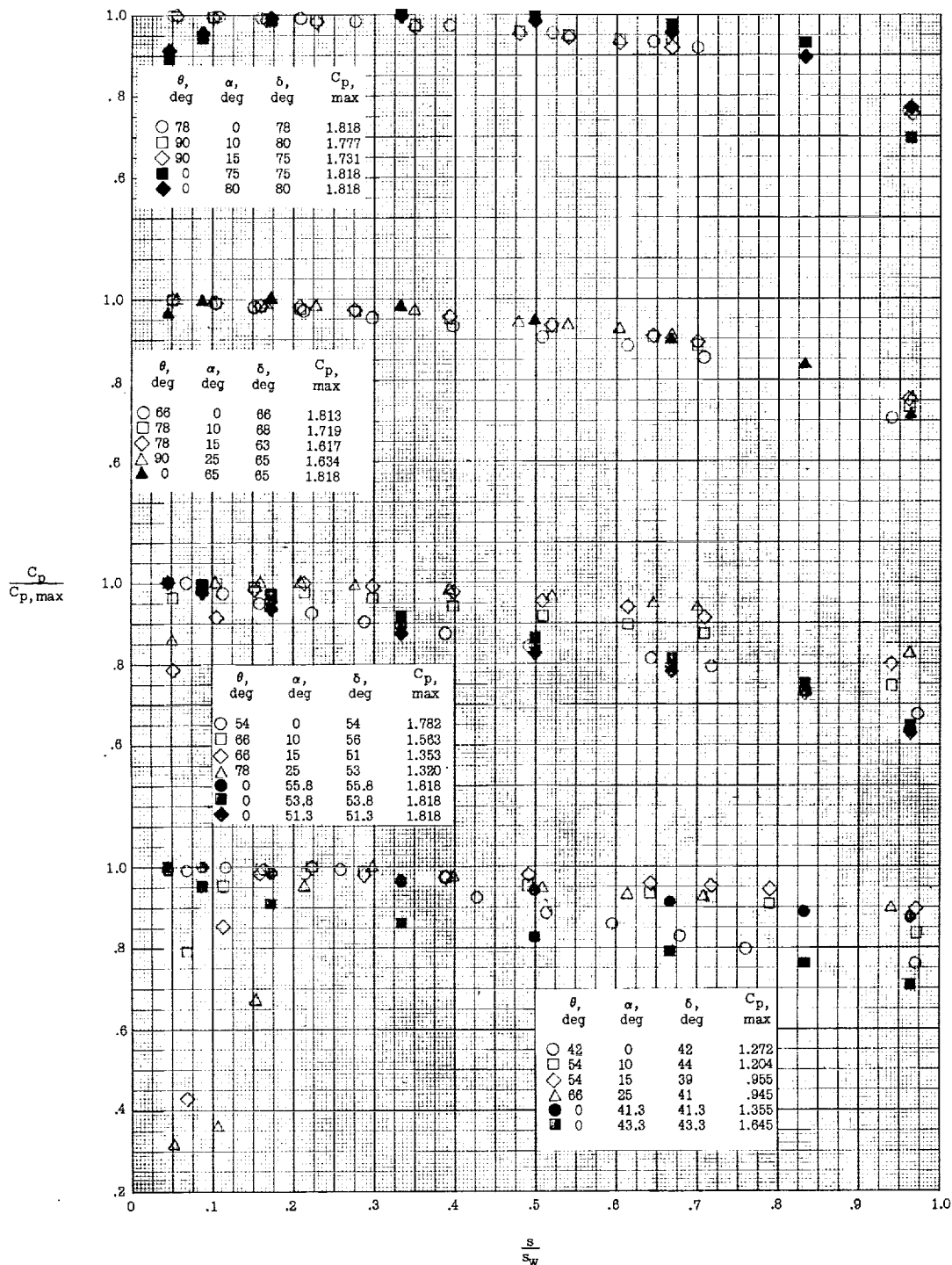
(a) Lower surface

Figure 12.- Comparison of geometric and measured slopes at which maximum pressure occurred for various angles of attack on the parabolic and circular arc bodies.



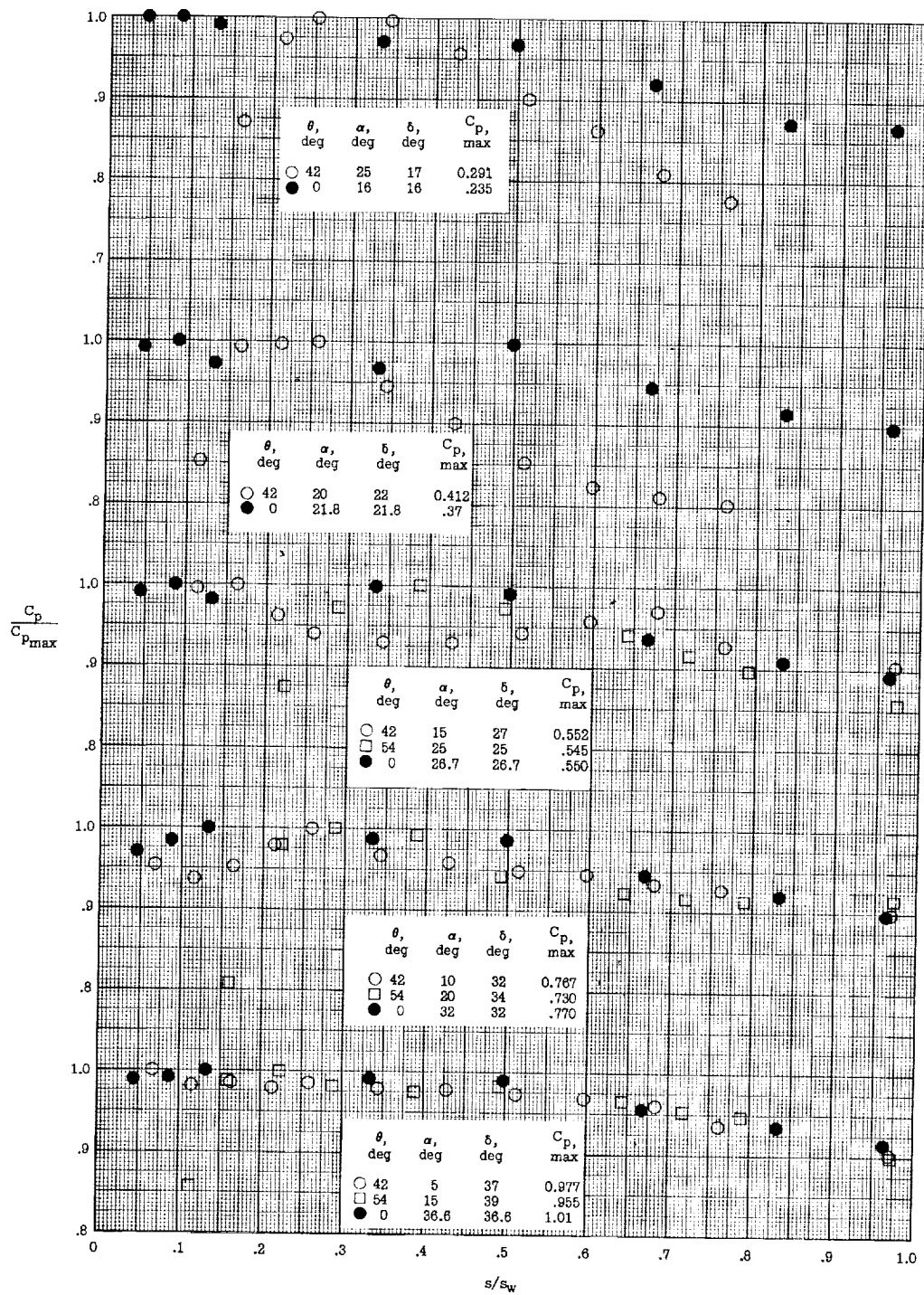
(a) Lower surface.

Figure 13.- Comparison of pressure distributions on wedges with constant deflection angles. Solid symbols are for flat-plate data at approximately the same deflection angles (ref. 2).



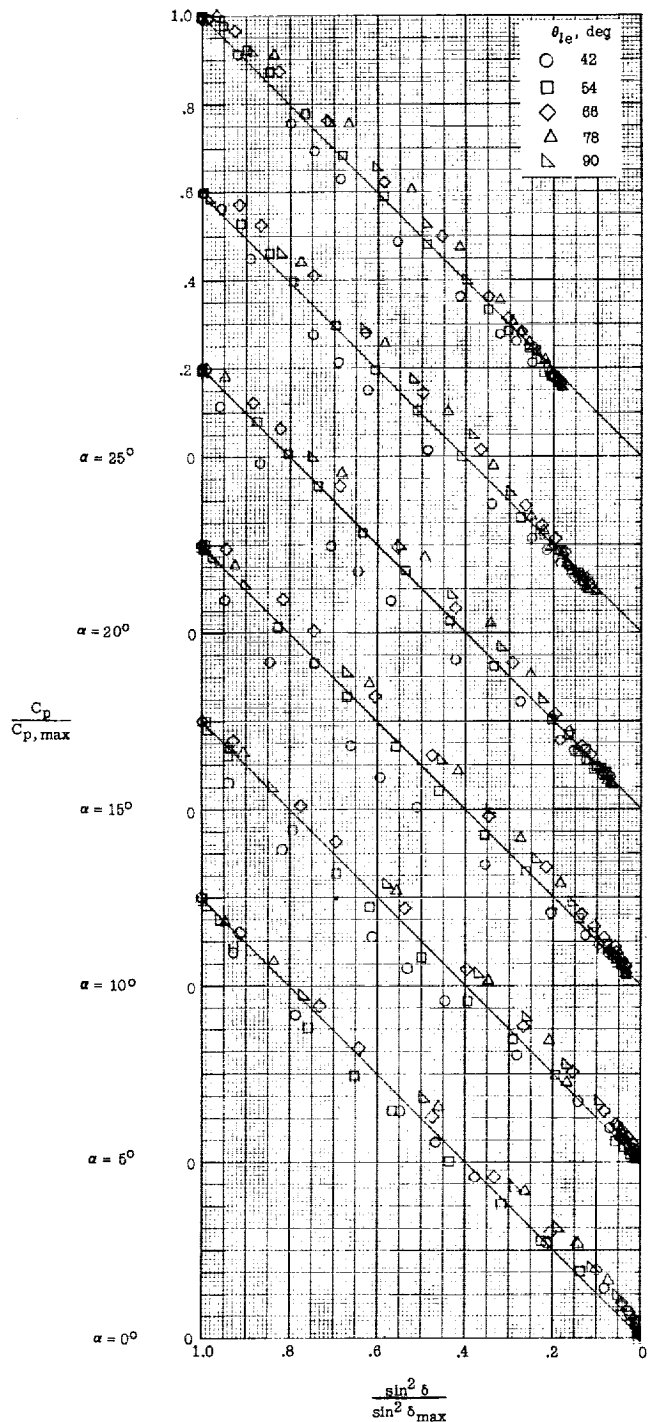
(b) Upper surface.

53

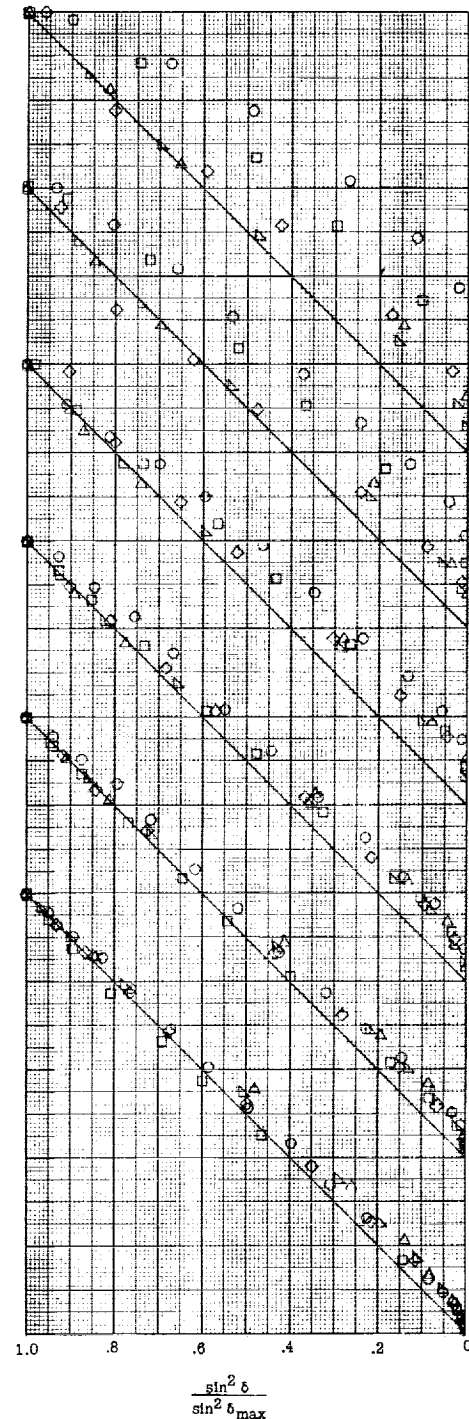


(b) Concluded.

Figure 13.- Concluded.

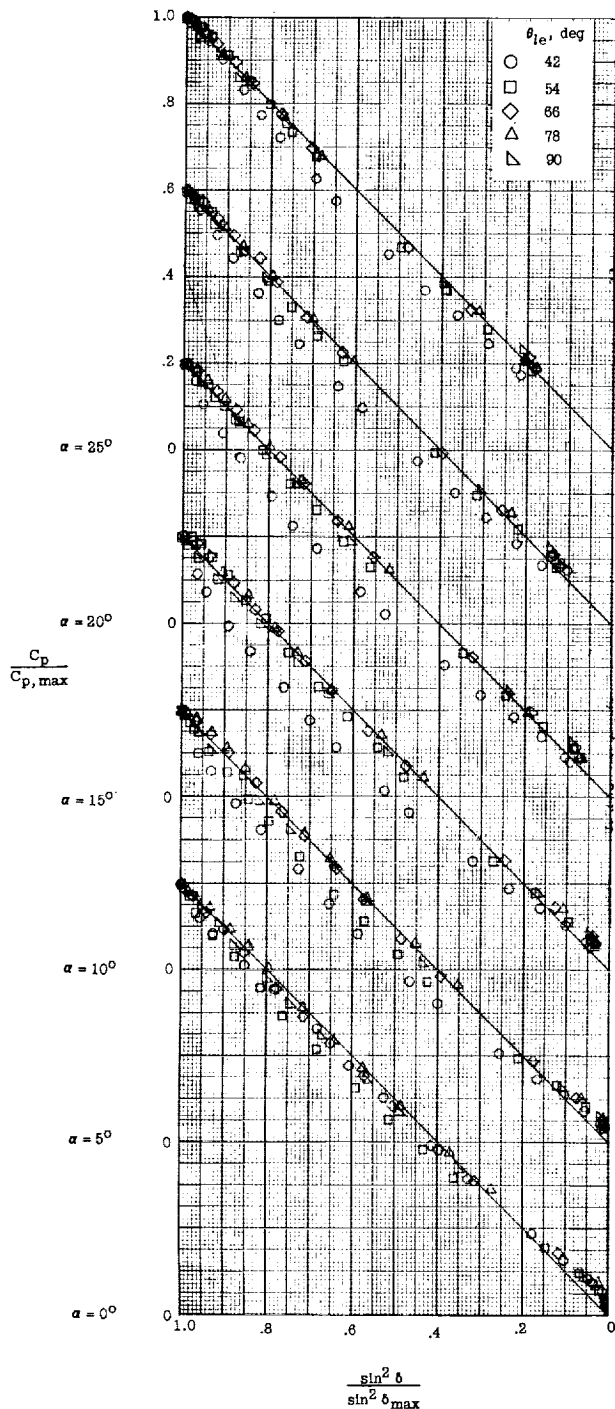


(a) Lower surface.

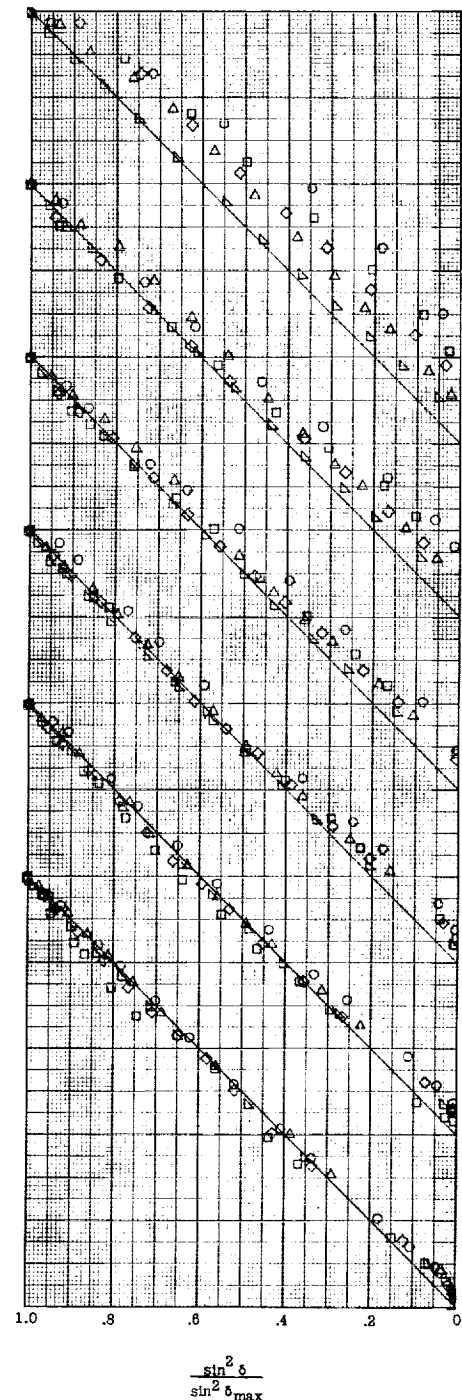


(b) Upper surface.

Figure 14.- Correlation of pressure distributions with generalized Newtonian theory for two-dimensional parabolic arc models.



(a) Lower surface.



(b) Upper surface.

Figure 15.- Correlation of pressure distributions with generalized Newtonian theory for two-dimensional circular arc models.

